The Journal of Gemmology

Volume 36 / No. 3 / 2018

Bumble Bee Stone from Indonesia

Tracking and Traceability in the Gem Industry

Circling on Ming Cultured Pearls

The Journal of
Gemmology

Volume 36 / No. 3 / 2018

Cover photo: *Bumble Bee Stone from Indonesia is an unusual carbonate-rich rock that is coloured by arsenic sulphide minerals and may also contain black areas of 'sooty' pyrite. A pattern resembling an erupting volcano is seen in this cabochon (45 × 65 mm), and is reminiscent of the volcanic origin of this gem. Courtesy of Rare Earth Mining Company.*

COLUMNS

ARTICLES

208

Photo by Orasa Weldon

230

Photo by J. Ivey

213

Photo by L. E. Cartier

The Journal is published by Gem-A in collaboration with SSEF and with the support of AGL.

Gem-A THE GEMMOLOGICAL ASSOCIATION OF GREAT BRITAIN

SSEF SCHWEIZERISCHES GEMMOLOGISCHES INSTITUT SWISS GEMMOLOGICAL INSTITUTE INSTITUT SUISSE DE GEMMOLOGIE

AGL AMERICAN GEMOLOGICAL LABORATORIES

The Journal of Gemmology

CONTENT SUBMISSION

The Editor-in-Chief is glad to consider original articles, news items, conference/excursion reports, announcements and calendar entries on subjects of gemmological interest for publication in *The Journal of Gemmology*. A guide to the various sections and the preparation of manuscripts is given at www.gem-a.com/index.php/news-publications/publications/journal-of-gemmology/submissions, or contact the Editor-in-Chief.

SUBSCRIPTIONS

Gem-A members receive *The Journal* as part of their membership package, full details of which are given at www.gem-a.com/membership. Laboratories, libraries, museums and similar institutions may become direct subscribers to *The Journal*.

DATABASE COVERAGE

The Journal of Gemmology is covered by the following abstracting and indexing services: Australian Research Council academic journal list, British Library Document Supply Service, Chemical Abstracts (CA Plus), Copyright Clearance Center's RightFind application, CrossRef, EBSCO (Academic Search International, Discovery Service and TOC Premier), Gale/Cengage Learning Academic OneFile, GeoRef, Index Copernicus ICI Journals Master List, Mineralogical Abstracts, Cambridge Scientific Abstracts (ProQuest), Scopus and the Clarivate Analytics (formerly Thomson Reuters) Emerging Sources Citation Index (in the Web of Science).

Design & production by Zest Design, www.zest-uk.com

Printed by DG3 Group (Holdings) Ltd

ISSN: 1355-4565

Gem-A
THE GEMMOLOGICAL ASSOCIATION OF GREAT BRITAIN

21 Ely Place
London EC1N 6TD
UK

t: +44 (0)20 7404 3334
f: +44 (0)20 7404 8843
e: information@gem-a.com
w: www.gem-a.com

Registered Charity No. 1109555
A company limited by guarantee and registered in England No. 1945780
Registered office: Palladium House, 1–4 Argyll Street, London W1F 7LD

What's New

INSTRUMENTATION

Alrosa Diamond Inspector

Released in March 2018, the Diamond Inspector from Russian diamond mining company Alrosa was developed jointly with the Technological Institute for Super Hard and Novel Carbon Materials in Moscow. The instrument is designed for separating polished loose or mounted natural, treated and synthetic diamonds, as well as simulants. Testing takes less than one minute per sample and reportedly employs three analytical methods. Near-colourless (D–K) samples that range from 0.03 to 10 ct may be tested; the analysis is performed on a round flat area of the sample with a diameter of at least 1.5 mm. The Diamond Inspector weighs 1.8 kg (plastic frame) or 3.1 kg (metal frame), and measures 25 × 15 × 10 cm. Visit http://alrosa-inspector.com. *BML*

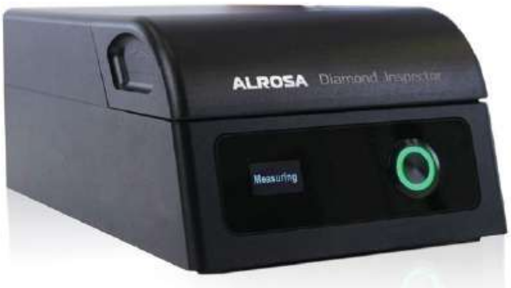

D-Tect for Synthetic Diamonds

In May 2018, HRD Antwerp in Belgium released its new D-Tect instrument. It is designed to be the final step in the identification of synthetic diamonds, following screening by HRD's M-Screen+ or any other diamond screening device that refers samples for further testing. D-Tect is a compact table-top instrument that can be used for both loose and mounted diamonds of all sizes and shapes in the D–Z colour range. It separates natural from laboratory-grown diamonds, as well as common diamond simulants. The unit is non-automated (requiring operator training) and is based on UV luminescence imaging and Raman and photoluminescence spectroscopy. For further information, or to request a demonstration, visit https://hrdantwerp.com/equipment/d-tect?language_content_entity=en. *CMS*

DiaColor Colorimeter from OGI Systems

OGI Systems Ltd (Ramat Gan, Israel) released two models of their DiaColor colorimeter in 2017: C-300 and C-1000. Both are designed to automatically measure the colour of rough diamonds in the D–Z range with about ½-colour-grade accuracy. The C-300 can accommodate samples weighing 0.30–300 ct, while the C-1000 can take diamonds up to 1,000 ct. The instrumentation reportedly can also indicate yellow and blue fluorescence, and detect diamonds that are type IIa (identifying those that are candidates for HPHT treatment), type IIb (blue or grey) and irradiated blue. Visit www.ogisystems.com/diacolor.html. *CMS*

Torcia 365 Long-wave LED Torch

During the June 2018 JCK Las Vegas show in Nevada, USA, the author obtained a new long-wave UV torch distributed by Mike Gray of Coast-to-Coast Rare Stones (Mendocino, California, USA). The flashlight, called the Torcia 365, is manufactured by Way Too Cool LLC (Glendale, Arizona, USA). The unit features a 3-watt Nichia 365 nm LED and a rechargeable battery. It produces a strong long-wave UV beam that can be used to check the fluorescence of a wide variety of gem materials. Its portable, battery-powered nature makes it useful for testing stones in the field (e.g. for quickly separating highly fluorescent stones such as ruby and spinel from non-fluorescent materials such as red garnet). Another potential application is checking for fracture fillings in emerald, as most emerald fillers show blue or yellow fluorescence. The author measured the flashlight's output with a spectrometer and confirmed it to be centred at approximately 368 nm (long-wave UV is 365 nm) with almost no visible-light component as a result of the unit's special filter. This waterproof flashlight is estimated to operate for approximately 1 hour per charge of the 18650 Li-ion battery. For more information, visit www.fluorescents.com/products-torcia.html.

Nathan D. Renfro FGA
Gemological Institute of America
Carlsbad, California
USA

NEWS AND PUBLICATIONS

Amberif 2017 and 2018 Conference Proceedings

Proceedings of conferences that took place during the 2017 and 2018 International Fair of Amber, Jewellery & Gemstones—Amberif—are available as free PDF files. The 42-page 2017 volume contains articles on 'amber personality' Wiesław Gierłowski, the origin of fossil resins, bio-inclusions in Burmese amber and the history of amber artefacts. The 167-page 2018 volume contains a much more extensive range of topics, including abstracts and full articles. The 2017 volume can be downloaded from http://tinyurl.com/y7u8k6u6 and the 2018 volume from http://tinyurl.com/y9ucpvxw. *CMS*

EGU General Assembly 2018 Gem Abstracts

Abstracts from the 8–13 April 2018 European Geosciences Union General Assembly in Vienna, Austria, are now available online. Of particular interest to gemmologists are poster presentations from the session 'Gem Materials: Properties and Genesis Processes', which can be viewed at https://meetingorganizer.copernicus.org/EGU2018/posters/27160. The abstracts cover a wide range of topics related to coloured stones. *CMS*

FTC's 'Jewelry Guides' Revised

In July 2018, the U.S. Federal Trade Commission (FTC) approved revision of its 'Jewelry Guides' (formerly 'Guides for the Jewelry, Precious Metals, and Pewter Industries'). The updated Guides incorporate public input invited with regard to specific topics since 2012. The revisions help align guidance with consumer expectations, and address technological and industry practice developments that affect nomenclature and terminology. Gem-specific revisions relate to 'composite gemstone products', 'varietals', 'cultured' diamonds, claims about synthetics, pearl treatment disclosures, use of the term 'gem', misleading illustrations and the definition of 'diamond'. For more information, and links to the full-text Guides, visit the FTC press release at www.ftc.gov/news-events/press-releases/2018/07/ftc-approves-final-revisions-jewelry-guides. *CMS*

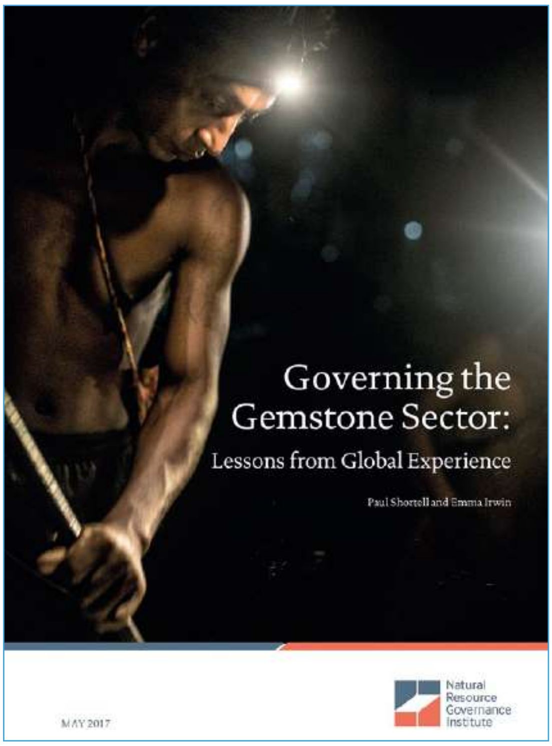

Governing the Gemstone Sector: Lessons from Global Experience

From the National Resource Governance Institute, this May 2017 report gathers and contextualises case studies on the management of gemstone resources and trade by governments of various gem-producing countries: Botswana, Brazil, Guyana, Madagascar, Myanmar, Pakistan, Sierra Leone, Sri Lanka, Tanzania, Thailand and Zambia. Topics cover citizen mining, modernisation of state-owned operations, fiscal terms, valuation processes, beneficiation, trade policies and accountability. To download the 72-page PDF, go to http://tinyurl.com/y9dt6xa8. *CMS*

GSJ 2018 Annual Meeting Abstracts

Abstracts of Special Lectures presented at the 2018 Annual Meeting of the Gemmological Society of Japan (held 9–10 June in Toyama, Japan) can now be accessed online. The 20 abstracts include a wide variety of topics on diamonds, coloured stones and cultured pearls. Downloadable PDFs are available (in Japanese and English) from www.jstage.jst.go.jp/browse/gsj/list/-char/en. *CMS*

PGI Insight 2018

Each issue of this publication from Platinum Guild International provides in-depth information on a focused topic regarding market trends in the platinum jewellery industry. The 2018 issue of *PGI Insight* addresses 'Rejuvenation of Platinum Jewellery in China'. The report opens by pointing out that China is the world's largest platinum jewellery market. However, demand has declined during the past four years. The report examines possible reasons for this decline and explores options to rebuild the market in China. The primary solution proposed is a change from weight-based to piece-based pricing. To download this and other PGI publications, visit http://platinumguild.com/research-publications/pgi-insight. *CMS*

Sapphires from Mogok, Myanmar

In June 2018, the Gemological Institute of America released a 56-page report titled 'Characterization of Blue Sapphires from the Mogok Stone Tract, Mandalay Region, Burma (Myanmar)'. It includes photos of mining areas and internal features in the sapphires, as well as UV-Vis-NIR and FTIR spectra and chemical data. The study concludes that a combination of features appear promising to identify the origin of Burmese sapphires. Download the report at http://tinyurl.com/y7d7h37l. *CMS*

Wooshin Gem Lab Magazine Vol. 5 2018

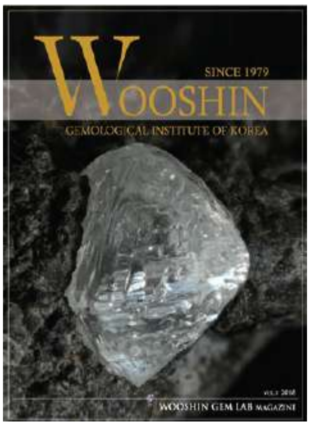

The 2018 issue of this publication from the Wooshin Gemological Institute of Korea is now available online in both Korean and English. Included are articles on the isotopic signatures of gem materials, the iridescence of mother-of-pearl, anorthite with uvarovite inclusions, identification of melee-size cubic zirconia diamond simulants in a ring, Raman spectroscopy of serpentine from Iran, and a review of colour-change gemstones, along with recent Wooshin events. To download the PDF, visit www.wooshinlab.com/LabStory/Research/Read.wgk?ArticleID=212, click the blue button, and select '2018WGK_EN.pdf'. *CMS*

OTHER RESOURCES

Yellow Diamonds Educational Video

In June 2018, the Natural Color Diamond Association (NCDIA) announced its first educational video, 'Natural Yellow Diamonds.' The 30-minute video is designed to appeal to both consumers and trade members. It covers the causes of yellow colour in diamond, range of colour, geographic origins, differences between natural and synthetic samples, comparison to other yellow gems, and more. The goal is to improve communication between consumers and trade professionals, as well as promote industry growth of affordable diamond jewellery. To order the video (US$100.00), visit https://ncdia.com/education. *CMS*

NCDIA NATURAL COLOR DIAMOND ASSOCIATION

MISCELLANEOUS

Call for Papers: Gem Issue of *The Extractive Industries and Society*

A special issue of *The Extractive Industries and Society* will focus on 'Gemstones: Perspectives and Trends in Mining, Processing and Trade of Precious Stones'. The goal is to attract papers from a broad range of contributors and disciplines associated with the production and trade of gem materials. The deadline to submit full papers is 1 December 2018. Authors will be notified of acceptance or rejection by 1 March 2019, and publication will occur in early 2019. For author guidelines, topic suggestions and a link to submit papers, visit http://tinyurl.com/yaw5e9qb. *CMS*

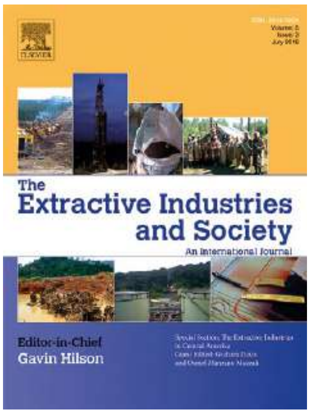

What's New provides announcements of new instruments/technology, publications, online resources and more. Inclusion in What's New does not imply recommendation or endorsement by Gem-A. Entries were prepared by Carol M. Stockton (CMS) or Brendan M. Laurs (BML), unless otherwise noted.

Diamond Museum Opens in Botswana

In March 2018, the Adrian Gale Diamond Museum opened in northern Botswana at Debswana's Orapa diamond mine. The museum is named after the late Dr Adrian Gale, who was general manager at the Orapa, Letlhakane and Damtshaa mines during 2012–2015. The museum showcases the discovery of diamonds in Botswana (in Orapa in 1967, a year after Botswana became independent from Britain), which have played an important role in the economic development of the country.

The museum is divided into two parts—a permanent and a temporary exhibition hall—with the latter to be developed in the future. The storyline follows six key thematic areas comprising: Introduction, The Formation of Earth and Geology, Diamond Prospecting and Exploration, Diamond Mining, Diamond Ore Processing, and Processing of the Final Diamonds. To visit, contact Debswana Corporate Affairs at Orapa by emailing kpilane@debswana.bw.

Mike Brook
Debswana, Gaborone, Botswana

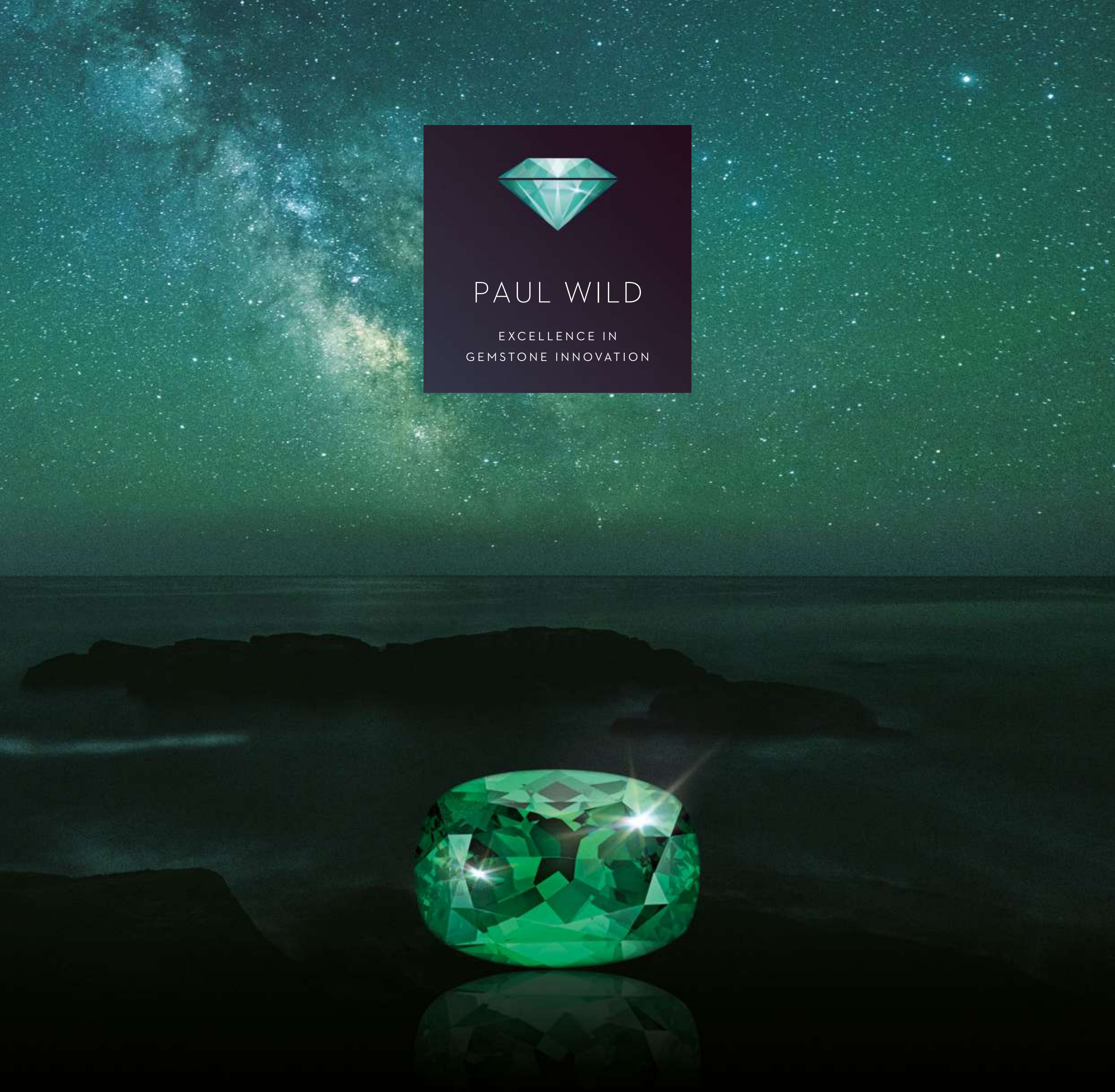
PAUL WILD
EXCELLENCE IN
GEMSTONE INNOVATION

Gem Notes

COLOURED STONES

Ametrine with Trapiche-like Patterns from Brazil

Ametrine is colour-zoned amethyst-citrine that is commercially known from only two deposits (approximately 50 km apart), which are both located in Bolivia (Vasconcelos et al., 1994; Laurs, 2010). It was with considerable interest, therefore, when ametrine reportedly from a new locality—Minas Gerais, Brazil—appeared at the February 2018 gem shows in Tucson, Arizona, USA. The stones were displayed by Dr Marco Campos Venuti (Seville, Spain), who obtained the rough material during the August 2017 Feira Internacional de Pedras Preciosas (FIPP) gem show in Teófilo Otoni, Brazil. The quartz crystals displayed corroded pyramidal terminations and commonly formed flared individuals that were bounded by irregular surfaces (i.e. contact points with adjacent crystals). Viewed in reflected light, they appeared mostly grey with central areas containing some amethyst (Figure 1, left). In transmitted light, the central portion of the crystals displayed a combination of amethyst and citrine colouration, while both the base and termination areas appeared very dark (Figure 1, right). Clearly, it was necessary to cut and polish these crystals before their inner beauty could be appreciated.

From approximately 400 kg of rough, Dr Campos Venuti cut about 36,000 carats of polished tablets and cabochons in various shapes up to 43 mm in maximum dimension. To best show their zoning patterns, the stones were oriented so that they are viewed down the c-axis. Those cut from the central part of the crystals displayed various colour-zoned patterns of amethyst and citrine (Figure 2, top left). Compared to ametrine from Bolivia, the colours were less saturated and the stones contained more abundant inclusions (mostly parallel bundles of feathers and veils, as well as black particles and filaments). More striking in appearance were stones cut from the dark area toward the base of the crystals. These showed patterned black cores of various size that were surrounded by amethyst-citrine zones, or in some cases the stones were cut entirely from the black areas of the crystals (again, see Figure 2). The black colour was due to dense networks of radiating inclusions that commonly formed segments which were separated by six radiating arms of clear quartz. Such spoked patterns are typical of the trapiche structure exhibited by some

Figure 1: The rough ametrine from Brazil typically consists of flared pieces that are bounded by corroded pyramidal terminations and appear mostly grey in reflected light (left). Transmitted illumination shows a central portion that displays a combination of amethyst and citrine colouration, with adjacent dark areas at the base and termination (right). Photos courtesy of Marco Campos Venuti.

Figure 2: These cabochons of trapiche-like quartz from Brazil show various patterns created by the amethyst-citrine colour zones and/or areas containing abundant black inclusions. The stones range from 15.5 × 11.7 mm to 21.3 × 15.9 mm. Gift of Marco Campos Venuti; photo by Jeff Scovil.

gem materials. However, rather than having transparent sectors separated by inclusion-rich arms, the black areas of this quartz consisted of included sectors that were separated by spokes of transparent quartz.

Sun et al. (2018) recently examined similar stones from Brazil (which they described as amethyst, rather than ametrine), and using Raman spectroscopy they identified the black inclusions as an iron sulfide mineral, likely pyrite. They also documented tiny brownish bullet-shaped inclusions in the arms of the trapiche-like structure that could not be identified but were probably goethite. The latter inclusions were only barely present in just one of the samples examined.

Brendan M. Laurs FGA

References

Laurs B.M., 2010. Gem News International: Update on ametrine from the Yuruty mine, Bolivia. *Gems & Gemology*, **46**(1), 58–59.

Sun Z., Muyal J. and Hand D., 2018. Gem News International: Trapiche-like amethyst from Brazil. *Gems & Gemology*, **54**(2), 237–238.

Vasconcelos P.M., Wenk H.-R. and Rossman G.R., 1994. The Anahí ametrine mine, Bolivia. *Gems & Gemology*, **30**(1), 4–23, http://doi.org/10.5741/gems.30.1.4.

Hessonite from Mogok, Myanmar

At the February 2018 gem shows in Tucson, Arizona, USA, gem cutter Meg Berry (Megagem, Fallbrook, California, USA) obtained some faceted garnets that were reportedly from a new occurrence in Mogok, Myanmar. The parcel consisted of 12 'native-cut' rectangular cushion-shaped gems. According to her supplier (Sai Tit of Cleopatra Gems, Chiang Rai, Thailand), who specialises in Burmese minerals, the stones came from the Lae Oo mine. This may be the same as the 'Le-U' mining area that was described by Themelis (2008) as lying below the well-known Dattaw deposit. According to Themelis (2008), Le-U has produced ruby, bicoloured tourmaline, moonstone, quartz, topaz, danburite and spinel (no garnet was listed), and the mines there were closed in 2001.

Eight of the stones were loaned to authors CW and BW for characterisation, weighing 0.68–1.14 ct (total weight 7.05 carats). Their colour ranged from light-to-medium 'golden' brown (Figure 3). Their RIs spanned from 1.740 to 1.748, with no consistent variation according to their tone. Due to the rather small size of the stones, no hydrostatic SG measurements were taken.

Figure 3: These garnets (0.68–0.99 ct) from Mogok, Myanmar, were identified as hessonite. Photo by Dean Brennan, Stone Group Laboratories.

The GemmoRaman-532SG identified all of them as grossular, and their colouration was fairly consistent with the hessonite variety. Energy-dispersive X-ray fluorescence (EDXRF) chemical analysis with an Amptek X123-SDD spectrometer revealed the expected high levels of Ca and Fe, with minor Mn, Ti and Cr. All samples were inert to long- and short-wave UV radiation, and exhibited some magnetic susceptibility (being just barely dragged by a magnet).

Viewed in the microscope between crossed polarisers, all of the stones exhibited various patterns of bright interference colours (Figure 4). This optical effect may

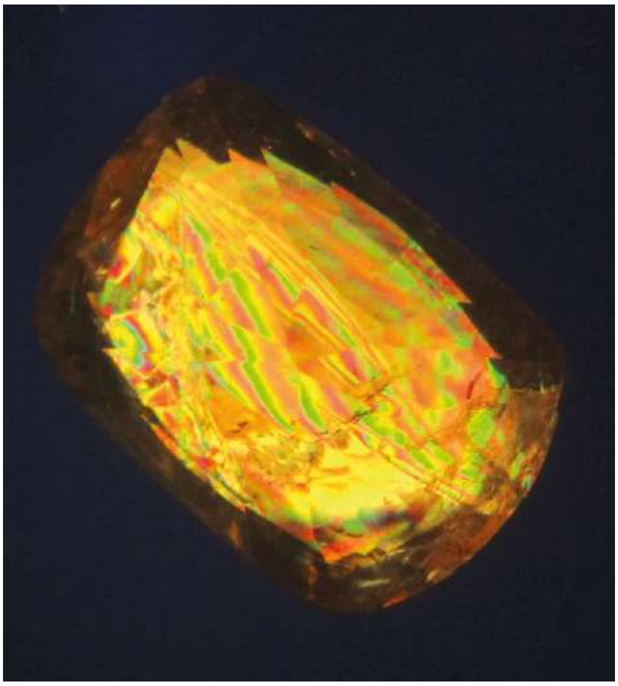

Figure 4: Viewed between crossed polarisers, this 1.14 ct hessonite displays bright interference colours. Photomicrograph by B. Williams.

Figure 5: Internal features in the hessonite consisted of (**a**) various fluid-filled inclusions hosted by partially healed fissures, (**b**) fluid-filled growth tubes and (**c**) an overall haziness in one stone. Photomicrographs by C. Williams; magnified 25× (a) and 40× (b and c).

have been caused by variously oriented twin planes (and associated internal strain) that were prevalent throughout the samples. The stones were moderately included to the unaided eye. The most common internal features were intricate, fluid-filled, partially healed fissures (Figure 5a). Several samples also exhibited a slightly roiled optical effect that was weaker than that typically seen in hessonite. In addition, fluid-filled growth tubes were common (Figure 5b). Similarly oriented, but non-parallel, growth lines were also seen. A hazy area was observed in one sample (Figure 5c).

According to Themelis (2008), facetable hessonite is often found in the Mogok area, particularly around Sakangyi, as crystals that commonly weigh 1–2 ct. The apatite inclusions that he mentioned occurring in the hessonite were not seen in the samples examined here.

Cara Williams FGA and Bear Williams FGA
(info@stonegrouplabs.com)
Stone Group Laboratories
Jefferson City, Missouri, USA

Brendan M. Laurs FGA

Reference

Themelis T., 2008. *Gems and Mines of Mogok*. Self-published, Bangkok, Thailand, 352 pp.

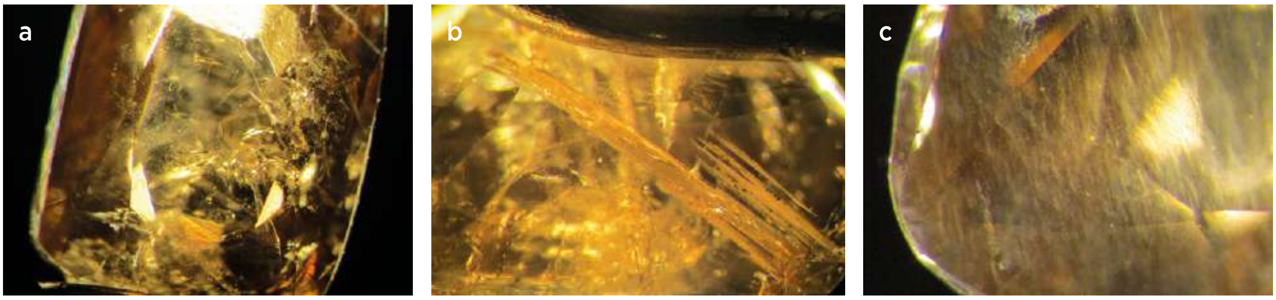

Yellowish Green to Yellow Opal from Brazil

Several occurrences and varieties of opal are known from Brazil (for a brief review, see Caucia et al., 2009). During the August 2017 FIPP gem show in Teófilo Otoni, Brazil, a purportedly new discovery of yellowish green to yellow ‘common’ opal (e.g. Figure 6) was brought to market by some artisanal miners. They had ~5 kg of rough material, which was purchased by gem and mineral dealer Dr Marco Campos Venuti. He polished dozens of cabochons and tablets in a variety

Figure 6: These cabochons (1.89–6.35 ct) show the range of colour in a new find of common opal from Brazil. Gift of Marco Campos Venuti; photo by Diego Sanchez, © GIA.

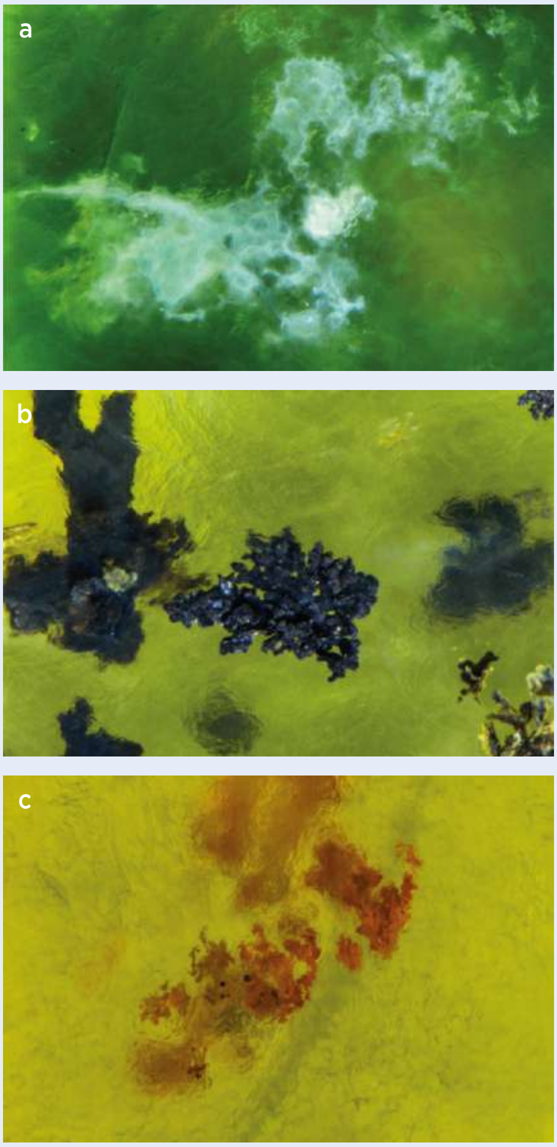

Figure 7: The yellowish green opal from Brazil contained distinct white clouds (**a**, image width 2.4 mm). Also present in the Brazilian opals were black plumes (**b**, image width 1.6 mm) and brown aggregates (**c**, image width 1.9 mm), which probably consist of manganese oxide and hematite, respectively. Photomicrographs by N. D. Renfro, © GIA.

of shapes that ranged from 5 to 20 mm in maximum dimension. He kindly donated three specimens to Gem-A's research and teaching collection that showed the range of colour for this new material (1.89–6.35 ct; again, see Figure 6).

Examination of the three stones by author NDR showed properties consistent with opal (spot RI of 1.44 and hydrostatic SG of 2.10). All three samples fluoresced a very weak red to orange to both long- and short-wave UV radiation. They were semi-transparent, and various inclusions were easily visible to the unaided eye. Viewed with the microscope, all three opals showed abundant swirl marks (Figure 7), similar to those documented in yellow opal from West Africa (Moe, 2012). The yellowish green stone contained some white clouds (Figure 7a), and Raman analysis of one such dense white area was inconclusive, giving only a weak signal consistent with quartz. Also present in the samples were irregular black and/or brown aggregates (Figures 7b and 7c). Unfortunately, no discernible signals could be obtained for these inclusions using Raman spectroscopy.

EDXRF analysis of the opals showed strong peaks for Ni, Fe and Cr. It is well known that Ni is involved with producing green colouration in silica minerals (Rossman, 1994) such as 'prase' opal, and Fe causes a yellow-to-brown body colour in common opal (Gaillou et al., 2008). Where black inclusions were present in our opal samples, EDXRF spectroscopy showed Mn in addition to Ni and Fe; this is consistent with their appearance as manganese oxide plumes. Where brown inclusions were present, EDXRF analysis showed only Fe and Ni. This suggests that the brown inclusions are likely hematite. The hematite inclusions were randomly scattered throughout the opal matrix, and therefore they may have been incorporated during its formation. Conversely, the black manganese oxide plumes were generally confined to specific linear or interconnected areas, indicating that they may have been introduced during a secondary process of cracking and re-healing of the opal.

Brendan M. Laurs FGA

Nathan D. Renfro FGA
Gemological Institute of America
Carlsbad, California, USA

References

Caucia F., Ghisoli C. and Adamo I., 2009. A study on the characteristics of some C- and CT-opals from Brazil. *Neues Jahrbuch für Mineralogie, Abhandlungen*, **185**(3), 289–296, http://doi.org/10.1127/0077-7757/2009/0125.

Gaillou E., Delaunay A., Rondeau B., Bouhnik-le-Coz M., Fritsch E., Cornen G. and Monnier C., 2008. The geochemistry of gem opals as evidence of their origin. *Ore Geology Reviews*, **34**(1–2), 113–126, http://doi.org/10.1016/j.oregeorev.2007.07.004.

Moe K.S., 2012. Gem News International: Yellow opal from West Africa. *Gems & Gemology*, **48**(3), 226–228.

Rossman G.R., 1994. Colored varieties of the silica minerals. In P.J. Heaney, C.T. Prewitt and G.V. Gibbs, Eds., *Silica—Physical Behavior, Geochemistry and Materials Applications*, Reviews in Mineralogy, Mineralogical Society of America, Chantilly, Virginia, USA, **29**, 433–467.

Ethiopian Opal with Dendritic Inclusions

Play-of-colour opal from Wollo Province, Ethiopia, has become well known in the gem trade since its discovery in early 2008. These opals were characterised in detail by Rondeau et al. (2010), who reported relatively few inclusion features in the stones they examined. Among these were cylindrical inclusions (most likely composed of chalcedony), dispersed micro-crystals of pyrite and, rarely, 'black minerals [that] were included in the body of the opal, filling fissures or forming dendrites' (Rondeau et al., 2010, p. 100).

Recently, an Ethiopian (Wollo) opal containing some conspicuous black inclusions was loaned for examination by rough stone dealer Farooq Hashmi (Intimate Gems, Glen Cove, New York, USA). The 4.34 ct partially polished sample contained a series of well-formed black dendrites (Figure 8). Raman analysis by author NDR was unable to identify the inclusions, perhaps because the opal matrix degraded the signal so that it was not resolvable. Nevertheless, EDXRF spectroscopy confirmed that the inclusions were Mn rich, which is consistent with their being composed of manganese oxide (presumably pyrolusite).

Figure 8: This 4.34 ct partially polished sample of Ethiopian opal contains eye-visible black inclusions. Photo by Robison McMurtry © GIA.

Rather than forming two-dimensional dendrites like those commonly seen in some gem materials as epigenetic fillings along fissures, the inclusions in this Ethiopian opal occurred as three-dimensional plumes that radiated in various directions (Figure 9). One set of plumes formed along an elongate structure that was reminiscent of a plant fossil, such as those documented in Wollo opal by Chauviré et al. (2017).

Brendan M. Laurs FGA *and*
Nathan D. Renfro FGA

References

Chauviré B., Rondeau B., Mazzero F., and Ayalew D., 2017. The precious opal deposit at Wegel Tena, Ethiopia: Formation via successive pedogenesis events. *Canadian Mineralogist*, **55**(4), 701–823, http://doi.org/10.3749/canmin.1700010.

Rondeau B., Fritsch E., Mazzero F., Gauthier J.-P., Cenki-Tok B., Bekele E. and Gaillou E., 2010. Play-of-color opal from Wegel Tena, Wollo Province, Ethiopia. *Gems & Gemology*, **46**(2), 90–105, http://doi.org/10.5741/gems.46.2.90.

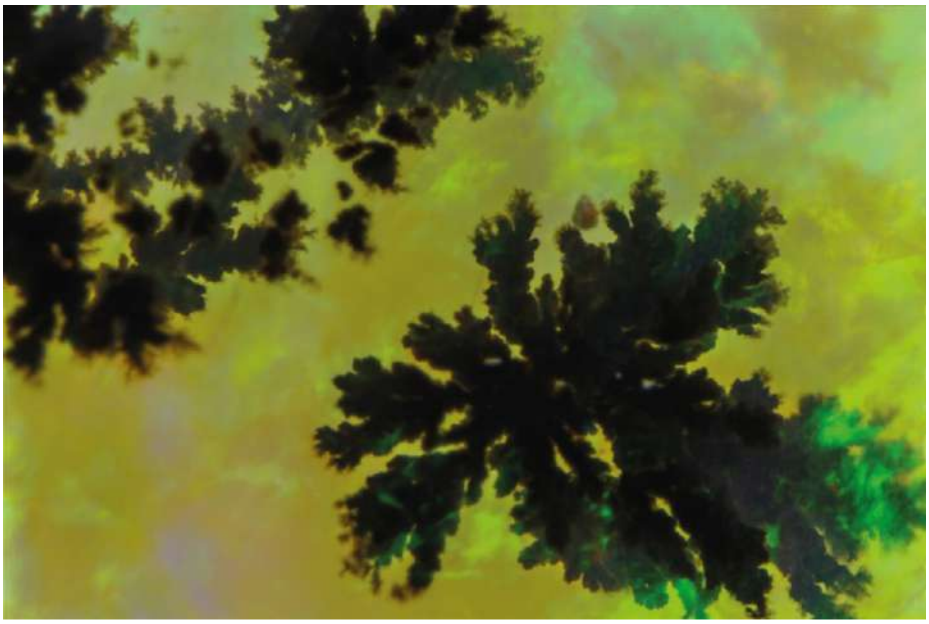

Figure 9: A closer view of the black inclusions shows a three-dimensional array of dendrites. Their Mn-rich composition is consistent with a manganese oxide mineral such as pyrolusite. Photomicrograph by N. D. Renfro, © GIA; image width 3.6 mm.

Figure 10: A 203.41 ct phenakite from Madagascar is shown together with another large phenakite (105.74 ct) that reportedly came from the Anjanabonoina pegmatite. Both stones were obtained by Dudley Blauwet, although the smaller gem was purchased significantly earlier (June 2014) than the larger one (November 2017). Photo by Jeff Scovil.

Large Phenakite from Madagascar

Madagascar is known as a source of fine-quality crystals of colourless phenakite (e.g. Wilson, 1989). The main source is the Anjanabonoina pegmatite in central Madagascar, which occasionally produces large crystals, such as 'a rather flattened, doubly terminated, fully transparent gem crystal weighing 1.1 kg' that was mentioned by Weiss (1995). As Malagasy phenakite crystals tend to be well formed, most of them are sold to mineral collectors rather than as gem rough.

Recently, however, Dudley Blauwet (Dudley Blauwet Gems, Louisville, Colorado, USA) obtained a large faceted phenakite from Madagascar that weighed 203.41 ct (Figure 10). He obtained the stone in Sri Lanka in November 2017, and his supplier reported that the original rough weighed 500 ct and was purchased in Mananjary on Madagascar's east coast.

Although phenakite is known to occur in phlogopite schist at the Ambodivandrika emerald mine in the Mananjary area (www.mindat.org/loc-45813.html), the large size and high clarity of the stone obtained by Blauwet strongly suggest that it came from a pegmatite deposit. In addition to Anjanabonoina, there are at least three other phenakite occurrences in Madagascar that are potential sources of large, gem-quality material, according to Frédéric Gautier (Little Big Stone, Antananarivo, Madagascar). One of these localities (Fianarantsoa area) produced several hundred grams of transparent phenakite in 2017 and continues to produce rough material. Since these pieces typically do not show any crystal faces, it seems likely that they would be sold as gem rough.

Brendan M. Laurs FGA

References

Weiss J.-P., 1995. Notes from Madagascar. *Mineralogical Record*, **26**(6), 579.

Wilson W.E., 1989. The Anjanabonoina pegmatite, Madagascar. *Mineralogical Record*, **20**(3), 191–200.

Recent Production of Poudretteite from Mogok, Myanmar

Poudretteite is an extremely rare borosilicate ($KNa_2B_3Si_{12}O_{30}$), and faceted examples are seldom encountered (cf. Smith et al., 2003; Mayerson, 2006). According to Dr Kyaw Thu (Macle Gem Trade Laboratory, Yangon, Myanmar), recently there were two new poudretteite discoveries in the Mogok area of Myanmar (e.g. Figure 11). First, an alluvial concentration of poudretteite was found by a miner looking for yellow danburite across the valley from Pein Pyit. Most of the rough material was colourless and had rough surfaces. Exactly when it was found and how much was produced is unclear. Then, in March 2018, a group of miners began working an area at Pyant Gyi (located in eastern Mogok, near Pein Pyit; Figure 12) and found both *in situ* and eroded poudretteite. This is the first time that a primary deposit of poudretteite has been found in Mogok.

Figure 11: This fine 2.6 g poudretteite crystal was mined from a newly discovered primary deposit in the Pyant Gyi area of Mogok. Photo by Thai Lanka Trading.

Figure 12: Local miners work the Pyant Gyi area of Mogok in search of poudretteite and other minerals. Photo by Kyaw Thu.

Pyant Gyi is a flat plain, and the *in situ* poudretteite was apparently found on the hill above it. The Pyant Gyi area was already a known source of alluvial poudretteite, and it also hosts primary and secondary deposits of spinel, ruby and sapphire, as well as rarer gems such as johachidolite and hackmanite (Themelis, 2008).

The recent mining has yielded a small quantity of poudretteite as broken pieces, well-formed crystals, and crude matrix specimens with smoky quartz. The best crystal known to author MHS is a 2.6 g bicoloured (colourless-pink) specimen that he purchased in May 2018 (again, see Figure 11). Most of the recently produced poudretteite is of low quality, being quite included with hollow tubes. The majority of the material is colourless with a pink 'skin' that is usually lost in faceting. The largest cut stone seen by author MHS weighed 9.59 ct but was heavily included and poorly cut. Some lightly included stones weighing more than 3 ct were obtained by this author, but after recutting to proper angles most of them weighed <2 ct. The faceted stones range from colourless to pink, or may display both colourless and pink areas (e.g. Figure 13). It is extremely rare to encounter a pure pink poudretteite that is nearly eye clean and >1 ct.

The total production of all grades of poudretteite from Pyant Gyi since March 2018 is estimated by Dr Kyaw Thu to be only about 100 g, so poudretteite remains a very rare gem material despite these recent discoveries.

Mark H. Smith (marksmithbkk@gmail.com)
Thai Lanka Trading Ltd Part.
Bangkok, Thailand

Brendan M Laurs FGA

References

Mayerson W.M., 2006. Lab Notes: Poudretteite. *Gems & Gemology*, **42**(4), 265–266.

Smith C.P., Bosshart G., Graeser S., Hänni H., Günther D., Hametner K. and Gübelin E.J., 2003. Poudretteite: A rare gem species from the Mogok Valley. *Gems & Gemology*, **39**(1), 24–31, http://doi.org/10.5741/gems.39.1.24.

Themelis T., 2008. *Gems and Mines of Mogok*. Self-published, Bangkok, Thailand, 352 pages.

Figure 13: Recent poudretteite production from Pyant Gyi ranges from colourless (**a**: 1.06 carats total weight) to pink (**b**: 0.73 ct), and some stones may show colourless/pink zones (**c**: 2.48 ct). Photos by Thai Lanka Trading.

Gem-quality Pseudomalachite from Slovakia

Pseudomalachite [$Cu_5(PO_4)_2(OH)_4$] is a mineral species named for its similarity in appearance to malachite [$Cu_2(CO_3)(OH)_2$]. There exist a number of dark green copper-phosphate minerals, including pseudomalachite and its polymorphs reichenbachite and ludjibaite (Hyršl, 1991). Before 1950 it was thought that dihydrite, lunnite, ehlite, tagilite and prasin were separate mineral species, but they all were found to be pseudomalachite (Berry, 1950). Compared to malachite, the much rarer pseudomalachite typically lacks pronounced light and dark banding and is slightly harder and denser. To verify an identification, pseudomalachite will not react to warm hydrochloric acid, while malachite will effervesce.

Pseudomalachite occurs as a secondary mineral in the oxidised zone of copper deposits. It usually forms botryoidal crusts and hemispherical aggregates of microscopic crystals. It also occurs as reniform, botryoidal or massive aggregates with a radial-fibrous structure and concentric banding in which the fibres are elongated, foliated and microcrystalline, or dense and colloform. Pseudomalachite is known from Slovakia as well as several other localities (e.g. Portugal, Namibia, Poland, Zambia, Chile, Germany and Australia).

The small region around the central Slovakian municipality of L'ubietová in the Banská Bystrica region has a rich mining history that dates back to the 14th century. There are three small copper deposits near L'ubietová called Podlipa, Svätodušná and Kolba (Luptáková et al., 2016). Extensive dumps as well as some accessible parts of the old mines are of interest to scientists and mineral collectors. The Podlipa deposit is situated in the Vepor Mountains of central Slovakia, about 1 km east of L'ubietová village, on the southern slope of the Carpathian mountain of Vysoká (995.5 m) above Zelená dolina (Green Valley). Podlipa is the type locality for libethenite (Breithaupt, 1823) and mrázekite (Řídkošil et al., 1992), and also hosts other rare minerals such as ludjibaite and reichenbachite (Hyršl, 1991).

Thin crusts of pseudomalachite are commonly found at all three of the Slovakian localities mentioned above. However, in 2016–2017 some gem-quality material was discovered in this area by author RG that consisted of coarser layers of relatively pure pseudomalachite that could be cut into cabochons without any accompanying matrix material. After separating these layers from the host rock, approximately 200 g of rough material was produced during the most recent mining activities. We polished 15 high-quality cabochons (e.g. Figure 14), ranging from 13.33 × 10.74 mm to 20.61 × 15.56 mm, and also cut a few dozen lower-quality cabochons of various shapes. The samples appeared greenish blue in daylight (again, see Figure 14) and green in incandescent light. They had RIs of 1.624–1.689 and hydrostatic SG values of 3.93–4.17. Their identity as pseudomalachite was confirmed by Raman spectroscopy, which showed peaks at 1084, 1055, 1004, 964, 886, 795, 748, 544, 482, 443, 364, 302 and 269 cm^{-1}.

Figure 14: These pseudomalachite cabochons (21.59–34.80 ct) are from the Ľubietová area in the Banská Bystrica region of central Slovakia. Photo by J. Štubňa.

Thin crusts of pseudomalachite combined with quartz and limonite matrix have been used by local Slovakian jewellers for a long time. The future potential for obtaining thicker, pure layers of gem-quality pseudomalachite from this area is unknown, as the site is not mined on a regular basis or with mechanised methods.

Dr Ján Štubňa (janstubna@gmail.com), Dr L'udmila Illášová and Radovan Galád Gemmological Institute, Constantine the Philosopher University, Nitra, Slovakia

Dr Radek Hanus Gemological Laboratory of e-gems.cz Prague, Czech Republic

References

Berry L.G., 1950. On pseudomalachite and cornetite. *American Mineralogist*, **5**(2), 365–385.

Breithaupt J.F.A., 1823. *Vollständige Charakteristik des Mineral-Systems*. Arnoldischen Buchhandlung, Dresden, Germany, 292 pp.

Hyršl J., 1991. Three polymorphs of $Cu_5(PO_4)_2(OH)$ from Ľubietová, Czechoslovakia. *Neues Jahrbuch für Mineralogie, Monatshefte*, **6**, 281–287.

Luptáková J., Milovská S., Jeleň S., Mikuš T., Milovský R. and Biroň A., 2016. Primary Cu ore mineralization at the Ľubietová-Podlipa locality (Slovakia). *Acta Geologica Slovaca*, **8**(2), 175–194.

Řídkošil T., Šrein V., Fábry J., Hybler J. and Maximov B.A., 1992. Mrázekite $Bi_2Cu_3(OH)_2O_2(PO_4)_2 \cdot 2H_2O$, a new mineral species, and its crystal structure. *Canadian Mineralogist*, **30**(1), 215–224.

Figure 15: These quartz slices (3.7 and 4.0 cm tall) from Madagascar contain attractive patterns created by amethystine colour zoning and oriented inclusions. Photo by Diego Sanchez, © GIA.

Quartz Slices from Madagascar with Interesting Inclusions

During the February 2018 Tucson gem shows, Madagascar mineral dealer Frédéric Gautier had some new quartz specimens containing attractive inclusion patterns. He reported that the rough material was found in August 2017 in the Mandritsara District (in former Mahajanga or Majunga Province) of north-central Madagascar. The exterior faces of the crystals were rather crudely developed, and to best show their internal beauty Gautier prepared polished slices from the larger crystals. Of the approximately 10 kg of quartz that he purchased, only about 4–5 kg were large enough to cut into attractive slices. From six crystals he obtained 25 slices measuring 1.5 to 5.0 cm across, which showed attractive 'phantoms' formed by a combination of inclusions and amethystine colour zoning. The slices were oriented perpendicular to the c-axis, and their edges (parallel to the prism faces) were also cut and polished.

Gautier loaned two samples of the quartz for examination (3.7 and 4.0 cm tall; Figure 15). Their cores contained distinct amethystine zones, and one of them also had an additional area of amethyst positioned between the core and the rim, together with some planar smoky zones that were parallel to two adjacent prism faces. Both slices contained abundant fluid inclusions and linear arrays of brownish red to black inclusions that extended toward the prism faces (e.g. Figure 16). Flat 'sheets' of the brownish red inclusions were also present in the amethyst zones. Based on their colour and appearance, both the linear and sheet-like inclusions consisted of hematite (sometimes referred to in the literature as 'lepidocrocite'). Primary fluid inclusions formed along growth zones as minute parallel aggregates or large conspicuous cavities. In addition, secondary fluid inclusions formed veils of particles along partially healed fractures.

The combination of the amethystine colour zoning and oriented inclusions made these slices both attractive and unusual. According to Gautier, this is the first time that quartz with this distinctive appearance has come from Madagascar.

Brendan M. Laurs FGA and Nathan D. Renfro FGA

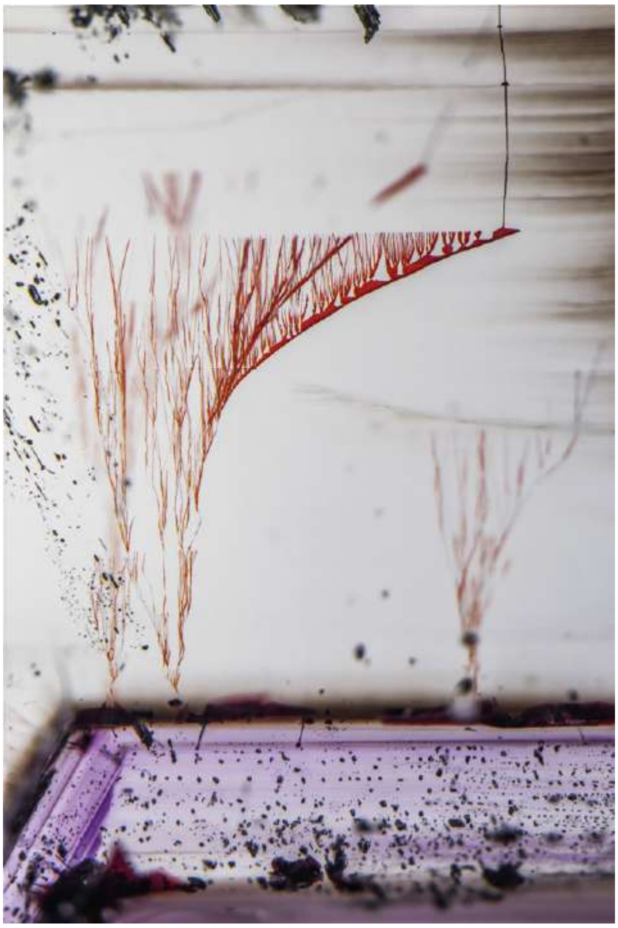

Figure 16: A closer view of one of the quartz slices shows a curved array of sub-parallel brownish red inclusions of hematite that abruptly end along a plane parallel to a prism face. In the underlying amethystine zone are planes of primary fluid inclusions that appear black in the brightfield lighting used to capture this image. Photomicrograph by N. D. Renfro, © GIA; image height 8.9 mm.

Red Aventurescent Quartzite from Tanzania

At the September 2016 Denver Gem & Mineral Show in Denver, Colorado, USA, red aventurescent quartzite from a new find in Tanzania was introduced to the USA market. According to Jonathan Bartky (Ariel Treasures, Livingston, New Jersey, USA), the material—also called 'Cherry Tanzurine' or 'Natural Cherry Quartz'—is mined in a joint venture on Maasai tribal land in northern Tanzania. Mining has been ongoing since early 2016. The material is extracted from an open pit using pneumatic hammers and hand tools but no explosives. Approximately 20 tonnes have been recovered so far, and about one tonne has been cut and polished into spheres and bookends (in Tanzania), beads (in Germany and India), pendants (in China) and eggs (in Germany). The first polished material was exhibited at the February 2017 Tucson gem shows (e.g. Figure 17).

Also debuting at the September 2016 Denver gem shows was a new green aventurescent quartzite from Tanzania (Stephan et al., 2018; White and Dickson, 2018). This material, coloured by inclusions of fuchsite (as in 'classic' green aventurine quartz), has some similarities to the red aventurescent quartzite. Recently, White and Dickson (2018) described the red material as quartzite of metamorphic origin that is coloured by pink-to-red mica inclusions. Based on SEM-EDS analyses, these authors reported that the inclusions are most likely lepidolite but possibly Mn-bearing muscovite.

For our investigations, we examined two pieces of rough red adventurescent quartzite (42.29 and 13.19 g), a polished egg (765 ct) and a beaded strand (with beads measuring ~10 mm in diameter), which were offered by the company Impexco (Idar-Oberstein, Germany). Wolfgang Weinz from Impexco received the material from a local Tanzanian miner and dealer in Dar es Salaam, Tanzania. One of the rough pieces was polished on both sides, and the other was used to prepare thin sections. For comparison we examined two tumbled pieces of red quartzite, one from India (196.86 ct) and one from South Africa (36.06 ct), from which thin sections were also prepared.

The rough and polished samples from Tanzania were translucent in smaller sizes (i.e. the beads and the smaller piece of rough), but appeared predominantly less translucent in larger sizes. Macroscopically it was obvious that the material was an aggregate of grains up to 10 mm in diameter, and it was coloured by pink-to-red inclusions. The polariscope gave a doubly refractive aggregate reaction, and RI and hydrostatic SG values

Figure 17: These bead necklaces (6–10 mm in diameter) and earrings (approximately 30 mm in diameter) are typical of the new red aventurescent quartzite from Tanzania. Photo by Jeff Scovil.

were consistent with quartz: n_o = 1.543, n_e = 1.552, birefringence = 0.009 and SG = 2.65. With magnification (Figure 18a), the inclusions were seen to have the same round, partially pseudo-hexagonal, platy shape as reported for the fuchsite grains in the green aventurescent quartzite from Tanzania (cf. Stephan et al., 2018).

Analysis of the pink-to-red inclusions with a Renishaw inVia micro-Raman spectrometer identified them as mica. A further comparison with reference spectra obtained from our database, and from muscovite and lepidolite samples in the collection of the German Gemmological Association, showed that the Raman spectra provided the closest match with muscovite. Nevertheless, both muscovite and lepidolite can have pink-to-red colouration caused by Mn^{3+} substituting for Al^{3+}, and to confirm our identification we performed X-ray powder diffraction. With these results, we were able to exclude lepidolite and identify the mica inclusions as most probably muscovite. The presence of muscovite inclusions in this quartzite is also consistent with the

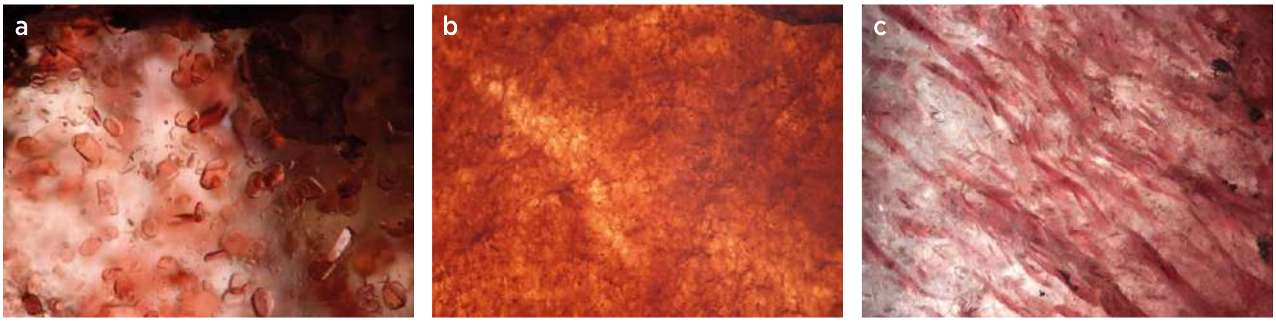

Figure 18: Polished slices of various types of red quartzite are viewed here in transmitted light. (**a**) The red aventurescent quartzite from Tanzania is coloured by muscovite inclusions. (**b**) In quartzite from India, the individual quartz grains are surrounded by thin films of hematite. (**c**) Quartzite from South Africa is also coloured by hematite, which forms platy, pink-to-red flecks oriented in one direction. Photomicrographs by T. Stephan; image widths 3.15, 7.14 and 3.32 mm, respectively.

material's geological occurrence, whereas lepidolite (a member of the polylithionite-trilithionite series of lithium micas) is not known to occur in quartzite.

By contrast, the red quartzites from India and South Africa were found to be coloured by hematite. In the sample from India, thin films of hematite surrounded the individual quartz grains (Figure 18b). It therefore showed no aventurescence because it lacked any reflective inclusions. However, the hematite in the red quartzite from South Africa formed platy inclusions (Figure 18c) that were present between the quartz grains. The inclusions were also oriented in a consistent direction, which produced aventurescence and implies schistosity. Further differences between these red quartzites and the new material from Tanzania were seen in their grain sizes: the Indian and South African quartzites were generally fine-to-medium grained (0.06–2 mm), while the Tanzanian material had much coarser overall grain sizes of 1–10 mm (Figure 19); this is even coarser grained than the new green aventurescent quartzite from Tanzania (1–5 mm; Stephan et al., 2018). As in the green material, the micas in the red aventurescent quartzite from Tanzania form inclusions within the single quartz grains and are not present as accessory phases between the grain boundaries.

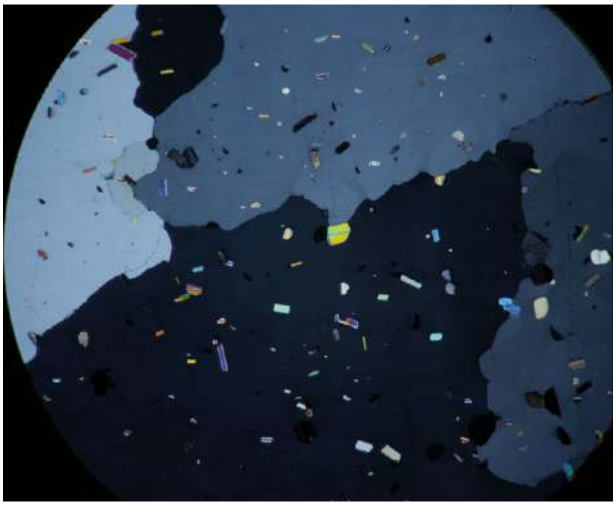

Figure 19: Viewed in cross-polarised light, a thin section of red aventurescent quartzite from Tanzania displays quartz grains with low-order grey-to-black interference colours, whereas the muscovite inclusions (up to 10 mm long) appear highly birefringent. The muscovite grains show no preferred orientation. Photomicrograph by T. Stephan; image width 8.14 mm.

Acknowledgements

The samples of the red aventurescent quartzite that were studied for this report were kindly donated by Impexco. One of the polished samples was loaned by Robert Myers. In addition, one slab and one polished lozenge were subsequently donated to Gem-A by Jonathan Bartky. We also thank Dr Tobias Häger (Institute for Gemstone Research, Johannes Gutenberg-University, Mainz, Germany) for performing the X-ray powder diffraction analysis.

Tom Stephan (t.stephan@dgemg.com),
Dr Ulrich Henn FGA and Fabian Schmitz
German Gemmological Association
Idar-Oberstein, Germany

Brendan M. Laurs FGA

References

Stephan T., Henn U., Schmitz F. and Laurs B.M., 2018. Gem Notes: Green aventurescent quartzite from a new find in Tanzania. *Journal of Gemmology*, **36**(2), 103–104.

White J.S. and Dickson L.D., 2018. Tanzurine, cherry-red and emerald-green quartz from Tanzania. *Rocks & Minerals*, **93**(3), 250–257, http://doi.org/10.1080/00357529.2018.1428863.

Yellow Scapolite from Tanzania Showing Peculiar Daylight Fluorescence

Yellow scapolite has been reported from two areas of Tanzania: the Umba area in the eastern part of the country (Zwaan, 1971) and in central Tanzania (Graziani and Gübelin, 1981). During the April 2016 Arusha Gem Fair in Tanzania, rough stone dealer Farooq Hashmi acquired a scapolite crystal that was reportedly found in Umba, and it was subsequently faceted by Peter Torraca (Torraca Gemcutting, Houghton, New York, USA). Due to the stone's unusual colour behaviour, it was loaned to author JCZ for further examination.

The cut-cornered rectangular modified brilliant (radiant cut) weighed 3.60 ct and measured approximately 10.93 × 7.13 × 6.83 mm. It was transparent, and when viewed in daylight-equivalent lighting it was slightly greenish yellow (Figure 20). In sunlight it appeared to turn to a purer, more vivid yellow, while peculiarly it looked slightly more orange in indirect sunlight (Figure 20, inset), particularly when tilted slightly.

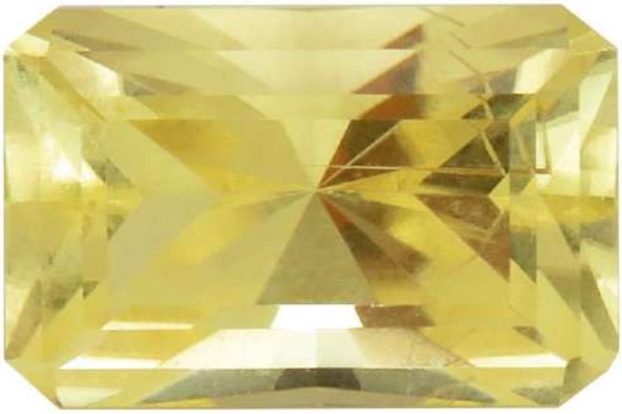

Figure 20: This 3.60 ct scapolite from Tanzania is slightly greenish yellow in daylight-equivalent lighting, but appears slightly more orange in indirect sunlight (right). Photos by Dirk van der Marel (main image) and B. M. Laurs (right).

RI readings gave 1.555–1.589, yielding a birefringence of 0.034, and the stone showed a uniaxial negative optic character. Hydrostatic measurements yielded an SG value of 2.73. The dichroscope revealed only weak dichroism, in slightly greenish yellow and yellow. The stone was free of inclusions except for one large, spiky, needle-like growth channel. This inclusion had a rhomb-shaped cross-section, and where it reached the surface it appeared to be filled with some secondary, fine-grained material. As shown in Figure 21, the stone luminesced a very strong yellow to long-wave (365 nm) and a moderate orangey yellow to short-wave (254 nm) UV radiation. In both cases, no phosphorescence was observed. A photoluminescence (PL) spectrum excited by a green (532 nm) laser showed a strong band centred at 620 nm in the orange-red region (Figure 22).

The RI and SG values, and especially the high birefringence, of this scapolite correspond to a meionite composition, which has RIs of 1.556–1.600, birefringence values of 0.024–0.037 and an SG of ~2.78 (Deer et al., 2004). Meionite ($Ca_4Al_6Si_6O_{24}CO_3$) is isomorphous with marialite ($Na_4Al_3Si_9O_{24}Cl$) in a series that constitutes 'scapolite'. There is an approximate linear variation between mean RI and scapolite composition (expressed as %Me or mol.% meionite), as well as between birefringence and %Me (Deer et al., 2004). Using the mean RI

Figure 21: The 3.60 ct scapolite fluoresces a very strong yellow under long-wave UV (left) and a moderate orangey yellow under short-wave UV radiation (right). Photos by J. C. Zwaan.

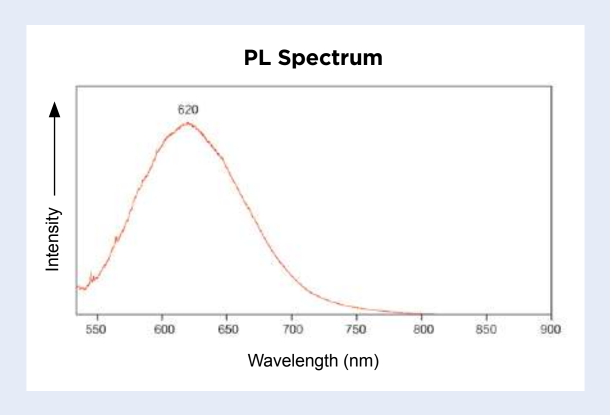

Figure 22: The yellow Tanzanian scapolite produced strong photoluminescence at 620 nm (orange-red region) when excited with a green (532 nm) laser. The small peaks on the left are Raman features.

$(\varepsilon+\omega)/2$ = 1.572 in the expression $(\varepsilon+\omega)/2$ = 1.5346 + 0.000507 %Me, the present scapolite is estimated to consist of 74 mol.% meionite. However, based on its high birefringence of 0.034, a composition of ~85 mol.% meionite would be expected. Thus, the stone's composition is inferred to be somewhere in the 74–85 mol.% meionite range.

Raman spectra most closely matched the spectra of meionite in the RRUFF database. Semi-quantitative EDXRF chemical analyses confirmed the dominance of Ca over Na, in accordance with a meionite composition, and also showed traces of sulphur (0.6 wt.% SO_3) and iron (0.03–0.04 wt.% FeO). In the mid-infrared spectrum, the presence of a sharp feature at ~2560 cm^{-1} confirmed the presence of HCO_3^- (an associated part of the scapolite crystal structure; Swayze and Clark, 1990) in the anion site.

Strong yellow fluorescence in scapolite is attributed to the presence of S_2^- in the anion site (Burgner et al., 1978), but as suggested by the PL spectrum (again, see Figure 22), the emission spectrum appears to be dependent on excitation wavelength. Burgner et al. (1978) also showed that the luminescence emission spectrum displays a series of distinct bands covering the region from 500 to 700 nm, which according to them indicates that S_2^- occupies a number of different sites. At room temperature and under long-wave UV excitation, Kirk (1955) recorded the PL spectrum of scapolite with a most intense peak at 570 nm. However, the strongest emission peak in scapolite recorded by Sidike et al. (2008) was 596 nm (slightly yellowish orange) using 390 nm (violet) excitation. The latter study also showed that the excitation efficiency is lower at 365 nm than in the violet range. For the present scapolite, the orangey yellow fluorescence that was evidently excited by the violet component of daylight was strong enough to be seen in indirect sunlight.

During the February 2018 Tucson gem shows, one of the authors (BML) was shown another yellow scapolite from Tanzania with very similar colour and fluorescence behaviour (Figure 23). This 11.52 ct scapolite in the collection of Herb and Monika Obodda (Warwick, Rhode Island, USA) had been recut by gem dealer Mark Smith from a stone that he obtained in Sri Lanka in late 2017. Herb Obodda reported that he first encountered such scapolite in the late 1970s as two stones in a parcel of rough yellow grossular from the Leletema Hills of north-eastern Tanzania. They were identified as meionite by Dr Pete Dunn at the Smithsonian Institution (Washington DC, USA). Their yellow fluorescence made them easy to separate from the garnet parcel.

Dr J. C. (Hanco) Zwaan FGA
(hanco.zwaan@naturalis.nl)
Netherlands Gemmological Laboratory
National Museum of Natural History 'Naturalis'
Leiden, The Netherlands

Brendan M. Laurs FGA

Figure 23: Weighing 11.52 ct, this scapolite from Tanzania has similar colour and long-wave UV fluorescence as the stone documented in this report. Photo by Thai Lanka Trading.

References

Burgner R.P., Scheetz B.E. and White W.B., 1978. Vibrational structure of the S_2^- luminescence in scapolite. *Physics and Chemistry of Minerals*, **2**(4), 317–324, http://doi.org/10.1007/bf00307574.

Deer W.A., Howie R.A., Wise W.S. and Zussman J., 2004. *Rock-Forming Minerals, Vol. 4B: Framework Silicates – Silica Minerals, Feldspathoids and Zeolites*, 2nd edn. The Geological Society of London, Bath, 982 pp.

Graziani G. and Gübelin E., 1981. Observations on some scapolites of central Tanzania. *Journal of Gemmology*, **17**(6), 395–405, http://doi.org/10.15506/jog.1981.17.6.395.

Sidike A., Kusachi I., Kobayashi S., Atobe K. and Yamashita N., 2008. Photoluminescence spectra of S_2^- center in natural and heat-treated scapolites. *Physics and Chemistry of Minerals*, **35**, 137–145, http://doi.org/10.1007/s00269-007-0205-3.

Swayze G.A. and Clark R.N., 1990. Infrared spectra and crystal chemistry of scapolites: Implications for Martian mineralogy. *Journal of Geophysical Research*, **95**(B9), 14481–14495, http://doi.org/10.1029/JB095iB09p14481.

Zwaan P.C., 1971.Yellow scapolite: Another gem-mineral from Umba, Tanzania. *Journal of Gemmology*, **12**(7), 304–309, http://doi.org/10.15506/JoG.1971.12.7.304.

Cr-bearing Green Spodumene from Northern Nigeria

During a buying trip to Nigeria in October 2017, rough stone dealer Farooq Hashmi obtained a few broken pieces of a green gem material that was sold to him as hiddenite. Its exact origin was not disclosed, but he was told it came from northern Nigeria.

Hashmi provided two of the pieces to author PK for faceting, and unfortunately the first stone cleaved during pre-forming of the pavilion. Cutting of the second stone yielded a 3.32 ct rectangular brilliant. Author PK has faceted numerous hiddenites from North Carolina, USA, and by comparison the material from Nigeria seemed harder, but it split much more easily along cleavages. During the cutting process, it was necessary to use nothing coarser than a worn-out 1,200 grit lap. Even so, the stone developed minor cleavage separations just from polishing the first crown main.

The faceted stone and cleaved preform were examined by authors CW and BW, together with three pieces of rough weighing 1.69–7.34 g (e.g. Figure 24) that Hashmi supplied. The faceted gem measured 9.98 × 7.21 × 5.48 mm, and the cleaved preform was incipiently polished for examination and weighed 5.62 ct. The stones were a pale, slightly bluish green and showed strong pleochroism in bluish green, light green and pale greenish yellow. RIs of the faceted stone were 1.662–1.679 (birefringence = 0.017) and of the preform were 1.663–1.680 (also birefringence = 0.017). Hydrostatic SG values were 3.19 for the faceted stone and 3.20 for the largest piece of rough. The samples appeared pink with the Chelsea Colour Filter, and they fluoresced weak-to-moderate yellow to long-wave UV and were inert to short-wave UV radiation. These properties are comparable to those of Cr/V-bearing green spodumene from Afghanistan documented by Chadwick et al. (2007), except the Afghan material showed no UV fluorescence and yielded a somewhat higher SG value (3.25).

The rough and preformed Nigerian stones exhibited prominent cleavage faces and some conchoidal fractures; no natural crystal faces were present. Internal features consisted of parallel, rain-like, colourless solid inclusions and fluid trapped within cleavage fractures. The faceted stone contained prominent cleavage cracks and incipient fissures, as well as some very fine, parallel needles that were probably growth tubes.

To test the colour stability of the material, one of the rough pieces was placed in a window where it was subjected to direct sunlight. No fading was seen after a period of three days.

Raman spectroscopy with a GemmoRaman-532SG instrument confirmed the stones were spodumene. Ultraviolet-visible–near infrared (UV-Vis-NIR) spectroscopy of the faceted stone with a MAGI GemmoSphere instrument revealed sharp peaks at 685 and 689 nm due to Cr^{3+}, as well as strong features at 370 and 379 nm and at 432 and 437.5 nm (Figure 25) that are ascribed to Fe^{3+} (cf. Walker et al., 1997; Anderson and Payne, 1998). The green colouration corresponds to a transition window that is formed by the prominent band at 620 nm

Figure 24: This Cr-bearing spodumene is reportedly from northern Nigeria. The cut stone is 3.32 ct and the larger piece of rough weighs 7.34 g. Photo by Dean Brennan, Stone Group Laboratories.

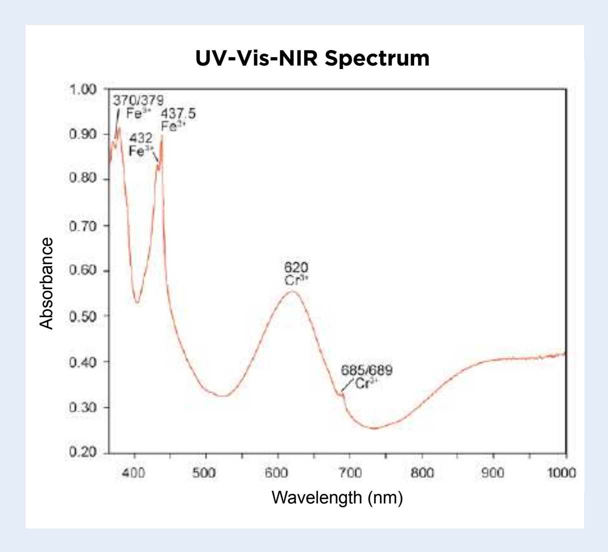

Figure 25: UV-Vis-NIR spectroscopy of the faceted green Nigerian spodumene showed features due to Cr^{3+} and Fe^{3+}.

and another underlying band near 450 nm, both due to Cr^{3+}; the latter feature is obscured by Fe^{3+} bands in the 430–440 nm region, which also contribute to the transmission window (and therefore the green colouration).

EDXRF spectroscopy with an Amptek X123-SDD spectrometer indicated prominent Fe and Mn, minor Cr, and traces of Ni, Zn and K. By comparison, the green Afghan spodumene documented by Chadwick et al. (2007) likewise contained Fe>Mn>>Cr, as well as 59–72 ppm V.

Regarding the proper use of the term *hiddenite*, Chadwick et al. (2007) indicated 'there is no consistent definition for this variety of spodumene. Although this term is typically used to refer to yellow-green to green Cr-bearing spodumene, it is unclear if the saturation of the green colour is important to the definition.' These authors also mentioned that in addition to the classic locality at Hiddenite, North Carolina, Cr-bearing spodumene is known from Brazil, India, Siberia and Afghanistan.

Although spodumene (kunzite) has previously been reported from northern Nigeria (Laurs, 2001), this is the first time that the green Cr-bearing variety has been documented from there.

Cara Williams FGA *and Bear Williams* FGA

Patrick Kelley
PAK Designs
Charlotte, North Carolina, USA

Dr George R. Rossman
California Institute of Technology
Pasadena, California, USA

Brendan M. Laurs FGA

References

Anderson B.W. and Payne C.J., 1998. Absorption spectra of spodumene. In R.K. Mitchell, Ed., *The Spectroscope and Gemmology*, GemStone Press, Woodstock, Vermont, USA (p. 123).

Chadwick K.M., Shen A.H., Laurs B.M., Simmons W.B. and Falster A.U., 2007. Gem News International: Cr/V-bearing green spodumene from Afghanistan. *Gems & Gemology*, **43**(3), 265–267.

Laurs B.M., Ed., 2001. Gem News International: Kunzite from Nigeria. *Gems & Gemology*, **37**(1), 70–71.

Walker G., El Jaer A., Sherlock R., Glynn T.J., Czaja M. and Mazurak Z., 1997. Luminescence spectroscopy of Cr^{3+} and Mn^{2+} in spodumene ($LiAlSi_2O_6$). *Journal of Luminescence*, **72–74**, 278–280, http://doi.org/10.1016/s0022-2313(97)00046-x.

Titanite (Sphene) from Zimbabwe

In early 2017, a new deposit of gem-quality titanite (sphene) was found in north-east Zimbabwe. According to Bill Larson (Pala International, Fallbrook, California, USA), the titanite comes from the Homestead mines in the Merewa area of Mutawatawa District in Mashonaland East Province. Although titanite has previously been reported from at least four Zimbabwean localities (www.mindat.org/locentries.php?p=21891&m=3977), none of them are located in this province. The stones were recovered as loose broken crystals in the soil. Shallow pits were dug with hand tools (e.g. Figure 26), but the miners soon encountered bedrock, and titanite production ceased.

Larson obtained about 4.5 kg of rough material, of which 10% was of fine quality. Some large crystals were recovered (up to ~12 cm in maximum dimension), and many pieces of the titanite contained cuttable areas between fractures. Faceted stones have ranged up to 40 ct (Stone-Sundberg and Schumacher, 2018), with fine clean gems weighing up to 30 ct (see www.palagems.com/gem-news-2017-11/#Sphene). Several hundred carats have been faceted so far by Pala International, mostly as calibrated stones of 1–3 ct for sale through Jewelry Television. The colour ranges from greenish yellow to yellowish green (Figure 27).

Chemical analysis of multiple spots on two fragments of light yellowish green titanite by author GRR using an INAM Expert 3L X-ray fluorescence unit revealed the presence of several trace elements: 0.20–0.40% Fe, 0.16–0.25% V, 0.01–0.13% Nb, 0.03–0.05% Mn, 26–47 ppm Zr, 15–20 ppm Y and 10–20 ppm Sr.

The Vis-NIR absorption spectra in Figure 28 were obtained from a 5.0-mm-thick slab—taken from one of the titanites which was chemically analysed—with a centred Bxa orientation (i.e. in the optical plane containing the acute bisectrix; see Thomas et al., 2014). Both polarisations showed a single absorption band centred at ~619 nm (and an absorption edge extending inward from the UV region). This absorption band is in the region where V^{3+} absorption occurs in other minerals (Schmetzer, 1982). The presence of trace amounts of V in the chemical analysis is also consistent with vanadium being the origin of the yellow-green colouration in this titanite.

Brendan M. Laurs FGA and
Dr George R. Rossman

References

Schmetzer K., 1982. Absorptionsspektroskopie und Farbe von V^{3+}-haltigen natürlichen Oxiden und Silikaten – ein Beitrag zur Kristallchemie des Vanadiums. *Neues Jahrbuch für Mineralogie, Abhandlungen*, **144**(1), 73–106.

Stone-Sundberg J. and Schumacher K., 2018. Gem News International: Vibrantly colored gems. *Gems & Gemology*, **54**(1), 87–88.

Thomas T., Rossman G.R. and Sandstrom M., 2014. Device and method of optically orienting biaxial crystals for sample preparation. *Review of Scientific Instruments*, **85**(9), article 093105, 7 pp., http://doi.org/10.1063/1.4894555.

Figure 26: A new deposit in north-east Zimbabwe has yielded gem-quality titanite (sphene) from the soil in shallow pits. Production ceased when the miners encountered bedrock. Photo courtesy of Bill Larson.

Figure 27: These titanites from Zimbabwe weigh 12.45–14.46 ct and show the range of colour for material from the new deposit. Photo by Mia Dixon.

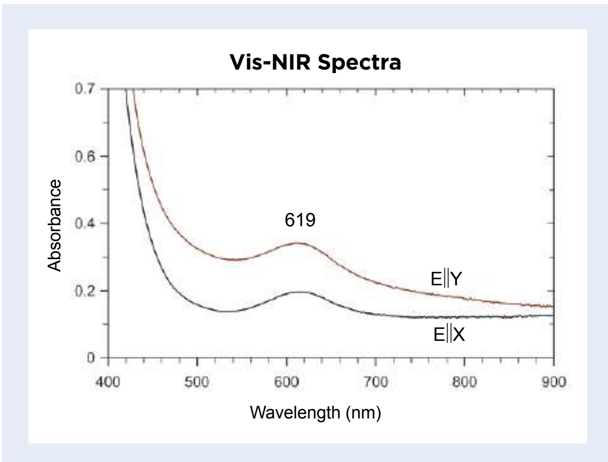

Figure 28: These polarised Vis-NIR absorption spectra of a 5.0-mm-thick slab of light yellowish green titanite from Zimbabwe were taken in the X=α and the Y=β extinction directions (E||X and E||Y, respectively).

Native Copper Inclusions in a Cu-bearing Tourmaline

Since the 1989 discovery of bright blue-to-green Cu-bearing tourmaline in Brazil's Paraíba State (Fritsch et al., 1990), these gems have completely changed how the global marketplace appreciates and values tourmaline as a gemstone. In addition to the array of 'electric' colours that have been seen in Cu-bearing tourmaline from Brazil (and subsequently from Nigeria and Mozambique), some intriguing new inclusion features have also come to light.

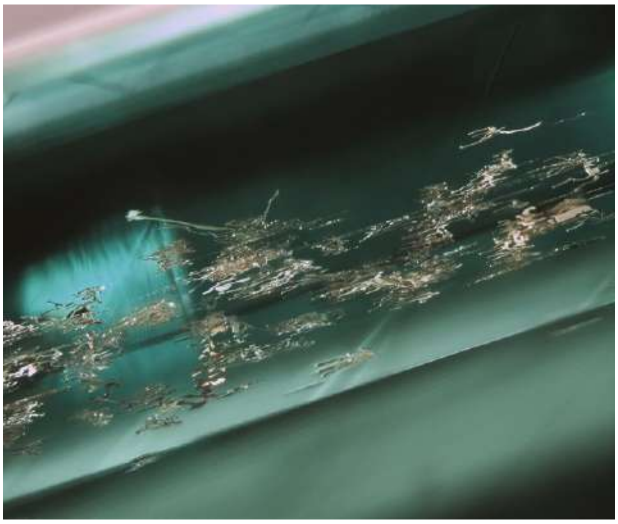

Figure 29: Dendritic platelets of native copper are oriented primarily along the c-axis of this Cu-bearing tourmaline. Photomicrograph by Bilal Mahmood; magnified 58x.

Recently, the American Gemological Laboratories received a 1.35 ct Cu-bearing tourmaline for identification and enhancement determination. The moderately saturated blue-green colour of the stone was not typical of the intensely coloured Paraíba-type tourmalines revered by the industry. Gemmologically, however, the stone was of much greater importance. Orientated primarily along the c-axis were numerous skeletal clusters of native copper inclusions (Figure 29).

Early publications on Cu-bearing tourmaline from Brazil make reference to native copper inclusions (e.g. Brandstätter and Neidermayr, 1994), however, they are only very rarely observed in cut stones found on the market. For gemmologists and mineralogists, inclusions such as these are paramount to understanding the environment in which minerals and gems form, particularly when chromophores are involved.

Adrian Hartley (ahartley@aglgemlab.com)
American Gemological Laboratories
New York, New York, USA

References

Brandstätter F. and Neidermayr G., 1994. Copper and tenorite inclusions in cuprian-elbaite tourmaline from Paraíba, Brazil. *Gems & Gemology*, **30**(3), 178–183, https://doi.org/10.5741/gems.30.3.178.

Fritsch E., Shigley J.E., Rossman G.R., Mercer M.E., Muhlmeister S.M. and Moon M., 1990. Gem-quality cuprian-elbaite tourmalines from São José da Batalha, Paraíba, Brazil. *Gems & Gemology*, **26**(3), 189–205, https://doi.org/10.5741/gems.26.3.189.

Tourmaline Mining at Ijero, Nigeria

In October 2017, rough stone dealer Farooq Hashmi visited an active tourmaline mining area near Ijero (or Ijero-Ekiti), which is located ~200 km by road (about 2.5 hours) north-east of Ibadan in the south-western part of Nigeria. The mines have been worked since the early 1990s, and have produced pink, green, blue and multi-coloured tourmaline. In addition, the deposit is a source of industrial minerals such as feldspar and sheet mica, as well as tantalum-niobium and lithium mineralisation (Ale et al., 2014).

At the time of Hashmi's visit, there were five different areas being worked for tourmaline by separate groups who leased the digging rights from a local pastor who owned the mine. Most of the tourmaline production at Ijero has come from eluvial deposits explored by open pits ranging from 10 to 30 m deep (e.g. Figure 30). When the miners encounter the underlying primary (granitic pegmatite) deposits, they dig vertical shafts for several more metres (Figure 31). Much of the work is done by hand, although one excavator was active during Hashmi's visit (Figure 32).

During his visit to Nigeria in 2017, Hashmi personally saw recently produced tourmaline that amounted to hundreds of kilograms of cabochon-quality rough material and 5–10 kg of facet-grade crystals. In addition, he saw 10–20 kg parcels of this tourmaline during a recent trip to gem markets in Bangkok. Shortly before his mine visit, most of the tourmaline from Ijero that Hashmi saw on the market was bright pink with colourless zones (Figure 33a), in pieces up to 3 g (although larger stones were produced). The production then transitioned into somewhat darker material, much of it multi-coloured (Figure 33b); some clean crystals exceeding 50 g were available. More recently, in early 2018, a small

Figure 30: Miners have removed eluvial material from this pit in the Ijero area of south-western Nigeria in search of gem tourmaline. Photo by Farooq Hashmi.

Figure 31: Once the Ijero miners reach the unweathered pegmatite, they dig shafts in search of tourmaline. Photos by Farooq Hashmi.

Figure 32: An excavator is used to dig into the eluvial deposit adjacent to a tourmaline-bearing pegmatite at Ijero. Several shafts are evident in the unweathered pegmatite. Photo by Farooq Hashmi.

amount of green tourmaline entered the market from Ijero (Figure 33c). In addition, a sizable quantity of brownish pink or 'peach' coloured tourmaline was produced, sometimes as large gemmy crystals (e.g. Figure 33d).

The Ijero area has produced large amounts of gem tourmaline in the nearly three decades that it has been mined. As exploitation of the deposit proceeds to deeper levels, requiring more hard-rock mining, it is expected that tourmaline production from this area will decrease.

Brendan M. Laurs FGA

Reference

Ale P.T., Dada J.A. and Adewumi A.J., 2014. Industrial minerals potentials [*sic*] of Ijero pegmatite in Ekiti State, southwestern Nigeria. *World Applied Sciences Journal*, **29**(3), 415–420.

Figure 33: Recent tourmaline production from Ijero has consisted of (**a**) bright pink/colourless, (**b**) multi-coloured, (**c**) green and (**d**) brownish pink crystals. The tourmalines in photos (a)–(c) typically range up to 3 g, while the unusually large crystal in (d) weighs 52 g. Photos by Farooq Hashmi.

DIAMONDS

Reduced Phosphorescence of Type II HPHT-grown Synthetic Diamonds After Electron Beam Irradiation

Since about 2015, large amounts of melee-size high-pressure, high-temperature (HPHT) synthetic diamonds have entered the market, and the gem and jewellery industry is struggling to discriminate them from natural ones. Several screening devices have been developed for making this separation. Most of them are based on measuring properties such as UV transmission, UV luminescence and IR absorption, although the methods used by some devices are undisclosed. The detection of phosphorescence is widely used among them since both loose and mounted stones can be rapidly inspected. HPHT-grown type II synthetic diamonds are known to show phosphorescence (e.g. Eaton-Magaña et al., 2017)—ranging in duration from milliseconds to tens of seconds—allowing their separation from most natural diamonds, which do not show phosphorescence (the main exception being type IIb stones).

However, in April 2018 an instrument developer in Hong Kong issued an alert that cautioned against using screening devices that look for phosphorescence at room temperature to detect irradiated HPHT-grown synthetic diamonds (Diamond Services, 2018). The alert claimed that the phosphorescence of such samples may be quenched by irradiation. In response, both the International Institute of Diamond Grading & Research and GIA reported that their identification instruments have no problem separating irradiated HPHT-grown synthetics (Meirovich, 2018).

With this background, we investigated the influence of electron-beam irradiation on the phosphorescence of HPHT-grown synthetic diamond melee. We used 10 samples (0.008–0.032 ct) of apparently colourless synthetics that were grown in China. They were divided into two groups (A and B) of five samples each (Figures 34 and 35), and were irradiated at 2 MeV in a stepwise fashion using an electron beam from a Cockcroft Walton-type radiation generator. Group A was irradiated with 1.0×10^{15}, 10.0×10^{15} and then 50.0×10^{15} electrons/cm^2, and Group B with 5.0×10^{15}, 25.0×10^{15} and then 100.0×10^{15} electrons/cm^2. Fluorescence and phosphorescence images were taken before and after irradiation using a GLIS-3000 screening device by Biaoqi Scientific Corp. (Guangzhou, China). The samples were excited by UV radiation from a deuterium arc lamp that covered a wide wavelength range between

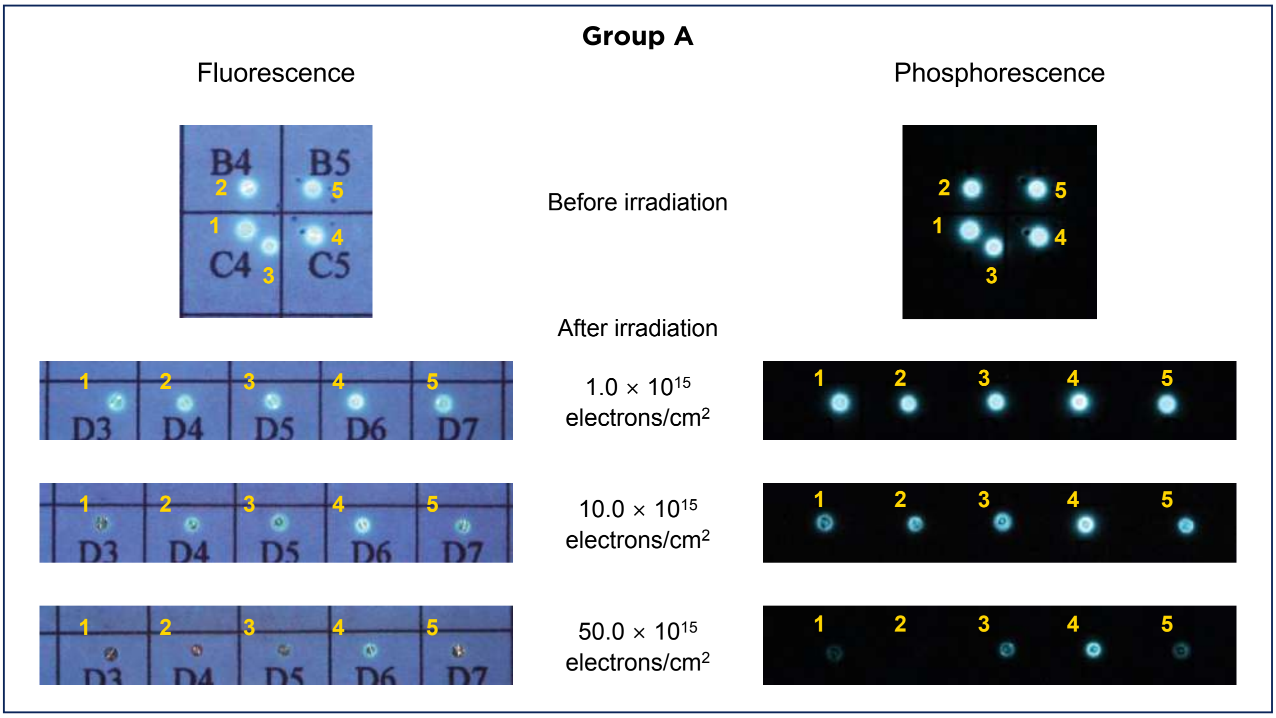

Figure 34: Fluorescence and phosphorescence images are shown for Group A synthetic diamonds (0.008–0.017 ct) before and after sequential irradiation with an electron beam. Photos by K. Koide.

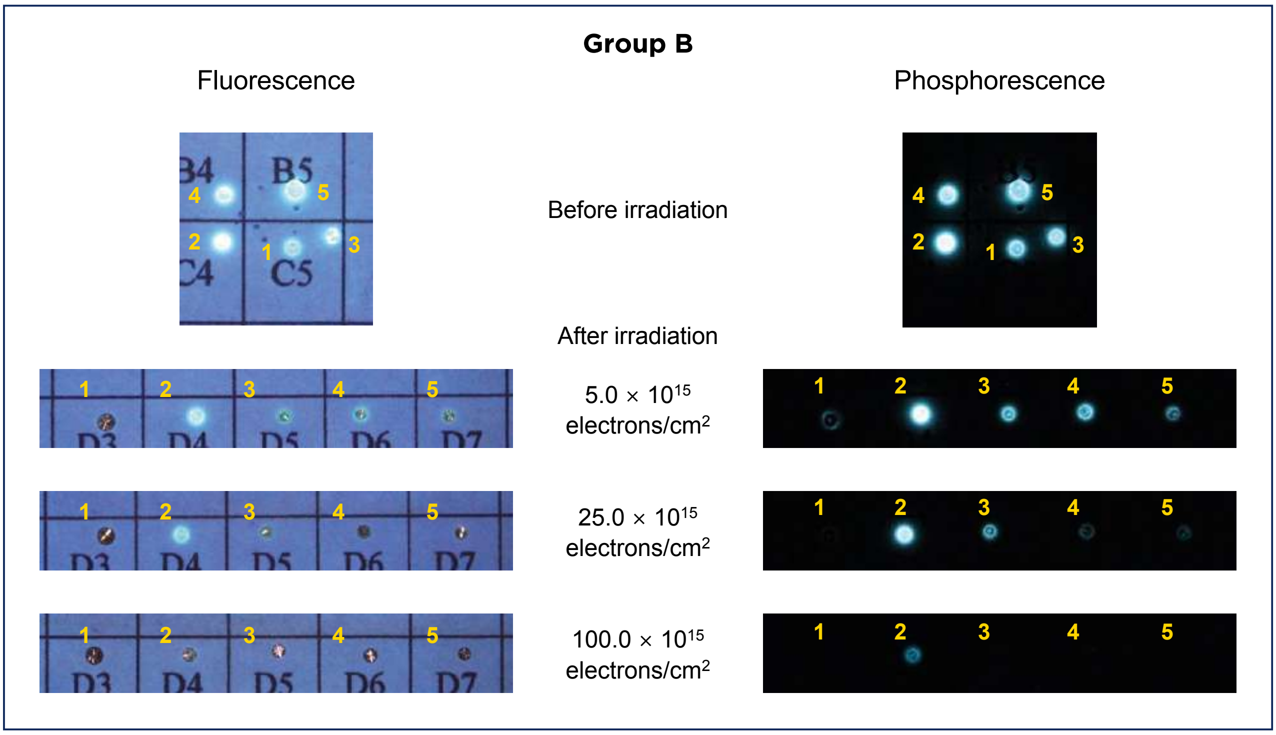

Figure 35: Fluorescence and phosphorescence images are shown for Group B synthetic diamonds (0.013–0.032 ct) before and after sequential irradiation with an electron beam. Photos by K. Koide.

180 and 250 nm. Phosphorescence photos were taken 200 milliseconds after turning off the lamp.

As shown in Figure 34, the synthetic diamonds in Group A displayed no reduction in fluorescence and phosphorescence after irradiation with 1.0×10^{15} electrons/cm^2, and a slight reduction after 10.0×10^{15} electrons/cm^2, although the intensity of the phosphorescence decrease was not uniform in the five samples. Irradiation with 50.0×10^{15} electrons/cm^2 caused the fluorescence and phosphorescence intensity to be reduced considerably, with no phosphorescence seen in one of the samples (no. 2).

Group B samples were exposed to a larger dose of electron-beam irradiation, causing their fluorescence and phosphorescence to be reduced more conspicuously (Figure 35). After irradiation with 100.0×10^{15} electrons/cm^2, all but one sample showed undetectable phosphorescence. Sample no. 2 displayed exceptionally strong phosphorescence before irradiation, and therefore it was not completely quenched by the treatment.

Figure 36 shows Group A samples after irradiation with 50.0×10^{15} electrons/cm^2, as illuminated by a daylight-equivalent lamp and while they phosphoresced. The daylight images were taken on a white, fluorescence-free tray used for diamond grading. Sample nos. 1, 3 and 5 appeared faint blue, which is due to the GR1 centre generated by the irradiation. However, their faint colour intensity would look almost colourless when set in jewellery. The strength of the samples' phosphorescence was not consistent with the presence or absence of blue colouration.

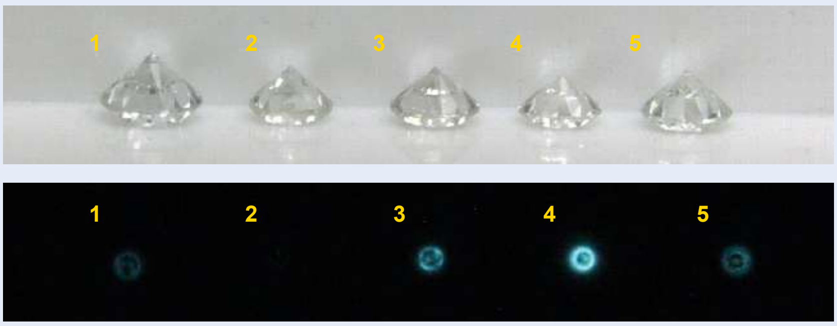

Figure 36: Group A synthetic diamonds (0.008–0.017 ct) irradiated with 50.0×10^{15} electrons/cm^2 are shown in daylight-equivalent illumination and after UV excitation. Some blue colouration is seen in nos. 1, 3 and 5, which emit variable amounts of phosphorescence. Photos by H. Kitawaki (top) and K. Koide (bottom).

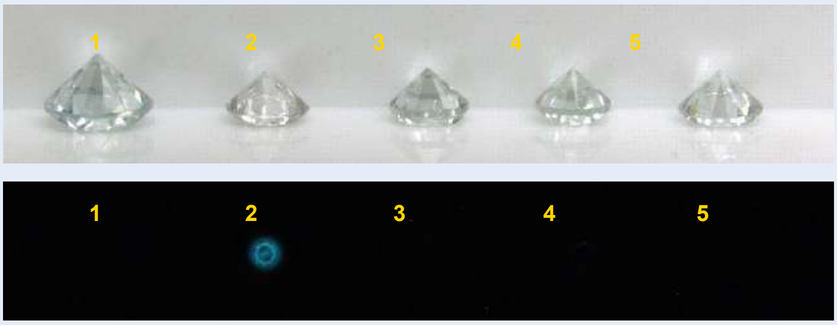

Figure 37: Group B synthetic diamonds (0.013–0.032 ct) irradiated with 100.0 x 10^{15} electrons/cm^2 are shown in daylight and after UV excitation. All samples except no. 2 exhibit some blue colouration but no phosphorescence. Photos by H. Kitawaki (top) and K. Koide (bottom).

Figure 37 shows Group B samples after irradiation with 100.0 × 10^{15} electrons/cm^2. All except no. 2 show some blue colouration, and their phosphorescence is undetectable. Sample no. 2 remained colourless and showed some phosphorescence.

According to our experiments, increasing the dose of electrons reduced both fluorescence and phosphorescence, and induced blue colouration as well. In particular, the irradiated synthetic diamonds that showed no phosphorescence also changed to light blue, although a few irradiated samples with undetectable phosphorescence remained colourless. We confirmed that the phosphorescence shown by HPHT-grown synthetic diamonds is reduced, and may finally disappear, after sequential irradiation with an electron beam. Therefore, by only measuring phosphorescence one may overlook these treated synthetics. However, detailed observation of their colour will help separate them from natural diamonds because the irradiation usually induces a blue colouration if the dose is high enough.

Dr Hiroshi Kitawaki FGA (kitawaki@cgl.co.jp), Kentaro Emori and Keiji Koide
Central Gem Laboratory, Tokyo, Japan

References

Diamond Services, 2018. Lab Alert: HPHT-grown diamonds might escape detection as synthetics, once they are treated with irradiation, 17 April. http://tinyurl.com/yah5w8ud, accessed 7 August 2018.

Eaton-Magaña S., Shigley J.E. and Breeding C.M., 2017. Observations on HPHT-grown synthetic diamonds: A review. *Gems & Gemology*, **53**(3), 262–284, http://doi.org/10.5741/GEMS.53.3.262.

Meirovich L., 2018. Labs refute claims HPHT escaping detection. Rapaport News, 25 April, http://tinyurl.com/y9x8kmm2, accessed 7 August 2018.

ORGANIC MATERIALS

Ammonites Inlaid with Ammolite and Turquoise

For many years, ammonite fossils from Madagascar have been used for decorative and ornamental purposes, including jewellery (e.g. Laurs, 2001). They are commonly sliced in half and polished to display their attractive coiled pattern and the suture lines separating their chambers.

During the June 2018 JCK show in Las Vegas, Nevada, USA, Bill Heher (Rare Earth Mining Co., Trumbull, Connecticut, USA) displayed some Madagascar ammonites that were inlaid with Ammolite from Canada and turquoise from the Sleeping Beauty mine in Arizona (Figure 38). He debuted these ammonites at the February 2018 Tucson gem shows. The individual chambers in the ammonite slices were hollowed out

Figure 38: These ammonites from Madagascar are inlaid with Ammolite (left, 27 mm long) and turquoise (right, 30 mm long). Photo by Orasa Weldon.

and then filled with pieces of these gem materials. The filled cavities were sealed with colourless lacquer, and then the pieces were ground and polished.

Depending on the inlay material used, the mosaic-set fossils showed colourful areas of iridescence (Ammolite) or a pleasing colour contrast (turquoise). They typically ranged from 30 to 75 mm long with some larger pieces available, and approximately 500 of them are being produced each month by artisans in Bali, Indonesia. Production will continue until Heher's stock of Ammolite and Sleeping Beauty turquoise pieces are consumed.

Brendan M. Laurs FGA

Reference

Laurs B.M., 2011. Gem News International: Iridescent ammonite from Madagascar. *Gems & Gemology*, **47**(3), 235–236.

SYNTHETICS AND SIMULANTS

Figure 39: These two oval specimens, weighing approximately 750 ct each, were represented as black opal. They proved to be imitations made with a magnesite core coated with a layer of grey cement that locally contains tiny grains having the appearance of opal. The lower edge of the left specimen was chipped off for study. Also note the uneven colour patches, suggesting that different materials were used in their manufacture. Photo by G. Choudhary.

Unusual Matrix Opal Imitations

Matrix opal from Andamooka, South Australia, is a well-known gem material that may be used to imitate black opal. It is primarily a porous rock that has been infiltrated by play-of-colour opal, and it is commonly carbonised (or 'sugar treated') to produce its dark colour (e.g. Brown, 1991). Recently Amit Soni of Jaipur showed this author two large oval-shaped specimens with the appearance of matrix opal (and sold as black opal), both of which turned out to be unusual imitations.

The samples were rather large, with each weighing approximately 750 ct and measuring ~82.0 × 60.0 × 16.0 mm. They displayed uneven body colours with brown, grey and black areas (Figure 39). Specks of spectral colours, suggesting the presence of opal, were restricted mainly to the brown portions (Figure 40), while other areas had a granular texture composed of angular fragments but lacked any play-of-colour. Such restricted areas of 'opal' raised suspicion about the origin of the specimens, so further testing was performed. Observation with long- and short-wave UV radiation revealed blue-white fluorescence (Figure 41) that was confined to the brown areas (i.e. containing the 'opal' specks), while the rest of each sample was inert. The hydrostatic SG was ~3.26 (although SG is of no significance for a matrix opal), and no shadow edge could be resolved with a refractometer. Qualitative EDXRF analysis revealed the presence of S, Ca, Ba, Fe and Sr, in addition to Si. Recently, we have seen quite a few ceramic turquoise imitations with similar chemical elements, which further raised our suspicion of these samples.

With permission from the owner, the edge of one of the specimens was chipped off (again, see Figure 39), which revealed a thick grey granular layer over an underlying blue-green-white material (Figure 42); this core was

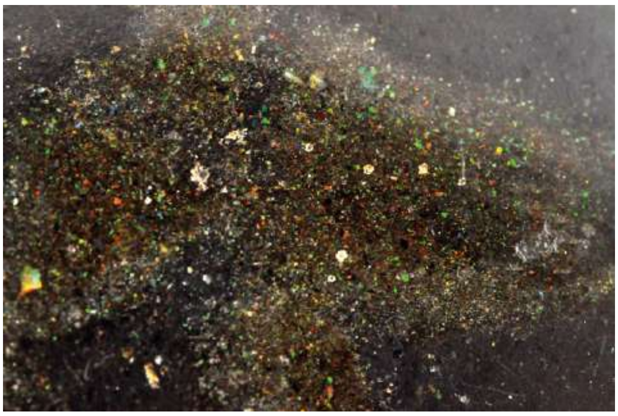

Figure 40: Grains showing play-of-colour are mainly restricted to the brown areas of this imitation matrix opal. The have been embedded into the top layer of grey cement. Photo by G. Choudhary.

Figure 41: The brown areas (containing the grains showing play-of-colour) of this imitation matrix opal fluoresce blue-white, while the other areas remain inert. The reaction to long-wave UV (shown here) was stronger than it was to short-wave. Photo by G. Choudhary.

blue-green towards the rim and white at the centre, with a chalky to powdery appearance. No play-of-colour was seen in the core or in the overlying grey layer. Raman spectroscopy of the blue-green and white areas of the core identified it as magnesite, and the colour of the blue-green rim suggested the presence of a dye.

On the basis of our observations and analysis, we deduced that these opal imitations were produced using a pre-form of dyed magnesite, which was first coated with a thick layer of grey cement (barium sulphate based). Next, cavities or pits were etched on the top surface and filled with a paste containing opal grains. Finally, the specimens were finished off with a polish.

It is difficult to understand the purpose of using magnesite as the core material and putting so much effort into manufacturing such imitations. Further, it is relatively easy to find treated black matrix opal in the marketplace (but not in such large pieces). Although it was straightforward to identify these samples as imitations and separate them from matrix opals, their true nature was only revealed with destructive testing. They proved highly unusual in both the materials used and the method of production.

Gagan Choudhary FGA *(gagan@gjepcindia.com)*
Gem Testing Laboratory, Jaipur, India

Reference

Brown G., 1991. Treated Andamooka matrix opal. *Gems & Gemology*, **27**(2), 100–106, http://doi.org/10.5741/gems.27.2.100.

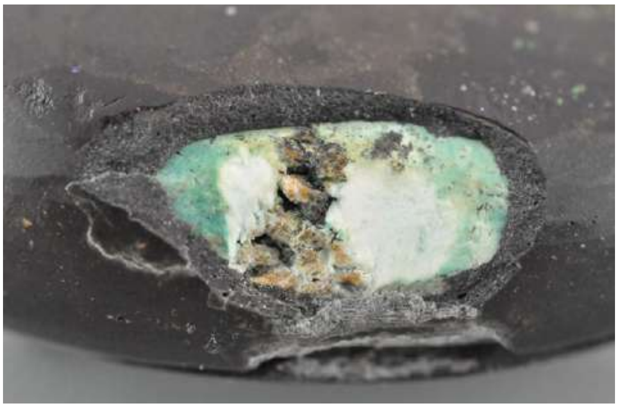

Figure 42: The chipped edge of one of the imitation matrix opals reveals the underlying magnesite used as the core, which was coated with a thick layer of granular grey cement. Also note the blue-green rim and white centre of the core, which suggests the local presence of dye in the magnesite. Photo by G. Choudhary.

MISCELLANEOUS

55th Myanmar Gems Emporium

On 20–29 June 2018, the 55th Myanmar Gems Emporium took place in Nay Pyi Taw. It was attended by about 2,800 foreign merchants and 1,200 local buyers. In addition, 500 local gem companies were in attendance, and they offered a variety of rough and polished gems.

Of the 336 'Gems' lots that were offered during this Emporium, 69 of them sold for a total of €1.379 million. In addition to ruby and sapphire, the Gems lots included spinel, peridot, topaz, petalite and amber. The highest Gems sale was a parcel of rough ruby (lot no. 175) weighing 2,997 carats that sold for €152,999.

There were 360 'Pearl' lots offered, and 341 of them sold for €2.598 million. Pearl lot no. 524 received the highest price of €32,999.

Of the 6,795 'Jade' lots offered, 5,259 sold for a total of €423.118 million. The highest Jade sale was lot no. 1796, which consisted of two pieces weighing a total of 83 kg that sold for €9,000,099.

The total sales for the event were €427.095 million, a decrease compared to €516.50 million at the 54th Emporium.

Dr U Tin Hlaing (p.tinhlaing@gmail.com)
Dept. of Geology (retired)
Panglong University, Myanmar

Letters

Transparency of Emerald Tanzurine

In the Gem Note titled 'Green aventurescent quartzite from a new find in Tanzania' (Vol. 36, No. 2, 2018 , pp. 103–104) authors Tom Stephan, Dr Ulrich Henn, Fabian Schmitz and Brendan Laurs describe Emerald Tanzurine as 'predominantly opaque'. Yet the polished egg and cabochon illustrated in their Figure 24 strongly suggest otherwise. There is a very simple test for opacity in gem materials: if inclusions within the gemstone are clearly visible, as they are in the objects in Figure 24, then it cannot be opaque. By definition you cannot see into an opaque material. In fact, not only is the Emerald Tanzurine not opaque, but one can reasonably argue that it is actually transparent. If it were not transparent, one would certainly not be able to view the fuchsite inclusions which can easily be seen in Figure 24. Admittedly, some of the Emerald Tanzurine is quite dark, but being dark does not make it opaque.

We have another modest concern with the article in general. Jonathan Bartky, the discoverer of Emerald Tanzurine, claims that the location of his deposit is undisclosed. The authors of the Gem Note did not use samples in their study supplied by Bartky, but instead their samples were donated by Impexco (Idar-Oberstein, Germany). There is no information provided regarding Impexco's source of their samples, so the possibility exists that it is not the same material as Bartky's. Samples could have been obtained from Bartky for this study, thereby eliminating this possibility.

John S. White
Stewartstown, Pennsylvania, USA

Dr Loretta D. Dickson
Lock Haven, Pennsylvania, USA

Authors' Reply

We thank Mr White and Dr Dickson for their comments. In our Gem Note on green aventurescent quartzite, we described the samples not only as 'predominantly opaque', but more precisely as follows: 'The rough material from Tanzania was predominantly opaque, but appeared translucent in strong transmitted light. The translucency was better in the polished samples (e.g. Figure 24)…' However, we use the following definitions for a gem's transparency: transparent—one can see through it; translucent—light can pass through it; opaque—one cannot see light pass through it. Furthermore, our description gave the sample's overall appearance, and not just on a micro-level relative to its inclusions. When investigating the samples shown in Figure 24, we observed that no light could pass through them under normal lighting conditions. Only by using very strong transmitted illumination could we observe a slight translucency at the edges. According to this observation, we maintain that these samples were '…predominantly opaque, but appeared translucent in strong transmitted light.'

On the samples' origin: The material was offered on the German market by Impexco in Idar-Oberstein, Germany. Wolfgang Weinz of Impexco received the material from a local Tanzanian miner and dealer in Dar es Salaam, Tanzania. Given the timing of these samples' arrival on the market and their close resemblance to material obtained from Jonathan Bartky, it seems reasonable to assume that they constitute the same material that Bartky sells as Emerald Tanzurine.

Tom Stephan, Dr Ulrich Henn FGA *and Fabian Schmitz*
German Gemmological Association
Idar-Oberstein, Germany

Brendan M. Laurs FGA

Erratum

In the Gem Note titled 'More on Black Star Rutile Imitations' (see *The Journal*, Vol. 36, No. 1, pp. 21–23), the title of Figure 33 should have been 'XRD Pattern'.

Blockchain, Chain of Custody and Trace Elements: An Overview of Tracking and Traceability Opportunities in the Gem Industry

Laurent E. Cartier, Saleem H. Ali and Michael S. Krzemnicki

ABSTRACT: Recent developments have brought due diligence, along with tracking and traceability, to the forefront of discussions and requirements in the diamond, coloured stone and pearl industries. This is a result of consumer demands for detailed information on the provenance of gems, banking requirements aiming to reduce risk, industry and company initiatives seeking to bring greater transparency, and growing government legislation on mineral supply chains. To address this trend, certification mechanisms and technologies (such as blockchain) are being developed to solve inherent traceability challenges. As applied to gems, such standards and associated technology could benefit from the support of existing gemmological approaches (e.g. geographical origin determination) to enhance traceability and transparency measures. Recent initiatives are not just limited to corporate social responsibility reporting and due diligence requirements, but they also embrace supply chain management (including quality control and process improvements)—for example, to correctly identify and disclose treated and synthetic materials throughout the jewellery industry—as well as address consumer demand for provenance information. This article provides an overview of current trends and developments in the tracking and traceability of gems, along with an explanation of the terms used in this context.

The Journal of Gemmology, **36**(3), 2018, pp. 212–227, http://doi.org/10.15506/JoG.2018.36.3.212

Traceability and transparency—including tracking (from mine to market) and tracing (from market to mine)—of coloured stones, diamonds and pearls is an increasingly important topic in the industry, as shown by recent research and reports (Archuleta, 2016; Walker, 2017; CIBJO, 2018; Human Rights Watch, 2018). The complex and fragmented nature of the global gem industry means that little information is typically available about these supply chains and how specific gem materials are mined, manufactured and sold. Traceability is one way to provide more transparency, and it is argued that by increasing transparency, supply chain issues can be better mapped and understood, ultimately helping to improve the environmental and social impact of a supply chain (Mol, 2015). Consumers are increasingly interested in knowing where and how the materials they consume are extracted and manufactured (Nash et al., 2016; De Angelis et al., 2017; see also Figure 1). Media and non-governmental organisations are placing the gem industry under increased scrutiny regarding the origin and sustainability footprint of various stones (Cross et al., 2010; IndustriALL et al., 2013; Global Witness, 2015, 2016; RESP, 2016). At the same time, some companies want to be proactive so as to mitigate risks and better understand their own supply chains and potential

Figure 1: An artisanal miner in Madagascar holds a treated blue topaz set in a ring. As the gem trade and consumers become increasingly interested in tracing the history and provenance of a gemstone or piece of jewellery, technological solutions and management models need to be developed to respond to these needs. Photo by L. E. Cartier.

sustainable development impact (Bloomfield, 2017). Governments want to improve the management and revenue collected from gem resources, and global governing bodies have highlighted issues such as smuggling and money laundering in recent years (Schroeder, 2010; 'Expert meeting to discuss…', 2013; Financial Action Task Force, 2013; OECD, 2016; Shortell and Irwin, 2017). Both the USA (through the Dodd-Frank Wall Street Reform and Consumer Protection Act) and the EU (through the upcoming Conflict Minerals Regulation in 2021) are requiring that companies carry out due diligence to ensure that the trade in four minerals—tin, tantalum, tungsten and gold—does not fund conflict in certain countries and regions. Although gold is presently the only commodity of concern to the jewellery industry in this context, such regulations could be expanded to diamonds and coloured stones in the future. The jewellery industry has been less scrutinised than other sectors (particularly in terms of legislation) and has been relatively late in responding to some of these concerns in a manner that integrates all materials used in jewellery products.

To further address these issues, a multi-fold approach is required—for example, strengthening specific ethical and sustainability standards and improving resource governance pertaining to the mining, processing and selling of gem materials worldwide (Cartier, 2011; Ali et al., 2017). Documenting the provenance and sources of gems through traceability schemes is one way to increase transparency and provide a supporting mechanism to strengthen the accountability and credibility of sustainability-certification schemes. In this article, we focus on gems (e.g. Figure 2) rather than jewellery as a whole, as track-and-trace in jewellery would also cover more wide-ranging issues such as quality control and inventory management in manufacturing. We briefly address the historic role of provenance in gems and jewellery, and how scientific origin determination of gemstones emerged in recent decades, thereby providing some knowledge about a stone's origin in the absence of a clear paper trail. We then review general concepts of traceability and track-and-trace approaches and how these might apply to gems through a compilation of various industry initiatives. Then, an overview of blockchain technology is given along with examples of emerging projects in the gem industry. A Glossary is included that defines key terms pertaining to provenance, traceability and related topics that are covered in this article. Finally, we conclude with an outlook on traceability, and argue that there is no 'silver bullet', but rather that multiple approaches and technologies are likely to spur greater transparency in the industry.

SIGNIFICANCE OF THE GEOGRAPHICAL ORIGIN OF GEMS

Historical Perspectives

Gems have been coveted by humans for millennia (e.g. Ali, 2009). Traded as precious objects or used for personal adornment, they have long been linked to different symbols and represented as commercial valuables. In some cases, the origin and nature of the minerals unearthed and traded was vital because of historical and spiritual connotations (Raden, 2016).

In the early days of gem commerce, only a few sources were known. With expanding global exploration and trade, new and diverse gem deposits were discovered. Traditionally, diamonds were sourced from India (Golconda) and Borneo until the discoveries in Brazil in the 18th century and in South Africa in the 19th century, which revolutionised the diamond industry. Similarly, the emerald sector experienced a surge in the 16th century with the discovery of Colombian deposits by the Spanish (Giuliani et al., 2000). Due to the emotional connection with gem materials from specific localities, knowing the provenance of these gems continued to be of interest for both traders and consumers, and was largely built on a system of trust and experience (Bernstein, 1992; Brazeal, 2017).

Opportunities and Limitations

As the science of gemmology emerged in the early 20th century, and synthetics and treatments became critical research issues, interest grew in carrying out structured investigations on gem materials from different origins to better characterise their properties. For example, Chesley (1942) attempted to correlate spectroscopic features of diamonds to their source localities. Geographical origin determination of coloured stones as we know it today appeared in the 1980s, and at the beginning focused on characterisation of typical microscopic inclusions from a deposit (Gübelin and Koivula, 1986). This was subsequently complemented by chemical and spectroscopic work on gem materials from various localities (Hänni, 1994; Krzemnicki, 2007; Rossman, 2009; Bui et al., 2012; Ogden, 2017), such as the early work on Kashmir sapphires by Hänni (1990). For more than a decade, the use of laser ablation inductively coupled plasma mass spectrometry (LA-ICP-MS) has provided greater quantitative insight into the trace- and ultra-trace-element composition of gems for fingerprinting their origin (Guillong and Günther, 2001; Rankin et al., 2003; Abduriyim and Kitawaki, 2006a,b). Recent work using GemTOF (SSEF's time-of-flight LA-ICP-MS instrument) in combination with complex multivariate statistical analysis has shown the potential to improve

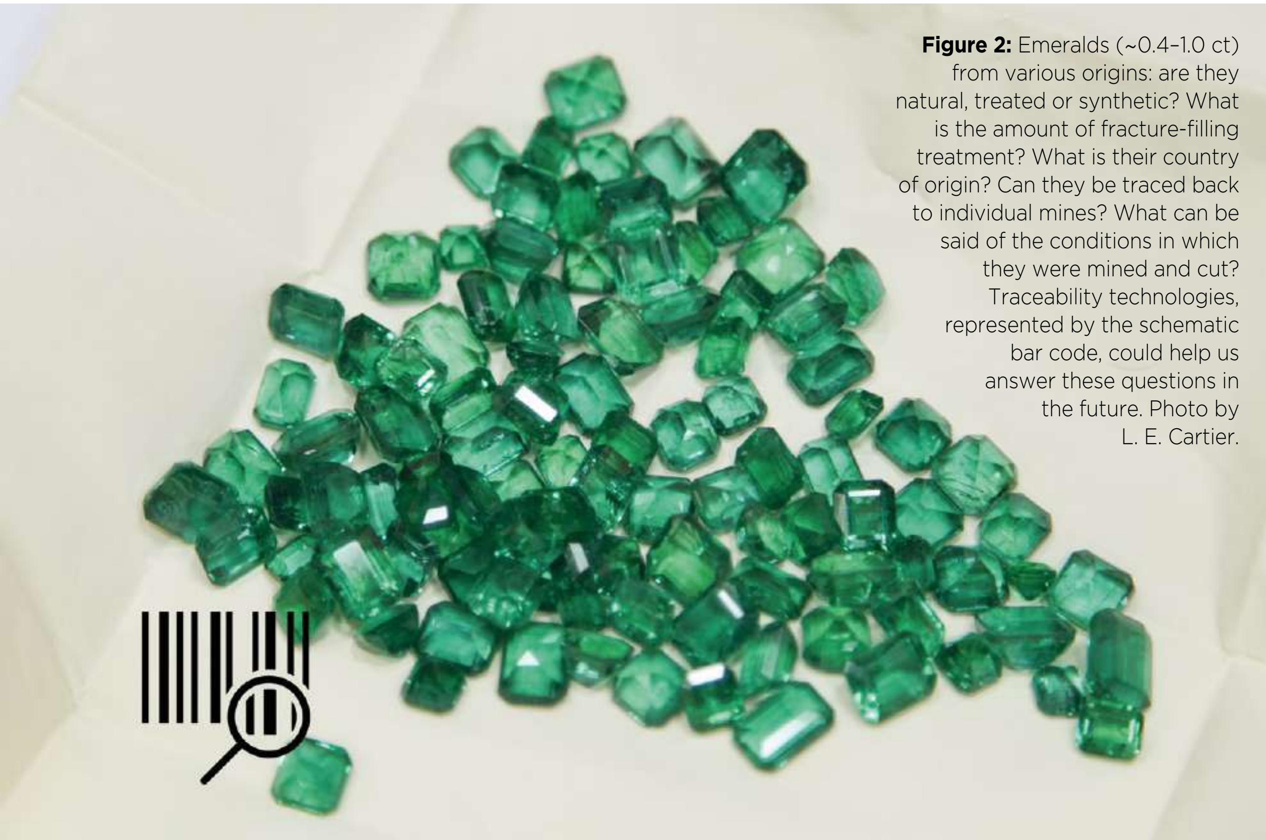

Figure 2: Emeralds (~0.4–1.0 ct) from various origins: are they natural, treated or synthetic? What is the amount of fracture-filling treatment? What is their country of origin? Can they be traced back to individual mines? What can be said of the conditions in which they were mined and cut? Traceability technologies, represented by the schematic bar code, could help us answer these questions in the future. Photo by L. E. Cartier.

Glossary*

Blockchain: A system for storing data in which groups of valid transactions, called blocks, form a chronological chain, with each block securely linked to the previous one. Originally invented for the digital currency bitcoin, a blockchain is a permanent, unalterable digital file of encrypted transactions that can be distributed in multiple copies across a network of devices linked to the blockchain. Given that every storage device has an exact and updated copy of the ledger, data can be verified and is considered immutable—an important property when transactions are occurring among users that do not know or trust each other.

Chain of custody: Under OECD's 2016 Due Diligence Guidance, chain of custody refers to the document trail recording the sequence of companies and individuals that have custody of minerals as they move through a supply chain.

Code of Practices: The Responsible Jewellery Council (RJC) Code of Practices defines responsible ethical, human rights, social, and environmental practices for businesses in the diamond, gold and platinum-group metals jewellery supply chain. It is being expanded to include coloured stones as well ('RJC to expand…', 2016).

Corporate social responsibility (CSR): 'A management concept whereby companies integrate social and environmental concerns in their business operations and interactions with their stakeholders' ('What is CSR?', 2018).

Disclosure: The release of information by companies required by regulators or requested by business partners in the supply chain.

Due diligence: The act of proactively ensuring that the products sourced and traded by companies within a supply chain conform to national and international regulations. This can include treatment disclosure, banning child labour and money laundering, and a wide range of other issues. For further information, see OECD (2016).

Geographical origin: In gemmological terms, this is commonly understood to be the country of origin of a gem provided as a scientific opinion based on microscopic, spectroscopic and chemical properties of a stone compared to a reference collection of samples and the gemmological literature. Ultimately this is linked to the geological origin of a stone. In some cases, such as rubies from Thailand and Cambodia, geologically similar or identical deposits are found on both sides of the border and thus cannot be separated by country.

Geological origin: The type of geological deposit in which a gem formed. In some countries (e.g. Madagascar), gem deposits may have different geological origins and thus can be separated accordingly (e.g. Ambondromifehy basaltic sapphires and Ilakaka metamorphic sapphires).

Origin determination: Origin determination of gems is an expert scientific opinion on the origin (country) of a stone, based on characteristic inclusions and chemical and spectroscopic features.

Provenance: A (documented) claim made on the origin (e.g. country or mine), source (e.g. recycled, mined, artisanally mined, natural, synthetic), previous ownership (e.g. a historic gemstone or a piece of jewellery formerly in a royal collection) or extraction and processing practices (e.g. conflict free, untreated, responsibly sourced).

Supply chain transparency: The extent to which information about the companies, suppliers, sourcing locations (including mines) and processing conditions (cutting and treatment processes) is available to end consumers and to other companies in the supply chain. There is growing demand for transparency in supply chains, as consumers and companies want detailed information about the origin of products.

Sustainable development: Defined in 1987 by the Brundtland Commission report as 'development that meets the needs of the present without compromising the ability of future generations to meet their own needs' (Brundtland, 1987, p. 15). This integrates economic, environmental and social pillars.

Tracing: The use of traceability records or an object's properties to identify the origin, attributes or history of a product within the supply chain. In the case of gemmology, this comes down to country-of-origin determination where documents are not available but physical and chemical properties allow for a conclusion of possible country-of-origin. If a gem has been tagged using tracking technology, it can be traced back upstream using this information.

Tracking: The use of traceability records to track an item from its origin to the end consumer through the supply chain. This is often complemented by the use of tracking technology such as radio-frequency identification (or RFID) chips, near-field communication, synthetic DNA implantation, barcodes or other forms of tagging.

Traceability: 'The ability to identify and trace the history, distribution, location, and application of products, parts, and materials' (Norton et al., 2014, p. 6, as per the International Organization for Standardization or ISO).

* Sources: Norton et al. (2014); OECD (2016); RJC (2017); Future of Fish et al. (2018); 'What is CSR?' (2018)

the precision and reliability of origin determinations (Wang et al., 2016).

Thus, today's laboratory reports offer origin opinions for certain coloured stones based on the scientific interpretation of their microscopic, spectroscopic and chemical properties compared to a reference collection of samples and the gemmological literature. Table I lists the gem varieties submitted to labs for origin reports and their common sources. As databases for tested gems grow and further research is carried out, origin determination will likely be extended further to include other gem varieties. Although it is not possible to trace a coloured stone back to a specific mine, origin determination can help validate claims made by companies regarding country of origin. For example, in the context of the now-defunct Tom Lantos Block Burmese JADE (Junta's Anti-Democratic Efforts) Act of 2008 that banned the import of Burmese rubies and jade (Dickinson DeLeon, 2008) into the USA, gemmological methods were useful for providing information to clients.

Origin reports are an important part of today's high-end gem and jewellery markets, where factors such as rarity, branding and provenance are critical to some consumers, investors and traders (Shor, 2013; Ogden, 2017). Rather than providing definitive proof of a stone's source, a country-of-origin report is used in general to support a claim made about the geographical origin of a high-end gemstone (e.g. at auction). This is very similar to expert-opinion reports on ceramics, furniture, paintings and wine (e.g. Spencer, 2004; Bull, 2016). Gemmological origin interpretations can vary in certain cases, and such variations in origin reports may show up between different labs (Gannon, 2004; Ogden, 2017). As accessibility to advanced analytical instrumentation improves, and as databases of documented rough material from different mines become more robust, the scope of geographical origin determination will also expand.

Table I: Selected gem varieties for which geographical origin determination can commonly be performed by gem laboratories.

Gem variety	Commonly identifiable (and commercially relevant) sources
Alexandrite	Africa (Madagascar, Tanzania), Brazil, Russia, Sri Lanka
Cu-bearing tourmaline	Brazil, Mozambique, Nigeria
Demantoid	Madagascar, Namibia, Russia
Emerald	Afghanistan, Brazil, Colombia, Ethiopia, Zambia
Ruby	Afghanistan, Madagascar, Mozambique, Myanmar, Tanzania (Winza), Thailand, Vietnam
Sapphire	Kashmir, Madagascar, Myanmar, Sri Lanka
Spinel	Madagascar, Myanmar, Sri Lanka, Tajikistan, Tanzania, Vietnam
Tsavorite	East Africa (Kenya, Tanzania)

Although considerable research on the origin determination of diamonds was conducted at the turn of the 21st century due to the issue of 'blood diamonds', until now no technique has been found to conclusively identify faceted stones from various origins based on scientific means (Dalpé et al., 2010). As such, it is not possible to determine the country or mine source for a cut diamond of unknown origin through commercially available geochemical, isotopic or spectroscopic methods. The diamond industry has thus had to focus on chain of custody and other mechanisms to support origin claims on sold diamonds (e.g. Table II). This includes the Kimberley Process Certification Scheme, the De Beers Best Practice Principles, the Signet Responsible Sourcing Protocol for Diamonds (D-SRSP) and the Responsible Jewellery Council's consultation for its chain of custody to become applicable to diamonds (RJC, 2017).

Research on pearls has focused on distinguishing natural from cultured and freshwater from saltwater samples, rather than geographical origin determination. However, recent work (Hänni and Cartier, 2013; Meyer et al., 2013; Cartier et al., 2018) has increasingly looked at mollusc species and the potential geographical origin determination of cultured pearls.

TRACKING AND TRACING

Tracking (from origin to market, or forward traceability) and tracing (from market to origin, or backward traceability) conceptualise the path of an item and how it can be identified within a supply chain (Schwägele, 2005). Whereas tracking and tracing describe path direction of goods, traceability is a more overarching term (see Glossary). Various sectors, such as the food and pharmaceutical industries, use both track and trace for different purposes. In such contexts, tracking can locate an item based on specific criteria (e.g. vital when recalling non-compliant items) whereas tracing is the basis for finding the cause of non-compliance (Bechini et al., 2008).

Table II: An overview of industry initiatives in responsible business practices and traceability programmes (modified from Solomon and Nicholls, 2010).

Initiative	Year founded	Target material	Chain of custody model (or model provided)	Strategy	Claim made/ aim of initiative	Supply chain segment
World Jewellery Confederation (CIBJO)	1961	Jewellery, metals, diamonds, coloured stones, pearls and coral	Product disclosure	Publish 'Blue Books' that cover industry-wide accepted nomenclature for claims made about gems and metals in the jewellery industry	Provide material disclosure guidelines for the jewellery industry	Entire jewellery industry
Kimberley Process Certification Scheme	2000	Diamonds	Bulk commodity (traceability)	Packages of rough diamonds are certified by exporting governments as conflict free	Diamonds are conflict free	Country of export, only for rough stones
CanadaMark (Dominion Diamond Mines)	2003	Diamonds	Bulk commodity (traceability)	Diamonds are certified to be of Canadian origin (from Diavik or Ekati mines)	Canadian origin (not tracked back to individual mine)	Diamond industry, from mine to end consumer
Extractive Industries Transparency Initiative (EITI)	2003	Oil, gas and mineral resources	EITI Standard	Annual EITI Progress Report to disclose information on: contracts and licences, production, revenue collection and allocation, and social and economic spending	Improve transparency in extractives sector	Mining company payments made to governments
Diamond Development Initiative	2005	Diamonds	Maendeleo Diamond Standards (MDS)	Standards and certification for responsible artisanal small-scale mining (ASM) diamond production	Responsibly mined ASM diamond according to MDS standards	ASM diamond mines (e.g. Sierra Leone)
Responsible Jewellery Council	2005	Coloured stones, diamonds, gold, platinum and silver	Code of practices and chain of custody (gold only)	RJC members commit to and are independently audited against the RJC Code of Practices, an international standard on responsible business practices for diamonds, gold and platinum-group metals	Responsible practices	Entire jewellery supply chain (coloured stones are currently under review)
Initiative for Responsible Mining Assurance	2006	Minerals and metals	Independent third-party verified responsible mining assurance system for mining companies	Certify mine-site practices	Certified to follow best practices for mining	Mining companies
Love Earth (Walmart)	2008	Gold and diamonds	Identity preservation (traceability)	Traceability of product back to mine (by consumer), with mining company, refiner and manufacturer self-reporting against a set of environmental and social criteria along with third-party audits	Jewellery material components are traceable and comply with Wal-Mart's responsible sourcing practices	Select mines, refineries, manufacturers and retailers
OECD Due Diligence Guidance for Responsible Supply Chains of Minerals from Conflict-Affected and High Risk Areas	2009	Minerals (including diamonds and coloured stones)	Due diligence guidelines for sourcing of minerals	Provide due diligence recommendations for mineral sourcing	(Not applicable)	Entire supply chain

Table II (continued): An overview of industry initiatives in responsible business practices and traceability programmes (modified from Solomon and Nicholls, 2010).

Initiative	Year founded	Target material	Chain of custody model (or model provided)	Strategy	Claim made/ aim of initiative	Supply chain segment
Diamonds with a Story (Rio Tinto)	2013	Diamonds	Identity preservation (traceability)	Australian (Argyle) origin certified as stones are tracked through supply chain	Argyle (Australia) origin	From mine to end consumer
Signet Responsible Sourcing Protocol for Diamonds (D-SRSP)	2016	Diamonds	Guidelines for responsible diamond sourcing	Protocol that provides transparency and to assure that all Signet diamonds are sourced through identified and verified sources, over time, through a process of continuous improvement	Compliant with D-SRSP	Suppliers to Signet Jewelers
Emerald Paternity Test (Gübelin Gem Lab)	2017	Coloured stones	Identity preservation and/or bulk commodity (traceability)	Rough stone batches (e.g. emeralds from Gemfields) are marked with unique ID nanoparticles that can be read downstream to provide data on the stones	Support provenance claims made by reading information contained in nanoparticles found in tagged emeralds	From mine to retail; information about a stone can be verified by a lab
M2M Program (GIA)	2017	Diamonds	Platform for consumers to visualise a diamond's story from rough to cut	GIA documents rough diamonds submitted by miner and then each stone is cut and sent back to GIA for grading; GIA confirms that each one is the same stone originally submitted	Story of the diamond from rough to cut, documented by GIA	A rough diamond submitted by a diamond mining company, tracked all the way through manufacturing and retail via M2M platform
Tracr (De Beers)	2017	Diamonds	Blockchain traceability	Develop mine-to-finger blockchain for diamonds	Demonstrate traceability of diamonds from mine to finger via blockchain	From mine to end consumer via blockchain
Diamond Time-Lapse Protocol	2018	Diamonds	Permissioned private blockchain	Show the journey of a diamond to an end consumer via blockchain and app; option for manufacturers to track stock through manufacturing process via blockchain	Journey of a diamond can be followed through manufacturing via blockchain and app	Manufacturer and retailer interface as well as a consumer interface
Provenance Proof	2018	Coloured stones	Blockchain traceability	Mine-to-finger blockchain for coloured stones developed by Everledger and the Gübelin Gem Lab	Demonstrate traceability of coloured stones from mine to finger via blockchain	From mine to end consumer, via blockchain
TrustChain	2018	Gold and diamonds	Permissioned private blockchain	Offer traceability of diamond jewellery via blockchain by working with selected certified miners, certifiers, manufacturers and retailers	Provenance claims for the source of metals and diamonds used in jewellery items	From mine to end consumer, via blockchain

Although traceability in current discussions in the gem and jewellery industry is often understood to mean an object is fully traceable (i.e. an individual gem is uniquely documented and identifiable at each step of the supply chain from mine/farm to market and end consumer), there are four different possible models of product traceability (Norton et al., 2014):

1) Identity Preservation or Track-and-Trace
2) Bulk Commodity or Segregation
3) Mass Balance
4) Book and Claim

The aim of these traceability approaches (see Table III) can be to substantiate sustainability and origin claims made by companies. A more detailed description of this, with examples for diamond and gold jewellery, can be found in Solomon and Nicholls (2010).

Clear guidelines exist for how chain of custody could be put in place in the jewellery industry (RJC, 2012, 2017) and how due diligence for responsible business practices can be carried out (OECD, 2018). Demand for both tracking and tracing within the gem industry is growing, as origin claims need to be verified. In addition, sustainability claims are increasingly being made about gems. In such cases, traceability is equally vital to uphold and validate such claims. In addition to improving chain-of-custody practices and auditing options, technology can provide solutions to verify such claims. Recent efforts have focused on individually marking and separating each stone or cultured pearl so that it can be identified and tracked back to its mine or farm of origin (Hänni and Cartier, 2013; Theodosi, 2017). The ultimate system of traceability should ideally offer a consumer transparent and proven access to the unique and complete story of a gemstone or piece of jewellery, and potentially

Table III: An overview of available traceability models used to support sustainability claims.

Traceability model	Approach	Level of traceability	Cost	General example	Gem example
Identity Preservation or Track-and-Trace	Certified materials and products are physically separated from non-certified materials and products at each stage along the supply chain.	Highest	Very costly	Consumer would know exact farm from which a banana or salad was sourced.	Exact mine-of-origin information is tracked through the supply chain.
Bulk Commodity or Segregation	Separates certified from non-certified materials but allows mixing of certified materials from different sources. All producers must comply with the certification standards.	High	Costly	An organic chocolate bar that contains cacao beans from various organically certified producers. Another example is Kimberley Process rough diamonds certified as 'conflict free'.	An aggregation of goods from one company that operates several mines; also useful for gem regions/ countries and could be complemented by gemmological analysis.
Mass Balance	Certified and non-certified materials can be mixed. However, the exact volume of certified material entering the supply chain must be controlled. Claims of 'this product contains X% of certified ingredients' can be made.	Low	Slightly costly	If 20% of the total cocoa purchased comes from fair-trade sources, 20% of a company's chocolate bars made with that mix of cocoa can include the fair-trade certified label.	Material from different mines (and certified and non-certified goods) can be mixed. Traceability information is lost.
Book and Claim	Allows all actors of a supply chain to trade in certificates for certified sustainable materials. Buying certificates allows retailers and manufacturers to claim that their business supports the production of sustainable materials. Claims of 'this product supports the sustainable sourcing and production of essential commodities' can be made.	Low	Reasonable	Companies wishing to make sustainability claims can purchase certificates (even though their goods may not be certified) that support sustainable production.	A synthetic diamond manufacturer may buy credits and contribute to sustainable mining activities.

continue to follow the piece as it is resold and recycled. Although the present consensus is that such a model is not feasible for the entire industry, research shows that many consumers want to know specific information about the origin of, for example, the cultured pearls they purchase (Nash et al., 2016). An integral part of this is marking or tagging—enabling an item to be uniquely tracked—so that it can be linked to the corresponding chain-of-custody document trail. Ultimately, combined approaches are necessary: solely marking a stone or a cultured pearl does not guarantee claims that are made about it; it must be uniquely identifiable in addition to having a chain of custody.

Laser inscription of diamonds has been offered for several years, whereby a logo or a report number is inscribed on the girdle of a stone after cutting. This is done by some natural diamond sellers (e.g. Forevermark) and synthetic diamond manufacturers to document the provenance of such products (Eaton-Magaña and Shigley, 2016). The inscription of a QR (quick response) code can link to further information about a stone that is accessible to consumers (Figure 3). The drawback associated with physically marking gems is linked to the fact that they are processed from rough to cut and thus initial surface markings would disappear. Furthermore, polished gemstones can be re-cut and such markings can be lost or fraudulently used or modified. In cultured pearls, tagging/marking techniques have ranged from inserting radio-frequency identification chips into composite nuclei (i.e. used in beaded cultured pearl production), chemically marking them via their inherent porosity (e.g. with fluorine) or trialling hologram surface markings (Hänni and Cartier, 2013; Segura, 2015). Most recently, in 2017, an 'Emerald Paternity Test' was developed that involves introducing unique synthetic DNA-based, nano-sized particles that can store specific information (e.g. mine location or mining period), which can later be retrieved and decoded in a laboratory (Branstrator, 2018). Clearly, there is no single solution or approach to providing traceability in the gem industry.

Know Your Source: Due Diligence, Chain of Custody and CSR

Several factors have spurred the jewellery industry to increasingly document its supply chains, including globalisation, greater reporting to shareholders by major groups due to 'conflict mineral' legislation, the need to reduce risk in order to secure financing, and pressure from the media and non-governmental organisations on issues such as 'blood diamonds' or 'dirty gold' (Bloomfield, 2017). It is widely argued that through increased transparency and knowledge of its supply chain, a company can better manage its risks and identify business opportunities (Carter and Rogers, 2008). In this context, chain of custody, a widely used concept in supply chain management, has become a pillar of reporting and verification in the industry (see Table II for various examples). The creation of the Responsible Jewellery Council (RJC) in 2005 further reinforced this trend with its strong focus on chain of custody to track and validate codes of practices by stakeholders (Solomon and Nicholls, 2010). To exemplify this trend further, Signet, a major American retail group, introduced its D-SRSP initiative in 2016 that vendors must adhere to if they want to be suppliers to Signet Jewelers (Bates, 2016).

The Organisation for Economic Cooperation and Development (OECD) recently developed the guidelines followed by companies seeking to respect human rights and avoid contributing to conflict through their mineral sourcing decisions and practices; these guidelines now

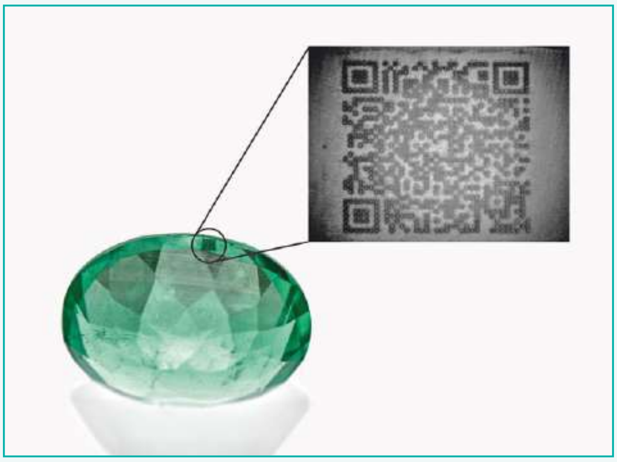

Figure 3: A tiny QR code can be inscribed on a gemstone during chemical analysis with GemTOF instrumentation (Wang and Krzemnicki, 2016). The QR code shown here measures 500 × 500 μm and has been inscribed on the girdle of an emerald weighing 2.5 ct. The material ablated during the inscription of the code is used to measure trace-element concentrations that are evaluated for determining country of origin. The code can be read (after magnification) using a QR reader on a smartphone, and gives the user access to various types of information on the stone. Composite photo by H. A. O. Wang and V. Lanzafame, SSEF.

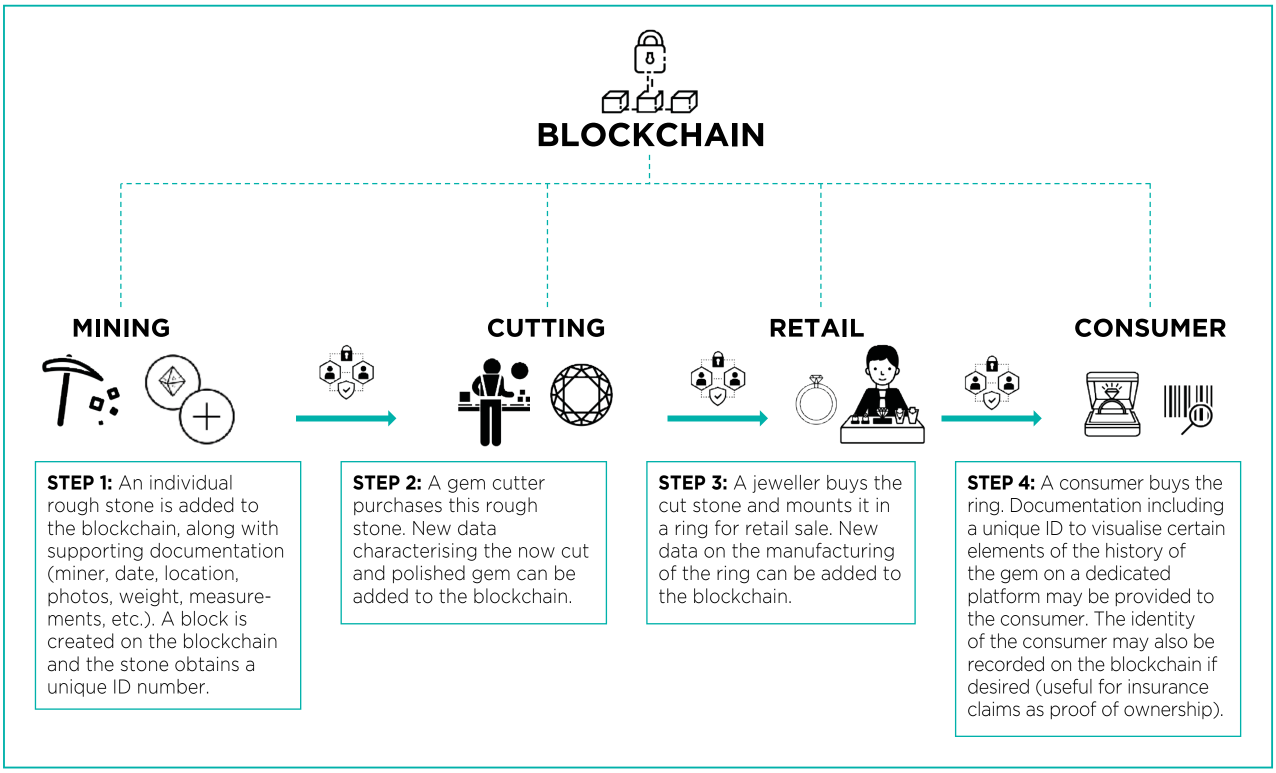

Figure 4: This generalised example of a blockchain serves to illustrate how information can be documented on a single gem's journey from mining to cutting and onward to retail and eventually the end consumer. After the stone is mined, the trade and transfer of ownership are validated at each step by both parties involved and recorded immutably to the blockchain. Illustration by L. E. Cartier.

apply to all minerals (OECD, 2016). Lombe et al. (2015, p. 15) in turn outlined due diligence and chain of custody in the following terms:

> Firstly, social and environmental risks are typically a product of an operator's behavior or environment, so knowing who has handled the material and where is an integral part of risk assessment and management. Secondly, tracking and traceability provide evidence to a company or auditor that a claim being made about a mineral (e.g. country of origin, sustainability dimensions, conflict free, etc.) is in fact true.

Traceability concerns and solutions are, thus, a natural, complementary extension to due diligence and chain of custody, depending on the context.

Blockchain Revolution: How Can It Be Applied to Gems?

Blockchain is a digitally distributed ledger technology that can support chain of custody through a system that makes documentation tamper-proof and, potentially, provides new opportunities for traceability in the highly complex and fragmented sectors of diamonds, coloured stones and pearls (e.g. Figure 4). Data added to the blockchain (e.g. by mobile phone, tablet or computer) at each recorded transaction step are verified, ownership is attributed, and the information is time stamped, encrypted, and stored permanently in a distributed and decentralised manner, providing an immutable record that is formed of a single, yet shared, source of information about a gem's journey from source to end consumer. As such, blockchain can be used to document the origin and path of a gem from mine to market, as well as verify ownership (and potentially possession, e.g. when a gem is out on memo). Blockchain technology has particularly grabbed the attention of the art world as a way to authenticate artwork back to its artist, and to record ownership and authenticity of artwork along a permanent and potentially anonymised chain of custody (O'Neill, 2018).

In blockchain, there are four types of ledgers: traditional (centralised), permissioned private, permissioned public and distributed permissionless public (Jeppsson and Olsson, 2017). A permissioned blockchain is a shared database that requires users to obtain permission before reading or writing to the chain. In permissionless blockchains, anyone can join. The rules in a blockchain are defined by the users, who can be either a private consortium (e.g. TrustChain) or public users. These rules are enforced as 'smart contracts' by computer software. Any computer that connects to the blockchain is called a node. The energy consumption of blockchain networks (documented to be very high in public ones such as

Figure 5: (a) Artisanal diamond miners sift gravels on the Sewa River in Sierra Leone. **(b)** A mixed parcel of rough diamonds from Sierra Leone was produced by such diggers. Programmes such as the GemFair initiative aim to bring certified responsibly produced artisanal diamonds to market, and complement this with blockchain to document the path of the diamonds. Photos by L. E. Cartier.

bitcoin using proof-of-work protocols; see O'Dwyer and Malone, 2014; Orcutt, 2017) must be taken into consideration when deciding what kind of ledger is selected and how it is managed and organised.

A so-called smart contract is software stored in a blockchain that automatically moves digital assets between accounts if pre-required conditions (collaboratively defined by the blockchain's users) are met, and it cannot be unilaterally changed (Iansiti and Lakhani, 2017). Smart contracts are being increasingly explored as solutions for ownership authentication and automatic validation of trades (Kim and Laskowski, 2018). They can potentially provide a huge gain in efficiency (especially with regards to demonstrating compliance and know-your-customer procedures), and they are one of the main reasons why blockchain is being widely investigated as a means of traceability and in logistics (Shrier et al., 2016). Depending on the type of blockchain, users may have transparent insight into the business rules by which the transactions are completed. Therefore blockchain can provide transparency to the regulators and other users who require it, while still providing the privacy and the specific views into the ledger that are relevant for each different type of user. This is an important factor for the gem and jewellery industry, which demands verified, but often anonymised, chain-of-custody solutions.

Blockchain is especially suitable for complex industries (Jansson and Peterson, 2017), and different variations of blockchain have been proposed for diamonds (Abeyratne and Monfared, 2016; Wall, 2016), diamond trading ('Singapore Diamond Investment Exchange…', 2017), jewellery (Irrera, 2018), art (O'Neill, 2018), coloured stones (Branstrator, 2018), minerals (RCS Global, 2017) and many other luxury products (Meraviglia, 2018). The Kimberley Process Certification Scheme has investigated blockchain as a solution for its system of warranties (Sulayem, 2016). The company Everledger recently developed the Diamond Time-Lapse Protocol ('Everledger announces…', 2018) to highlight the individual journey of a diamond that can be followed by a consumer through a smartphone application.

However, a blockchain is only as strong as the data supplied, because blockchain only verifies the data and not the event itself. Therefore, it does not replace robust standards in the supply chain (requiring external validation of data and production practices along with audits). However, it has the strong potential to reinforce claims by providing an immutable record of a product's history that can be verified (through the blockchain), and these data are secured using cryptography. A range of properties and information can be recorded in the blockchain, including: weight, quantity, photos, videos, certification/audits, reports, mine of origin, ownership at each step of the supply chain, workers who handle the material at each step, grade, and other factors. Blockchain clearly has enormous potential in the gem and jewellery industry, but more research is required to understand how the efficiency and transparency it can provide can best be put to use, and whether industry-wide consensus is possible or necessary. Further research is also required to understand how all levels of the supply chain (including artisanal miners) can benefit from traceability opportunities that blockchain technology could provide.

The recent launch of De Beers' GemFair programme with the Diamond Development Initiative (Sanderson, 2018) provides insight into how some key characteristics can be recorded in a blockchain. The programme involves a highly localised partnership with civil society groups in areas of artisanal and small-scale mining (Figure 5), with photographic evidence and verification mechanisms at the digging pit itself. De Beers is also investing heavily in developing a blockchain platform for tracking its diamonds more broadly, and in due course plans to link that platform with GemFair (Sanderson, 2018).

OUTLOOK—WHAT'S NEXT?

The informal and highly fragmented nature of some parts of the gem industry makes full transparency a complex and challenging undertaking. Sorting and aggregation steps in supply chains—in which goods may be sorted in terms of quality rather than origin—may further complicate this endeavour (see Figures 6 and 7). Regulatory requirements and consumer demands for supply chain integrity and knowledge of provenance will push the industry to find solutions. Due diligence and chain-of-custody requirements will continue to grow and, as such, all levels of the trade will need to find solutions to address these traceability and transparency challenges. This may also provide newfound opportunities if, for example, synthetics and treated stones can be separated more clearly from natural/untreated material in the supply chain based on traceability information to verify the ownership and authenticity of gem materials at all stages.

Technological solutions such as blockchain and various tagging methods will become increasingly important as complementary responses to improve chain of custody and provide increased transparency in the supply chain. Blockchain and other tracking methods can also provide much more data and information that are increasingly important to consumers and regulators. Importantly, gemmological science can continue to provide much-needed assistance regarding claims of origin (geographical and whether a gem is natural or synthetic) and whether or not a gem has been treated. A gem's inclusions and their location within the stone can be used to help verify its identity, as well as provide gemmological data that can later be compared to existing chain-of-custody information. The current focus on full mine-to-market traceability may not be as realistic as it has been shown for other sectors, nor may the market necessarily want or require it. For example, rather than focussing all efforts on uniquely tracking a stone from its individual mine, tracing gem materials from specific regions that can be verified through gemmological means may prove to be an alternative and complimentary model (Cartier, 2017).

Country-of-origin determination is not a stand-alone traceability solution, but it offers independent verification of claims made about a gem's locality. This model has also been explored for tin, tungsten and tantalum (coltan) supply chains via the analytical fingerprint method (Schütte et al., 2018). Gemmology can complement and supplement the claims and documentation made by more standard traceability approaches that are inspired from other industries. The informal and highly fragmented nature of the coloured stone industry is likely to place stronger reliance on innovations in traceability rather than common tracking techniques that are more feasible for gold, diamonds and other commodities.

Figure 6: At a processing facility in Hunan, China, freshwater cultured pearls are aggregated from different farms and sorted according to various characteristics. Such processing on the basis of quality rather than source poses a challenge for traceability. Photo by L. E. Cartier.

Figure 7: At an amethyst-cutting workshop in Jaipur, India, rough material is generally purchased and sorted by size and quality rather than according to specific sources. The cutting and polishing of gems is an under-researched bottleneck for traceability. Photo by L. E. Cartier.

REFERENCES

Abduriyim A. and Kitawaki H., 2006a. Applications of laser ablation–inductively coupled plasma–mass spectrometry (LA-ICP-MS) to gemology. *Gems & Gemology*, **42**(2), 98–118, http://doi.org/10.5741/gems.42.2.98.

Abduriyim A. and Kitawaki H., 2006b. Determination of the origin of blue sapphire using laser ablation inductively coupled plasma mass spectrometry (LA-ICP-MS). *Journal of Gemmology*, **30**(1), 23–36, http://doi.org/10.15506/JoG.2006.30.1.23.

Abeyratne S.A. and Monfared R.P., 2016. Blockchain ready manufacturing supply chain using distributed ledger. *International Journal of Research in Engineering and Technology*, **5**(9), 1–10, http://doi.org/10.15623/ijret.2016.0509001.

Ali S.H., 2009. *Treasures of the Earth: Need, Greed, and a Sustainable Future*. Yale University Press, New Haven, Connecticut, USA, 304 pp.

Ali S.H., Giurco D., Arndt N., Nickless E., Brown G., Demetriades A., Durrheim R., Enriquez M.A., Kinnaird J., Littleboy A., Meinert L.D., Oberhänsli R., Salem J., Schodde R., Schneider G., Vidal O. and Yakovleva N., 2017. Mineral supply for sustainable development requires resource governance. *Nature*, **543**(7645), 367–372, http://doi.org/10.1038/nature21359.

Archuleta J.-L., 2016. The color of responsibility: Ethical issues and solutions in colored gemstones. *Gems & Gemology*, **52**(2), 144–160, http://doi.org/10.5741/gems.52.2.144.

Bates R., 2016. Signet wants all its diamonds to come from identified sources. Is that possible? *JCK*, 17 February, www.jckonline.com/editorial-article/signet-wants-all-its-diamonds-to-come-from-identified-sources-is-that-possible, accessed 8 May 2018.

Bechini A., Cimino M.G.C.A., Marcelloni F. and Tomasi A., 2008. Patterns and technologies for enabling supply chain traceability through collaborative e-business. *Information and Software Technology*, **50**(4), 342–359, http://doi.org/10.1016/j.infsof.2007.02.017.

Bernstein L., 1992. Opting out of the legal system: Extralegal contractual relations in the diamond industry. *Journal of Legal Studies*, **21**(1), 115–157, http://doi.org/10.1086/467902.

Bloomfield M.J., 2017. *Dirty Gold: How Activism Transformed the Jewelry Industry*. MIT Press, Cambridge, Massachusetts, USA, 272 pp.

Branstrator B., 2018. Gübelin working to create blockchain for colored stones. *National Jeweler*, 10 January, www.nationaljeweler.com/diamonds-gems/social-issues/6197-guebelin-working-to-create-blockchain-for-colored-stones, accessed 17 May 2018.

Brazeal B., 2017. Austerity, luxury and uncertainty in the Indian emerald trade. *Journal of Material Culture*, **22**(4), 437–452, http://doi.org/10.1177/1359183517715809.

Brundtland G.H., 1987. *Report of the World Commission on Environment and Development: Our Common Future*. United Nations, New York, New York, USA, http://tinyurl.com/yam59pqz, accessed 31 July 2018.

Bui H.A.N., Fritsch E. and Rondeau B., 2012. Geographical origin: Branding or science? *InColor*, No. 19, 30–39.

Bull T., 2016. The grape war of China: Wine fraud and how science is fighting back. In N. Charney, Ed., *Art Crime: Terrorists, Tomb Raiders, Forgers and Thieves*, Palgrave Macmillan, London, 41–56, http://doi.org/10.1007/978-1-137-40757-3_5.

Carter C.R. and Rogers D.S., 2008. A framework of sustainable supply chain management: Moving toward new theory. *International Journal of Physical Distribution & Logistics Management*, **38**(5), 360–387, http://doi.org/10.1108/09600030810882816.

Cartier L.E., 2011. Gemstones. In D.E. Vasey, L. Shen, S.E. Fredericks and S. Thompson, Eds., *Berkshire Encyclopedia of Sustainability, Vol. 4: Natural Resources and Sustainability*, Berkshire Publishing, Great Barrington, Massachusetts, USA, 174–177.

Cartier L.E., 2017. Preserving the heritage of gemstone regions and resources worldwide: Future directions. *Episodes*, **40**(3), 233–236, http://doi.org/10.18814/epiiugs/2017/v40i3/017026.

Cartier L.E., Krzemnicki M.S., Lendvay B. and Meyer J.B., 2018. DNA fingerprinting of pearls, corals and ivory: A brief review of applications in gemmology. *Journal of Gemmology*, **36**(2), 152–160, http://doi.org/10.15506/JoG.2018.36.2.152.

Chesley F.G., 1942. Investigation of the minor elements in diamond. *American Mineralogist*, **27**(1), 20–36.

CIBJO, 2018. CIBJO sets up industry-wide working committee to formulate responsible sourcing guidance for gem and jewellery sectors. CIBJO—The World Jewellery Confederation, Milan, Italy, 8 May, www.cibjo.org/cibjo-sets-up-industry-wide-working-committee-to-formulate-responsible-sourcing-guidance-for-gem-and-jewellery-sectors, accessed 8 May 2018.

Cross J., van der Wal S. and de Haan E., 2010. *Rough Cut: Sustainability Issues in the Coloured Gemstone Industry*. Stichting Onderzoek Multinationale Omdernemingen, Amsterdam, The Netherlands, 44 pp., www.somo.nl/wp-content/uploads/2010/02/Rough-Cut.pdf.

Dalpé C., Hudon P., Ballantyne D.J., Williams D. and Marcotte D., 2010. Trace element analysis of rough diamond by LA-ICP-MS: A case of source discrimination? *Journal of Forensic Sciences*, **55**(6), 1443–1456, http://doi.org/10.1111/j.1556-4029.2010.01509.x.

De Angelis M., Adıgüzel F. and Amatulli C., 2017. The role of design similarity in consumers' evaluation of new green products: An investigation of luxury fashion brands. *Journal of Cleaner Production*, **141**, 1515–1527, http://doi.org/10.1016/j.jclepro.2016.09.230.

Dickinson DeLeon S.W., 2008. Jewels of Responsibility from Mines to Markets: Comparative Case Analysis in Burma, Madagascar and Colombia. M.S. thesis, University of Vermont, Burlington, Vermont, USA, 190 pp.

Eaton-Magaña S. and Shigley J.E., 2016. Observations on CVD-grown synthetic diamonds: A review. *Gems & Gemology*, **52**(3), 222–245, http://doi.org/10.5741/gems.52.3.222.

Everledger announces the industry Diamond Time-Lapse Protocol, 2018. *International Diamond Exchange* (*IDEX*), 22 February, www.idexonline.com/FullArticle?Id=43757, accessed 8 May 2018.

Expert meeting to discuss a new initiative on coloured gemstones traceability and certification of ethical origin, 2013. United Nations Interregional Crime and Justice Research Institute, Turin, Italy, 11 April, www.unicri.it/news/article/2013-04-11_Expert_meeting_Gemstones, accessed 8 May 2018.

Financial Action Task Force, 2013. Money laundering and terrorist financing through trade in diamonds. Egmont Group of Financial Intelligence Units, Paris, France, 148 pp., www.fatf-gafi.org/media/fatf/documents/reports/ML-TF-through-trade-in-diamonds.pdf.

Future of Fish, FishWise and Global Food Traceability Center, 2018. *Seafood Traceability Glossary—A Guide to Terms, Technologies, and Topics*, 12 pp., http://futureoffish.org/sites/default/files/docs/resources/Seafood%20Traceability%20Glossary_download.pdf.

Gannon F., 2004. Editorial: Experts, truth and scepticism. *EMBO reports*, **5**(12), 1103, https://doi.org/10.1038/sj.embor.7400302.

Giuliani G., Chaussidon M., Schubnel H.-J., Piat D.H., Rollion-Bard C., France-Lanord C., Giard D., de Narvaez D. and Rondeau B., 2000. Oxygen isotopes and emerald trade routes since antiquity. *Science*, **287**(5453), 631–633, http://doi.org/10.1126/science.287.5453.631.

Global Witness, 2015. *Jade: Myanmar's "Big State Secret"*. Global Witness, London, 127 pp., www.globalwitness.org/en/campaigns/oil-gas-and-mining/myanmarjade.

Global Witness, 2016. *War in the Treasury of the People: Afghanistan, Lapis Lazuli and the Battle for Mineral Wealth*. Global Witness, London, 100 pp., www.globalwitness.org/en/campaigns/conflict-minerals/war-treasury-people-afghanistan-lapis-lazuli-and-battle-mineral-wealth.

Gübelin E.J. and Koivula J.I., 1986. *Photoatlas of Inclusions in Gemstones*. ABC Edition, Zurich, Switzerland, 532 pp.

Guillong M. and Günther D., 2001. Quasi 'non-destructive' laser ablation-inductively coupled plasma-mass spectrometry fingerprinting of sapphires. *Spectrochimica Acta Part B: Atomic Spectroscopy*, **56**(7), 1219–1231, http://doi.org/10.1016/s0584-8547(01)00185-9.

Hänni H.A., 1990. A contribution to the distinguishing characteristics of sapphire from Kashmir. *Journal of Gemmology*, **22**(2), 67–75, http://doi.org/10.15506/JoG.1990.22.2.67.

Hänni H.A., 1994. Origin determination for gemstones: Possibilities, restrictions and reliability. *Journal of Gemmology*, **24**(3), 139–148, http://doi.org/10.15506/JoG.1994.24.3.139.

Hänni H.A. and Cartier L.E., 2013. Tracing cultured pearls from farm to consumer: A review of potential methods and solutions. *Journal of Gemmology*, **33**(7), 239–245, http://doi.org/10.15506/JoG.2013.33.7.239.

Human Rights Watch, 2018. *The Hidden Cost of Jewelry: Human Rights in Supply Chains and the Responsibility of Jewelry Companies*. Human Rights Watch, New York, New York, USA, 99 pp., www.hrw.org/sites/default/files/report_pdf/jewellery0218_web_0.pdf.

Iansiti M. and Lakhani K.R., 2017. The truth about blockchain. *Harvard Business Review*, **95**(1), 118–127.

IndustriALL, Construction, Forestry, Mining and Energy Union, United Steelworkers, Earthworks and MiningWatch Canada, 2013. *More Shine Than Substance: How RJC Certification Fails to Create Responsible Jewelry*, 124 pp., https://miningwatch.ca/sites/default/files/more-shine-than-substance-final.pdf.

Irrera A., 2018. Jewelry companies team up with IBM on blockchain platform. Reuters, 26 April, www.reuters.com/article/us-blockchain-diamonds/jewelry-companies-team-up-with-ibm-on-blockchain-platform-idUSKBN1HX1BD, accessed 2 June 2018.

Jansson F. and Petersen O., 2017. Blockchain Technology in Supply Chain Traceability Systems. M.S. thesis, Lund University, Sweden, 93 pp.

Jeppsson A. and Olsson O., 2017. Blockchains as a Solution for Traceability and Transparency. M.S. thesis, Lund University, Sweden, 102 pp.

Kim H.M. and Laskowski M., 2018. Toward an ontology-driven blockchain design for supply-chain provenance. *Intelligent Systems in Accounting, Finance and Management*, **25**(1), 18–27, http://doi.org/10.1002/isaf.1424.

Krzemnicki M.S., 2007. Origin determination of gemstones: Challenges and perspectives. *InColor*, Winter, 6–11.

Lombe J.E., Gilbert S., Levin E., Pandya A. and Runci M., 2015. *Due Diligence for Responsible Sourcing of Precious Stones*. Sustainable & Responsible Solutions, Suffolk, 85 pp., www.jewelers.org/images/files/psmswg-report.pdf.

Meraviglia L., 2018. Technology and counterfeiting in the fashion industry: Friends or foes? *Business Horizons*, **61**(3), 467–475, http://doi.org/10.1016/j.bushor.2018.01.013.

Meyer J.B., Cartier L.E., Pinto-Figueroa E.A., Krzemnicki M.S., Hänni H.A. and McDonald B.A., 2013. DNA fingerprinting of pearls to determine their origins. *PLoS ONE*, **8**(10), article e75606, 11 pp., http://doi.org/10.1371/journal.pone.0075606.

Mol A.P.J., 2015. Transparency and value chain sustainability. *Journal of Cleaner Production*, **107**, 154–161, http://doi.org/10.1016/j.jclepro.2013.11.012.

Nash J., Ginger C. and Cartier L., 2016. The sustainable luxury contradiction: Evidence from a consumer study of marine-cultured pearl jewellery. *Journal of Corporate Citizenship*, **63**, 73–95, http://doi.org/10.9774/GLEAF.4700.2016.se.00006.

Norton T., Beier J., Shields L., Househam A., Bombis E. and Liew D., 2014. *A Guide to Traceability: A Practical Approach to Advance Sustainability in Global Supply Chains*. United Nations Global Compact and BSR, 45 pp., www.bsr.org/reports/BSR_UNGC_Guide_to_Traceability.pdf.

O'Dwyer K.J. and Malone D., 2014. Bitcoin mining and its energy footprint. *25th IET Irish Signals & Systems Conference 2014 and 2014 China-Ireland International Conference on Information and Communications Technologies (ISSC 2014/CIICT 2014)*, Limerick, Ireland, 26–27 June, 280–285.

O'Neill J., 2018. Why the art world is looking to blockchain for tracking and provenance. *Medium*, 11 May, https://medium.com/ethereum-art-collective/why-the-art-world-is-looking-to-blockchain-for-tracking-and-provenance-f7329618f6f7, accessed 17 May 2018.

OECD, 2016. *OECD Due Diligence Guidance for Responsible Supply Chains of Minerals from Conflict-Affected and High-Risk Areas*, 3rd edn. OECD Publishing, Organisation for Economic Cooperation and Development, Paris, France, 120 pp., https://doi.org/10.1787/9789264252479-en.

OECD, 2018. *OECD Due Diligence Guidance for Responsible Business Conduct*. Organisation for Economic Cooperation and Development, Paris, France, 100 pp., http://mneguidelines.oecd.org/OECD-Due-Diligence-Guidance-for-Responsible-Business-Conduct.pdf.

Ogden J.M., 2017. Rethinking laboratory reports for the geographical origin of gems. *Journal of Gemmology*, **35**(5), 416–423, http://doi.org/10.15506/JoG.2017.35.5.416.

Orcutt M., 2017. Blockchains use massive amounts of energy—But there's a plan to fix that. *MIT Technology Review*, 16 November, www.technologyreview.com/s/609480/bitcoin-uses-massive-amounts-of-energybut-theres-a-plan-to-fix-it, accessed 26 July 2018.

Raden A., 2016. *Stoned: Jewelry, Obsession, and How Desire Shapes the World*. Ecco Press, New York, New York, USA, 368 pp.

Rankin A.H., Greenwood J. and Hargreaves D., 2003. Chemical fingerprinting of some East African gem rubies by laser ablation ICP-MS. *Journal of Gemmology*, **28**(8), 473–482, http://doi.org/10.15506/JoG.2003.28.8.473.

RCS Global, 2017. *Blockchain for Traceability in Minerals and Metals Supply Chains: Opportunities and Challenges*. International Council on Mining & Metals, London, 20 pp., www.icmm.com/website/publications/pdfs/responsible-sourcing/171220_rcs-global_-icmm_blockchain_final.pdf.

RESP, 2016. *Challenges to Advancing Environmental and Social Responsibility in the Coloured Gems Industry*. Responsible Ecosystems Sourcing Platform, Geneva, Switzerland, 44 pp.

RJC, 2012. *Frequently Asked Questions (FAQ's): Responsible Jewellery Council Chain of Custody Certification*. Responsible Jewellery Council, London, 9 pp., www.responsiblejewellery.com/files/FAQs-for-Chain-of-Custody-Certification-2012.pdf.

RJC, 2017. *Annual Progress Report 2017*. Responsible Jewellery Council, London, 28 pp., www.responsiblejewellery.com/files/RJC_AnnualProgressReport_17LR.pdf.

RJC to expand scope to include colored stones, 2016. *National Jeweler*, 22 March, www.nationaljeweler.com/diamonds-gems/social-issues/4047-rjc-to-expand-scope-to-include-colored-stones, accessed 28 May 2018.

Rossman G.R., 2009. The geochemistry of gems and its relevance to gemology: Different traces, different prices. *Elements*, **5**(3), 159–162, http://doi.org/10.2113/gselements.5.3.159.

Sanderson H., 2018. De Beers to pilot digital programme in Sierra Leone to sell ethically sourced diamonds. *Financial Times*, 19 April, www.ft.com/content/8ff2414c-43d6-11e8-93cf-67ac3a6482fd, accessed 30 July 2018.

Schroeder R.A., 2010. Tanzanite as conflict gem: Certifying a secure commodity chain in Tanzania. *Geoforum*, **41**(1), 56–65, http://doi.org/10.1016/j.geoforum.2009.02.005.

Schütte P., Melcher F., Gäbler H.-E., Sitnikova M., Hublitz M., Goldmann S., Schink W., Gawronski T., Ndikumana A. and Nziza L., 2018. *The Analytical Fingerprint (AFP): Method and Application Process Manual Version 1.4*. Federal Institute for Geosciences and Natural Resources, Hannover, Germany, 37 pp., www.bgr.bund.de/EN/Themen/Min_rohstoffe/CTC/Downloads/AFP_Manual.pdf?__blob=publicationFile&v=6.

Schwägele F., 2005. Traceability from a European perspective. *Meat Science*, **71**(1), 164–173, http://doi.org/10.1016/j.meatsci.2005.03.002.

Segura O., 2015. Gem Notes: Pearl marking: An innovative non-destructive method. *Journal of Gemmology*, **34**(6), 478–479.

Shor R., 2013. Auction houses: A powerful market influence on major diamonds and colored gemstones. *Gems & Gemology*, **49**(1), 2–15, http://doi.org/10.5741/gems.49.1.2.

Shortell P. and Irwin E., 2017. *Governing the Gemstone Sector: Lessons from Global Experience*. Natural Resource Governance Institute, New York, New York, USA, 72 pp., https://resourcegovernance.org/sites/default/files/documents/governing-the-gemstone_sector-lessons-from-global-experience.pdf.

Shrier D., Wu W. and Pentland A., 2016. *Blockchain & Infrastructure (Identity, Data Security)*. Massachusetts Institute of Technology, Cambridge, Massachusetts, USA, 18 pp., www.getsmarter.com/career-advice/wp-content/uploads/2017/07/mit_blockchain_and_infrastructure_report.pdf.

Singapore Diamond Investment Exchange (SDiX) partners with Kynetix and Everledger to trial first-ever blockchain verification and record-keeping service for diamond trading, 2017. Singapore Diamond Investment Exchange, Singapore, 15 June, www.sdix.sg/singapore-diamond-investment-exchange-sdix-partners-kynetix-everledger-trial-first-ever-blockchain-verification-record-keeping-service-diamond-trading, accessed 26 July 2018.

Solomon F. and Nicholls G., 2010. *Chain-of-Custody in the Diamond and Gold Jewellery Supply Chain – Issues and Options*. Responsible Jewellery Council, London, 11 pp., www.responsiblejewellery.com/files/RJC_Chain_custody_discn_paper_19_04_2010.pdf.

Spencer R.D., Ed., 2004. *The Expert Versus the Object: Judging Fakes and False Attributions in the Visual Arts*. Oxford University Press, Oxford, 268 pp.

Sulayem A.B., 2016. *Kimberley Process: Mid-term Report*. Kimberley Process, 24 pp., www.kimberleyprocess.com/en/system/files/documents/kimberley_process_mid-term_report.pdf.

Theodosi N., 2017. Gemfields partners with Gübelin Gem Lab on new emerald traceability technology. *WWD*, 27 March, https://wwd.com/fashion-news/fashion-scoops/gemfields-partners-gubelin-gem-lab-emerald-traceability-technology-10851799, accessed 18 May 2018.

Walker S., 2017. Diamond miners respond. *Engineering and Mining Journal*, **218**(9), 58–66.

Wall M., 2016. How blockchain tech could change the way we do business. BBC, 22 January, www.bbc.com/news/business-35370304, accessed 8 May 2018.

Wang H.A.O. and Krzemnicki M.S., 2016. System for marking and analysing gemstones. European Patent Application EP 3 305 461 A1, filed 4 October.

Wang H.A.O., Krzemnicki M.S., Chalain J.-P., Lefèvre P., Zhou W. and Cartier L.E., 2016. Simultaneous high sensitivity trace-element and isotopic analysis of gemstones using laser ablation inductively coupled plasma time-of-flight mass spectrometry. *Journal of Gemmology*, **35**(3), 212–223, http://doi.org/10.15506/JoG.2016.35.3.212.

What is CSR?, 2018. United Nations Industrial Development Organization, Vienna, Austria, www.unido.org/our-focus/advancing-economic-competitiveness/competitive-trade-capacities-and-corporate-responsibility/corporate-social-responsibility-market-integration/what-csr, accessed 11 May 2018.

The Authors

Dr Laurent E. Cartier FGA[1,2], Dr Saleem H. Ali[3] and Dr Michael S. Krzemnicki FGA[1]

[1] Swiss Gemmological Institute SSEF, Aeschengraben 26, 4051 Basel, Switzerland

[2] Institute of Earth Sciences, University of Lausanne, 1015 Lausanne, Switzerland

[3] University of Delaware, Department of Geography and Center for Energy and Environmental Policy, 220 Pearson Hall, Newark, Delaware 19716-2514, USA; Sustainable Minerals Institute, University of Queensland, Australia

Acknowledgements

The authors thank Pat Syvrud (University of Delaware) for discussions on initiatives in the industry and reviewing an earlier version of this article. Ron Martinez (Transium.io) is thanked for discussions on blockchain. Three peer reviewers are thanked for their constructive suggestions and comments that helped improve the focus and detail of this article. The information on specific initiatives (especially Table II) was prepared from publicly available sources and data, and any errors of interpretation or omissions are unintentional and are the responsibility of the authors.

Figure 1: These cabochons (up to 40 mm long) and rough pieces of Bumble Bee Stone (BBS) were produced in 2017. The samples are more orange than previously mined material that contained yellow areas. Photo by J. Ivey.

Bumble Bee Stone: A Bright Yellow-to-Orange and Black Patterned Gem from West Java, Indonesia

Emmanuel Fritsch and Joel Ivey

ABSTRACT: Bumble Bee Stone (BBS) is a bright yellow-to-orange and black patterned gem material. Although sometimes referred to as a jasper, it is actually a carbonate-rich rock rather than a silica-based gem. It is mined from sulphide-bearing veins near an active volcano in West Java, Indonesia. Its most remarkable characteristic is its bright yellow colour, which is caused by the presence of an unexpected sulfide, pararealgar. The orange colour in some samples consists of a mixture of pararealgar with realgar. Both minerals are polymorphs of As_4S_4, arsenic sulphide. Areas of black colouration are due to aggregates of micron-sized pyrite crystals ('sooty' pyrite). The successive growth layers, when cut through in different orientations, give rise to a variety of attractive patterns. BBS has been mined for the past 15 years, and new veins are still occasionally found.

The Journal of Gemmology, **36**(3), 2018, pp. 228–238, http://doi.org/10.15506/JoG.2018.36.3.228

Figure 2: The three polished specimens of BBS on the left (12–26 cm long) show spectacular orbicular (also called 'bull's-eye') patterns with a strong colour contrast. The typical bull's-eye pattern ranges from 10 to 14 mm in diameter, but may be much larger (see Figure DD-1 in *The Journal*'s online Data Depository). Such pieces are derived by cutting across botryoidal areas such as shown by the BBS slab on the right. The colourless calcite crystals (up to ~3 cm long) induce the botryoidal structure in the overlying sulphide-bearing layers. Photos by J. Ivey.

An attractive, generally opaque stone patterned in bright yellow-to-orange and black has been mined in Indonesia since 2003. It has been difficult for vendors to agree on a name for this unique material, and examples include Bumble Bee Stone (hereafter abbreviated BBS), 'Bumble Bee Jasper', 'Mustard Jasper' and 'Eclipse Jasper' (e.g. Overlin, 2014; Figures 1 and 2). Its main attraction is its saturated yellow-to-orange colour, as well as the striking contrast formed by black bands in the material. Other colours may be present, such as grey to near-white or near-colourless. Some pieces show a desaturated greyish yellow colour that is reminiscent of some mustards, hence the 'Mustard Jasper' appellation (Figure 3).

The term *jasper* was identified as a misnomer early on, as the material is a carbonate-rich rock (Serras Hermann, 2013). Bumble Bee Stone is easy to fashion, as its Mohs hardness is 5 or below (Overlin, 2014). The bright yellow-to-orange colouration is said to come from orpiment and realgar, which are both arsenic sulphides (raising the question about possible toxicity of the dust produced during fashioning), while the black layers are reportedly manganese rich (Serras Hermann, 2013).

Very few such opaque bright yellow-to-orange gem materials are known, with the possible exception of the little known Forcherite, a bright yellow variety of opal from Austria (Bojar and Taucher, 1994). In addition, opaque crusts of bright yellow opal are known from the town of Saint Nectaire in central France (Gaillou, 2006). Also, some unusual agates displaying yellow-to-orange and grey to near-colourless layers have been found in Xuanhau, Hebei Province, China (Meng et al., 2016).

In addition to its colouration, another interesting aspect of BBS is its range of patterns. Pieces with irregular striping are possibly the easiest to find on the market, whereas homogeneous yellow cabochons are quite rare. An orbicular variety is the most sought after, obtained by slicing across botryoidal concretions (Figure 2). Other eye-catching landscape and human-like patterns can be obtained by cutting the material at different angles. Some rare pieces may look like a volcano, which is reminiscent of the volcanic origin of this gem (see cover image of this issue).

Figure 3: These cabochons show various textures and colours, with typical 'Mustard Jasper' corresponding to the yellowish grey pieces. The orange piece in the centre is sample no. 1877, measuring 20 × 19 × 4 mm. Photo by Olivier Segura.

Figure 4: Eddie, a cutter at the CV Anugrah Alam workshop in Sukabumi, admires a 12.7 cm sphere of BBS he just fashioned (left). The bangle on the right was carved from a single piece of BBS. Photos by J. Ivey.

As it is opaque, BBS is mostly fashioned as cabochons, plaques or polished blocks for decoration. The cabochons are flat, and are often oval but also free-form. They typically measure a few centimetres across. Many have been cut into matched pairs extracted from the same piece of rough. Recently, several spheres have been fashioned, and even a hololith bangle was made from BBS (Figure 4).

This article reports on the location, geology and gemmological properties of BBS, focusing on the cause of its extraordinary colouration.

LOCATION

The mining area for BBS is situated on the lower slopes of an active volcano, Mt Ciremai (or Cereme), which is located about 25 km south-west of the coastal town of Cirebon in West Java (Figure 5). The diggings are located a few kilometres south of the resort town of Kuningan and about 20 km from the volcano's summit. Its eruptions are not frequent, but they have produced dangerous explosions and lahars. The summit area is

Figure 5: The BBS deposit is located at the base of Mt Ciremai, an active volcano, in the vicinity of Kuningan, West Java, Indonesia.

Figure 6: (a) Peak extraction of BBS occurred over a six-month period in mid-2011 with a rented excavator. Here, on the opposite side of the muddy pool, the flat, smooth, grey surface represents the outside surface of the vein. **(b)** Mt Ciremai, seen here, is an active stratovolcano where the world's only known deposit of BBS is found. **(c)** The BBS vein consists of layers of bright yellow sulphides and black areas coloured by sooty pyrite. Photos by J. Ivey.

formed by a caldera about 1 km in diameter. It is the highest peak in West Java, culminating at 3,078 m. The area is covered by the small Mount Ciremai National Park (Taman Nasional Gunung Ciremai; 155 km^2). The volcano may be climbed by hikers, but care is required.

HISTORY AND PRODUCTION

Some pieces of BBS initially appeared on the Jakarta market in 2003. The first rough material seen by one of the authors (JI) around 2005 was likely obtained close to the surface. It was a flat wedge with alternating bands of dusty yellow and dark grey (see Figure DD-2 in the online data depository on *The Journal*'s website). These bands were narrow (3–5 mm) and relatively straight. Although the name 'Bumble Bee' came immediately to mind, the colour contrast was not as striking as the deeper-mined material seen on the market today. A 50 kg sample brought to the gem shows in Tucson, Arizona, USA in 2005 was enthusiastically greeted by buyers, and was sold as 'Bumble Bee Jasper'. This was considered a good commercial name, even though many wholesalers were aware the gem was not silica-based. Unfortunately the material proved to be too soft for fashioning, and demand waned for pieces mined near the surface. In Indonesia, initial enthusiasm spurred the locals to dig up a large pile of the BBS, and it was sold in nearby towns and stone markets in Jakarta, and even exported to Bali. An American dealer (Zee Haag of Tucson, Arizona) bought up the villagers' stockpile and tried re-introducing it as 'Eclipse Jasper' around 2008. Around that time, gem dealer Paul Ingram in Bali marketed BBS in his customer newsletter as 'Mustard Jasper'.

In October 2010, locals started hand digging a small vein that ran across a hilltop in the area. Of the approximately 2 tonnes of material that was produced, 500 kg was brighter and showed higher contrast and more colourful patterns than the original surface rough. At that time, it was estimated that about 10 tonnes of BBS could be recovered from the deposit.

In May 2011, the landowner subcontracted an excavator from a road crew. In several months, they opened up access to one of the larger veins of BBS by removing the wall rock from one side to a depth of ~15 m (Figure 6a).

Figure 7: BBS rough material is washed and sorted (top). The largest piece of BBS to date was extracted in 2011 and weighed 222 kg (bottom). Photos by J. Ivey.

It appeared that as mining progressed deeper, the material became harder and showed more attractive patterns. The pyroclastic wall rock (andesitic tuff) was carefully chiselled off as much as possible. Consisting of 70%–80% lapidary material, 6 tonnes of BBS were collected from 2011 to 2013 (e.g. Figure 7). Container loads of lower-grade material were purchased by Korean and Taiwanese stone brokers.

In 2013, several large blocks containing narrow BBS veins were mined. They were interesting as specimens, but most of them were too fragile to process into lapidary rough. Some were sent to Bali to polish into free-form pieces like those in Figure 2. This material spurred local dealers to visit the mining area and buy the remaining stockpile of more than 110 tonnes of rough, which was shipped to Bali, and then onward to Hong Kong, Australia and the USA.

In the past few years only hand digging has taken place, but several new veins have been discovered across the hill, and mining still continues as of this writing. Although production varies according to season (greater in the dry period than in the rainy season from November to March), currently up to ~500 kg/month is being mined, of which about 30% is BBS vein material. The estimated total amount of rough BBS produced so far exceeds 500 tonnes. This includes a considerable amount of volcanic wall rock, and we estimate that the actual amount of lapidary material is about 150 tonnes.

There are several local workshops in the Sukabumi area of West Java that cut and polish BBS as their main product. This material is still very common on the local gem market and in tourist shops around Indonesia. Much BBS is actively traded on Instagram and Facebook by young locals. Indonesians highly value domestic gem materials, and they are often willing to pay more than buyers elsewhere.

LOCAL GEOLOGY

BBS formed within a solfatara (a fumarole that vents gases rich in sulphur) occurring in close proximity to the Mt Ciremai volcano (Figure 6b). This type of vent is common near active stratovolcanoes, and results from the heating of circulating groundwaters containing various elements or compounds extracted from the volcanic system—in this case iron, sulphur, calcium carbonate and arsenic. Such a system produces abundant 'sooty' pyrite, consisting of very small crystals of the iron sulphide, crystallising rapidly near the surface, which looks like black soot. As the gases escape the solfatara, minerals are deposited as more-or-less regular bands in fractures within the volcanic rock, which is here comprised of fine-bedded volcanic ash and intercalated pyroclastic tuff (an accumulation of volcanic ejecta of varied size). The veins are near vertical, with individual colour bands rarely exceeding 5 cm (e.g. Figure 6c). The tuffaceous wall rock contains marcasite, an iron sulphide that is unstable when exposed to air and moisture. After about 1–2 weeks in this environment, the breakdown of marcasite facilitates the separation of BBS vein material from its volcanic host rock.

BBS is thus not formed from 'a mixture of Indonesian volcano lava and sediment' (Overlin, 2014), but is the indirect result of volcanic activity.

MATERIALS AND METHODS

We analysed eight cabochons ranging from 9.48 to 96.90 ct, representing typical colours of BBS. The specimens were acquired on the open market: Nos. 1877–1882 were sold with others (Figure 3) as a necklace by Marcus McCallum, London; others were purchased at the Tucson gem shows or in Bangkok, Thailand. The samples used in this study are listed in Table I and illustrated in Figure 8.

Figure 8: BBS samples used for this study are shown here. From left to right and top to bottom: nos. 1591, 1877–1882 and 2396; see Table I for weights and dimensions. Photo by Philippe Deuxgniards.

Observations were undertaken using a Leica MZ6 binocular microscope with Nossigem gemmological observation attachments. SG values were measured with a calibrated Mettler Toledo XS104 electronic scale. Fluorescence was tested with a Vilber Lourmat UV lamp with a power of 6 W per tube emitting long-wave (365 nm) or short-wave (254 nm) radiation, with the stone being placed 7 cm from the lamp.

Visible-range absorption spectra were obtained using a PerkinElmer Lambda 1050 spectrometer in the range of 400–800 nm with a spectral bandwidth of 1 nm for a sampling of 1 nm. The spectra were obtained in reflectance mode on an accessory using a 150 mm integrating sphere with an InGaAs detector. Raman spectra were obtained using a Bruker MultiRAM Fourier-transform Raman spectrometer, with a 1064 nm Nd:YAG laser at a maximum power of 2 W. The spectral resolution was set at 4 cm^{-1}.

Observations and micro-chemical analyses were conducted with a JEOL 7600F scanning electron microscope equipped with an energy-dispersive spectrometer. Two additional BBS samples (not listed in Table I) were sacrificed for this analysis, as they needed to be metallised with platinum and the coating cannot be completely removed.

Table I: BBS samples and methods used for this report.

Sample number	Main colour(s)	Weight (ct)	Dimensions (mm)	Tests/Analyses
1591	Yellow and black	96.90	40.0 × 31.0 × 10.6	SG, microscopy, and Raman and visible-range spectroscopy
1877	Orange	9.48	20.0 × 19.0 × 4.0	SG, microscopy, and Raman and visible-range spectroscopy
1878	Yellow	11.29	19.0 × 13.0 × 5.2	SG, microscopy and Raman spectroscopy
1879	Black and yellow	10.62	19.0 × 13.0 × 5.0	SG, microscopy, and Raman and visible-range spectroscopy
1880	'Mustard'	10.61	19.0 × 14.0 × 5.5	SG, microscopy, and Raman and visible-range spectroscopy
1881	Yellow and orange	10.22	18.0 × 13.0 × 5.2	SG and visible-range spectroscopy
1882	Orange and black	11.22	20.0 × 13.0 × 5.2	SG and visible-range spectroscopy
2396	Yellow	50.36	40.0 × 30.0 × 5.3	Microscopy and Raman spectroscopy

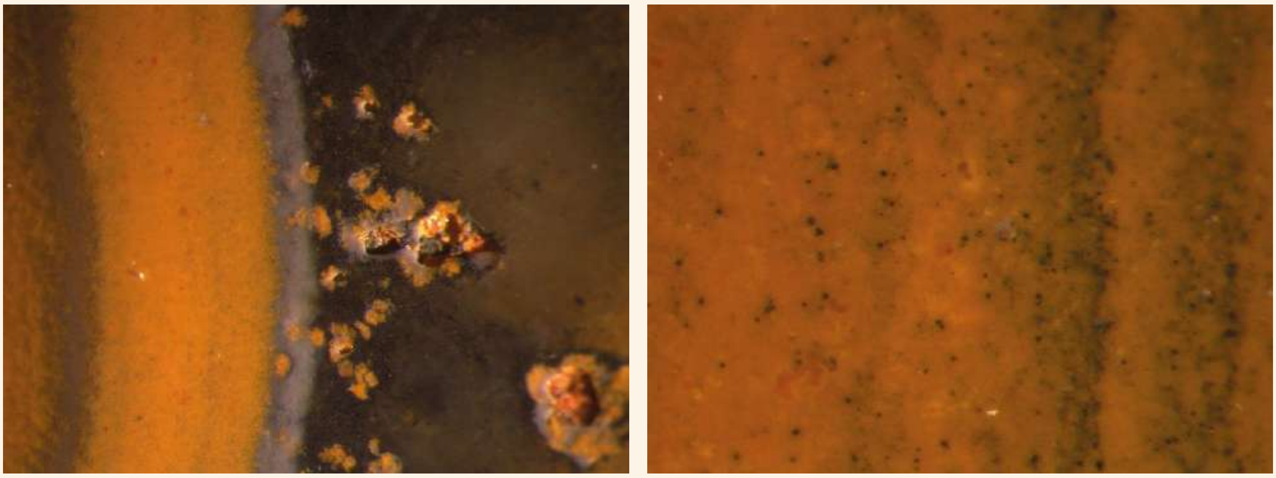

Figure 9: The pulverulent appearance of the colour banding in BBS is shown here under magnification in sample no. 1591. Left: Yellow-to-orange pigment is disseminated within the carbonate matrix, forming colour bands, within which micro-geodes are found. Right: The black pigment forms minute discs that are resolvable only at higher magnification. Photomicrographs by E. Fritsch; image width 3 mm (left) and 6 mm (right).

RESULTS

Refractive index values were difficult to measure because of the material's porosity. Some attempts were made to obtain a spot measurement, but the results were so variable that we decided not to use them. Specific gravity varied between 2.42 and 2.74; the average of seven measurements was 2.57. When exposed to the UV lamp, part of each sample (corresponding to transparent colourless areas) emitted some yellow fluorescence, while other parts remained inert; the yellow luminescence was slightly stronger in long-wave UV.

Bubbles appeared when a drop of diluted hydrochloric acid was placed on the surface, confirming that this material is carbonate rich. Therefore, it is not jasper, which is an opaque form of microcrystalline quartz.

Magnification

As the material is almost completely opaque, it does not show inclusions *per se*. However, when examined with the binocular microscope, the appearance was that of coloured powders cemented in the carbonate matrix (Figure 9). The black-appearing areas were due to the presence of many black dots; the larger ones formed discs (Figure 9, right). Small cavities were actually micro-geodes; many contained very small crystals that were orange or tended towards red. The overall colour of the samples varied according to the proportion and overall abundance of yellow, orange and black pigments in an otherwise colourless (transparent) or white (opaque) matrix.

Visible-range Absorption Spectroscopy

The visible-range reflectance spectra of all colours of BBS, except black, had an overall sigmoid shape (Figure 10). In general, the point of inversion of such a pattern marks the 'absorption edge' of a particular pigment. The steeper the slope at this point, the more saturated the colour. The higher the maximum of reflectance, the more luminous the colour appears, as more light is reflected towards the eye. In addition, the higher the step, the brighter the colour (more light participates in the perception of the colour).

In BBS, the absorption edge was at ~530 nm for the yellow areas. Thus, the colour perceived is a combination of all wavelengths above 530 nm (green), which is observed as yellow. The maximum reflectance was over 80% and the edge was roughly 50% high, although there were slight variations in the position of the absorption edge and in the slope at the inversion point within the bright yellow samples. The edge shifted towards 550 nm in the orange areas (again, see Figure 10), as is logical (less yellow equates to more red), still with a fairly high step of about 40% reflectance.

Black areas provided a nearly flat spectrum at about 35% reflectance, which is low (and subsequently, dark). 'Mustard' samples showed a maximum reflectance of about 50% and an edge height of approximately 15%. Both of these values are much lower than for the bright yellow areas, corresponding to the less saturated and luminous appearance of the 'mustard' samples.

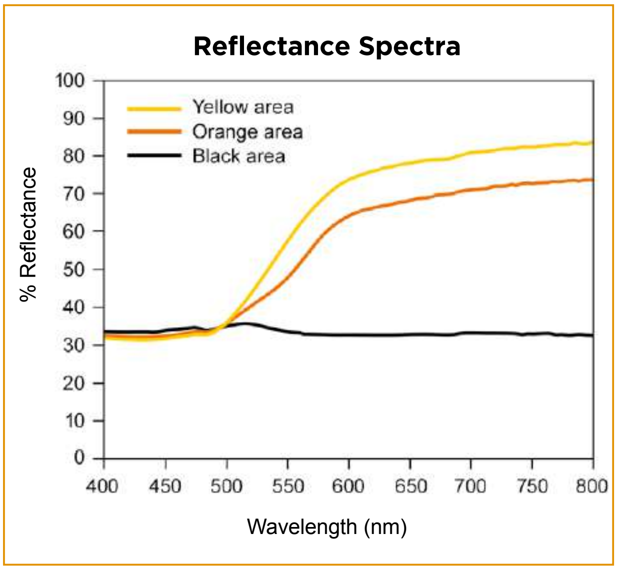

Figure 10: Visible-range reflectance spectra are shown for various coloured areas of BBS. The yellow regions have an absorption edge at ~530 nm, which is shifted towards 550 nm in the orange areas. The black portions show a nearly flat spectrum.

Raman Spectroscopy

The Raman spectra of all analysed samples of BBS consistently presented bands for calcite at about 285 and 160 cm^{-1} (Figure 11), indicating calcite as the major carbonate mineral present in this material. We obtained aragonite bands in only one part of one orange sample. Accordingly, we contend that calcite is the near-colourless transparent to white opaque matrix material seen in many pieces.

In 'mustard'-to-yellow parts of BBS, additional major bands were recorded at about 346, 284, 233 and 157 cm^{-1} (Figure 11). They correspond to pararealgar, which has the formula As_4S_4. It is a bright yellow monoclinic polymorph of realgar, a more common and better-known red arsenic sulphide, which is also monoclinic but with a different class of symmetry.

The Raman spectrum of realgar dominated the bright orange areas (Figure 11) and the reddish crystals in the micro-geodes mentioned above, with main peaks at approximately 355, 221, 194 and 184 cm^{-1}. It had a much higher Raman scattering intensity than pararealgar, thus it dominated the spectrum of a mixture of both polymorphs. As such, the orange areas appeared to be a mixture of pararealgar and realgar. The signal for orpiment, As_2S_3, previously reported as one of the BBS pigments, was looked for but not found.

In the black areas, a small Raman signal appeared at about 378 cm^{-1}. It was clearly not related to the calcite matrix. The closest signal we could find is pyrite, FeS_2, which has a strong doublet at 385 and 355 cm^{-1}. If one broadens the doublet significantly, it would give a single peak at about 378 cm^{-1}. This signal is difficult to attribute to manganese oxides, previously deemed as the possible origin of the black colour, as this class of black minerals has its most intense Raman bands at positions very different from 378 cm^{-1}.

Scanning Electron Microscopy and Microanalysis

Two pieces of BBS were mounted for this technique, and yellow, orange, and near-colourless areas were marked for observation and microanalysis, as well as the black disc-like particles. The nearly ubiquitous presence of Ca confirmed that the material is mostly calcite, although the consistent presence of a small Mg peak suggested it was a slightly magnesian calcite.

Yellow-to-orange areas were rich in S and As. The As-bearing particles, which were easy to recognise in backscattered electron images because of their very light tone, were of irregular shape and measured ~1–20 μm (see Figure DD-3 in *The Journal*'s online Data Depository). Because of their small or irregular nature and the abundance of calcite, no precise quantitative analysis could be performed, but various attempts were consistent with an overall composition of arsenic sulphide corresponding to the yellow-to-orange colouration. This supports the identification of pararealgar and realgar by Raman analysis.

Finally, the black discs were composed of circular aggregates with maximum diameters ranging from ~5 to 30 μm (Figure 12, left). They were composed

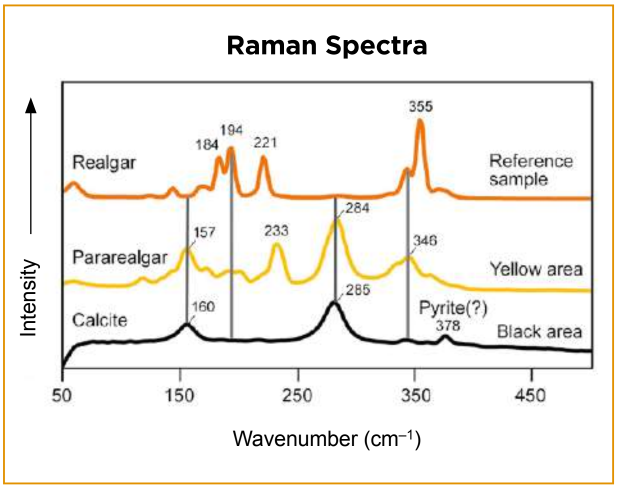

Figure 11: The Raman spectra of the BBS samples tested always showed peaks for calcite, with additional features corresponding to pararealgar and realgar in yellow and orange areas. The spectrum shown here for realgar is from a reference crystal, as no area of BBS we analysed consisted of pure realgar.

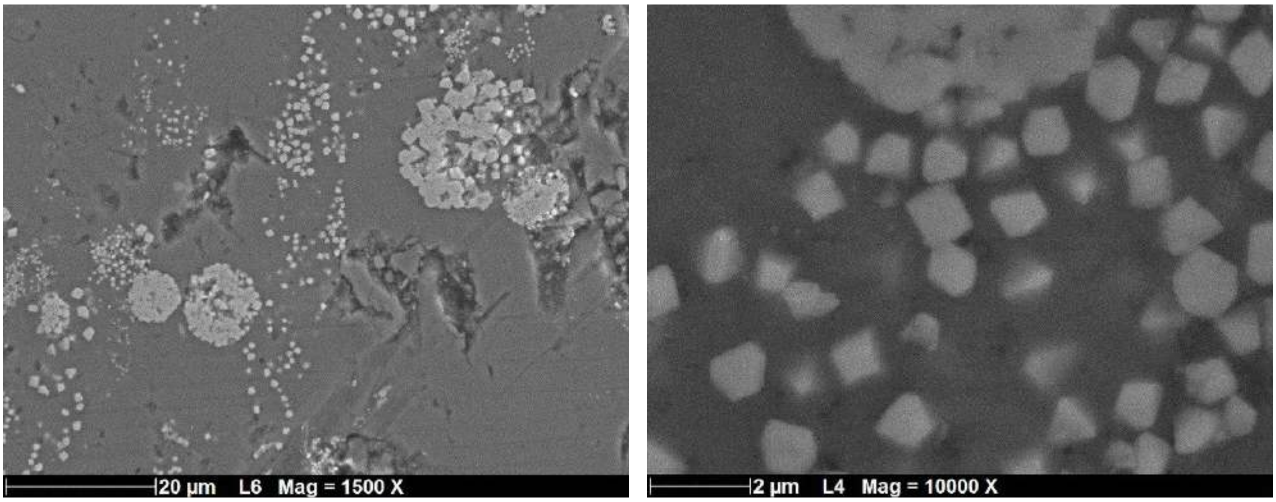

Figure 12: The black discs seen in the binocular microscope are actually aggregates of small pyrite crystals (left, light grey areas). The pyrite has a variety of micro-morphologies, ranging from cubic to octahedral (right). Micrographs by E. Fritsch.

of micrometre-sized crystals identified as pyrite. Curiously their morphology varied, from nearly cubic (square faces) to cubo-octahedral (pseudo-hexagonal faces) to octahedral (triangular faces), as illustrated in Figure 12-right. This is reminiscent of framboidal pyrite. The term *framboid* describes an aggregation of uniformly-sized particles of the same mineral, from the French *framboise* for raspberry, as this berry is composed of aggregated uniformly sized drupelets. Some additional micron-sized pyrite crystals were dispersed in the calcite matrix. The matrix was also commonly riddled with polishing marks, due to the low hardness of calcite, and many small pores were observed in all samples, confirming the micro-porosity noticed when using RI liquid.

DISCUSSION

BBS (Figure 13) is a type of carbonate-rich rock that is polycrystalline with a variety of minerals present, and therefore its measured properties can be quite variable. In addition, it is porous, with some pieces containing many vacuoles (see Figure DD-4 in *The Journal*'s online Data Depository), which further complicates RI and SG measurements. This explains why the hydrostatic SG values obtained from most of our samples were below that of calcite (2.71), despite the presence of the sulphides that are denser (realgar having an SG of 3.59). The yellow luminescence was observed only in the calcite areas of the samples. Although yellow is not a common luminescence colour for calcite, further research into this is beyond the scope of the present study.

The main attraction of BBS is its bright yellow -to-orange colour, caused by the presence of pararealgar ± realgar. The yellow colour is similar to that of orpiment, an arsenic sulphide, yet no trace of this mineral was found in Raman analyses of many yellow areas in our samples. This demonstrates the caution needed if determining the origin of colour on the basis of chemical composition alone, without confirmation by another type of spectroscopy (i.e. the Raman scattering performed here).

This is not the first time that pararealgar has been identified as the colouring agent in a gem material. Gaillou (2006) documented this pigment via Raman scattering in a little-known bright yellow opal from the area of Saint Nectaire in central France. Another bright yellow-to-orange opal, Forcherite, from Austria, is reportedly coloured by orpiment (on the basis of an X-ray diffraction analysis), but no Raman investigation was reported (Bojar and Taucher, 1994).

Yellow pararealgar is best known to be produced from red realgar in two different ways. First, through the action of light, in particular UV: in a well-known photo-induced phase transformation (Kyono, 2010), red realgar is slowly covered by a yellow dusting of pararealgar, a phenomenon feared by mineral museum curators. Second, this polymorph may be obtained by grinding (Gaillou, 2006). This is demonstrated in Figure 14, which shows how grinding a crystal of realgar in an agate mortar produced a yellow-orange powder. Its Raman signal was that of a mixture of pararealgar and realgar. As realgar is quite soft, it was difficult to crunch all the material into a fine powder, and in three experiments we consistently obtained a mixture of the two minerals as the final product. However, pararealgar in BBS formed as a primary product of the volcanic vent, and is unlikely to be the result of either transformation described above. (Note that any photo-induced phase transformation of realgar to pararealgar in the

Figure 13: A variety of BBS cabochons (30–50 mm long), including some matched pairs, display typical yellow-to-orange and black, grey and white colour contrast with crisp patterns. Photo by J. Ivey.

orange areas of BBS is expected to be minimal due to the small percentage of realgar present on the surface. In addition, no evidence of any instability due to this phase transition has been observed since BBS has been on the market.)

Regarding the presence of pyrite in black areas of BBS, it is not surprising that finely divided micrometric pyrite gives an overall black colour, rather than the golden yellow metallic colour that is commonly seen for macroscopic crystals of this iron sulphide. Commonly known as 'sooty' sulphides by miners, such material is black and composed of very small particles, reminiscent of soot. Framboidal pyrite, in particular, is associated with dark colour, often in the grey-to-black range (Wignall and Newton, 1998; Bond and Wignall, 2010; Wang et al., 2013). In addition, the micrometric size of the crystals might explain the broadening of the pyrite Raman doublet. (It is well known with Raman scattering that the more finely divided the material, the broader the band.) Furthermore, framboidal pyrite is often associated with

Figure 14: Grinding a red realgar crystal into powder produced a yellow-orange mixture of pararealgar and realgar. Photos by E. Fritsch.

amorphous iron sulfide, another factor which could explain a broader band. We could not find a published Raman spectrum of natural framboidal pyrite for comparison with our own. This unique variety of pyrite is found in many different environments that are strongly reducing (little oxygen available), and also in volcanic-associated massive sulphide deposits. This is somewhat consistent with what we know of the occurrence of BBS.

CONCLUSION

BBS is a carbonate-rich gem material with bright yellow-to-orange and black colour contrast, often in attractive patterns (e.g. Figure 13). It formed in a solfatara vent associated with an Indonesian volcano, as a rock that is dominated by slightly magnesian calcite coloured by sulphide pigments of pararealgar (yellow), realgar (giving an orange colour when mixed with pararealgar) and pyrite (producing black areas). Therefore, BBS belongs to a rare category of gems coloured by micro-inclusions of sulphide pigments, such as yellow opals from France and Austria, and myrickite, a bright orange-to-red silica-rich material coloured by cinnabar inclusions from various mercury deposits in California, USA (Wright, 1957). Considering the abundance of arsenic sulphides in BBS, lapidaries should wear protective gear to avoid toxicity of the dust produced during fashioning.

BBS is currently a single-source gem material, with no other deposit having been documented elsewhere. Production has been ongoing since 2003, yielding an estimated 150 tonnes of lapidary material. It is difficult to predict future production, due to the discontinuous nature of the veins and the traditional, labour-intensive methods of exploration and production. Although in 2013 it was thought the BBS deposit was exhausted, fortunately through hand trenching some additional discoveries of sub-parallel veins and extensions have been made, and mining is ongoing.

REFERENCES

Bojar H.P. and Taucher J., 1994. Arsenolith, Realgar und Auripigment im « Forcherit » vom Ingeringgraben bei Knittelfeld, Steiermark. In G. Niedermayr et al., *Neue Mineral Funde aus Östereich XIIIL, Carinthia II*, **184**(104), 265–266.

Bond D.P.G. and Wignall P.B., 2010. Pyrite framboid study of marine Permian–Triassic boundary sections: A complex anoxic event and its relationship to contemporaneous mass extinction. *GSA Bulletin*, **122**(7–8), 1265–1279, https://doi.org/10.1130/b30042.1.

Gaillou E., 2006. Relations Between Nanostructure, Physical Properties and Mode of Formation of Opal A and Opal CT. Ph.D. dissertation, University of Nantes, France, 181–186, www.gemnantes.fr/fr/recherche/theses/these-gaillou (in French).

Kyono A., 2010. Growth and Raman spectroscopic characterization of As_4S_4 (II) single crystals. *Journal of Crystal Growth*, **312**(23), 3490–3492, https://doi.org/10.1016/j.jcrysgro.2010.09.001.

Meng G., Chen M., Jiang J. and Chen S., 2016. Structural characteristic and cause of colour of "Zhanguohong" agate from Xuanhua, Hebei Province. *Journal of Gems & Gemmology*, **18**(6), 28–34 (in Chinese with English abstract).

Overlin S., 2014. Gem News: Bumble Bee "jasper" from Indonesia. *Gems & Gemology*, **50**(2), 166–167.

Serras Herman H., 2013. Bumble Bee "jasper" a colorful volcanic lapidary material. *Rock & Gem*, **43**(8), 26–29.

Wang P., Huang Y., Wang C., Feng Z. and Huang Q., 2013. Pyrite morphology in the first member of the Late Cretaceous Qinshankou Formation, Songliao Basin, northeast China. *Palaeogeography, Palaeoclimatology, Palaeoecology*, **385**, 125–136, https://doi.org/10.1016/j.palaeo.2012.09.027.

Wignall P.B. and Newton R., 1998. Pyrite framboid diameter as a measure of oxygen deficiency in ancient mudrocks. *American Journal of Science*, **298**, 537–552, https://doi.org/10.2475/ajs.298.7.537.

Wright L.A., 1957. Gem stones. In *Mineral Commodities of California*, California Division of Mines Bulletin 176, California Division of Mines and Geology, San Francisco, California, USA, 164–169.

The Authors

Dr Emmanuel Fritsch FGA
Institut des Matériaux Jean Rouxel CNRS (UMR 6502) and University of Nantes, BP 32229, F-44322, Nantes Cedex 3, France. Email: emmanuel.fritsch@cnrs-imn.fr

Joel Ivey
Geologist, www.IndoAgate.com, Bangkok, Thailand

Acknowledgements

Ekaterina Zviagina, then a first-year student at the University of Nantes, re-ran all of the visible spectra on the cited spectrometer, as the original spectrometer that was used broke down. Florian Massuyeau, IMN's engineer for UV-visible and luminescence spectroscopies, was helpful throughout the project. Jean-Yves Mevellec, IMN's vibrational spectroscopy engineer, was very instrumental in acquiring the most difficult Raman spectra of BBS. We thank Dace Irwan, CEO of CV Anugrah Alam in Sukabumi, West Java, Indonesia, for his assistance with materials and the use of his team and workshop facilities.

Figure 1: The Ming cultured pearls in these strands display several circles (top, 11–14 mm wide) or only one or two circles (bottom, 13–15 mm wide). Photo by J.-P. Gauthier.

An Explanation of a Specific Type of Circling as Observed on Ming Cultured Pearls

Jean-Pierre Gauthier, Jacques Fereire and Thanh Nhan Bui

ABSTRACT: The name *Ming pearls* refers to gonad-grown Chinese freshwater cultured pearls. In these beaded cultured pearls, the nuclei are predrilled and a tissue graft is placed into the drill hole at the same time the bead is inserted into the mollusc. A large number of these cultured pearls exhibit circling on their surface, typically with one or two main rings and sometimes additional ones. Examination of sliced samples by optical microscopy highlights the primary origin of the circling and the predominant role of predrilling the nucleus. As the cultured pearl rotates during its formation, each orifice on the drilled bead induces a groove on its surface with a spot defect right over the opening. When this drill hole is perpendicular to the rotational axis of the cultured pearl, only one 'equatorial' ring is generated. When there is a fairly large tilt angle between the bead's drill hole and the rotational axis, two grooves appear symmetrically relative to the equatorial plane, diametrically opposite with respect to the nucleus centre. With only a slight tilt angle between the drill hole and the rotational axis, the circles nearly overlap and a narrow ridge might eventually develop between the grooves. The disturbance created by the drill hole is generally more pronounced on the side where the graft was inserted. Round-, drop- and baroque-shaped non-circled Ming cultured pearls were also investigated to clearly understand the influence of the nucleus drill hole. This research raises awareness of one of the major causes of defects that result from grafting techniques using drilled nuclei.

The Journal of Gemmology, **36**(3), 2018, pp. 240–250, http://doi.org/10.15506/JoG.2018.36.3.240

Circling is a common surface feature on freshwater and saltwater cultured pearls (Ky et al., 2015a). Although this 'defect' is sometimes appreciated, it more often downgrades the value of the cultured pearls. In addition, the grooves that form the circling are often lined with brownish organic matter that further degrades their value. As a result, circling is of major concern to pearl farmers, and efforts have been made to reduce its frequency (Ito, 2009; Ky et al., 2014; Kishore and Southgate, 2015, 2016; Ky et al., 2015b,c).

The origin of such circling, however, has been little studied (Ito, 1996, 2011; Ogimura et al., 2012). Research on Polynesian black cultured pearls from *Pinctada margaritifera* has shown that, for this mollusc, the rings are related to surface defects resulting from the emergence of narrow holes that extend through the nacre layers to the bead nucleus (Gauthier et al., 2014; Cuif et al., 2018). However, the simple presence of spot defects is not sufficient to result in circling; there also must be rotation of the developing cultured pearl around a fixed axis. The rotation of bead nuclei inside the gonad was demonstrated conclusively by Gueguen et al. (2015).

This article sheds light on one of the likely prime causes of circling phenomena, using Ming cultured pearls as an example (e.g. Figures 1 and 2). Currently, this type of pearl is cultured in China and marketed under the names 'Ming' (Hänni, 2011) and 'Edison' (Laurs, 2012). The culturing process is actually of Japanese origin—having been practised in Lake Kasumigaura on hybrid varieties of the freshwater bivalves *Hyriopsis schlegeli* and *Hyriopsis cumingii* (Strack, 2011)—and consists of simultaneously introducing a bead and a tissue graft into the gonad of the pearl mussel. The implant location in freshwater molluscs is reportedly less accessible (Hänni, 2011) than in saltwater oysters (*P. margaritifera*, *P. maxima* and *P. martensii*). For this reason, the graft is partially recessed in a cylindrical cavity drilled into the bead, so the two elements, bead and graft, can be implanted in one single operation. The drill hole usually extends clear through the bead.

Following the layer-by-layer deposition of nacre, the harvested cultured pearls vary in shape—round, drop, button or baroque—but they often display coaxial rings or grooves. In such cases, the cultured pearls are then usually drilled perpendicular to the circling (i.e. parallel to the rotational axis). As for non-circled cultured pearls, the hole is drilled either partway through for mounting as a pendant or earrings, or all the way through for stringing on a necklace. This double drilling of bead and cultured pearl has been well illustrated by X-radiography of both Kasumiga (Hänni, 2000) and Ming (Hänni, 2011) cultured pearls (see also Karampelas, 2012).

MATERIALS AND METHODS

The affordability of Ming cultured pearls enabled us to acquire numerous (approximately 100) circled samples for possible destructive analyses in order to study their circling phenomena. Some of the purchased strands contained primarily multi-circled cultured pearls (e.g. Figure 1, top), while those in other strands had only one or two grooves (e.g. Figure 1, bottom). The latter constitute the main topic of this study. For comparison, we later acquired 26 non-circled Ming cultured pearls: eight drop-shaped (12–16 mm long), 15 round (11–15 mm in diameter) and three baroque (16–19 mm long). In addition, a non-beaded mantle-grown Chinese freshwater cultured pearl was also investigated to evaluate potential confusion with the beaded Ming products.

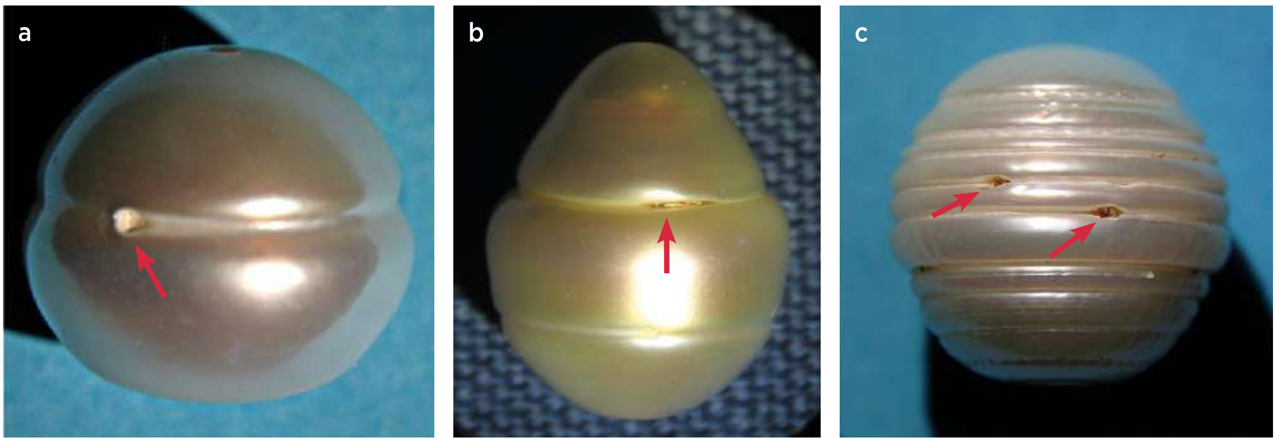

Figure 2: Shown here are three examples of circling on Ming cultured pearls with a rotational axis displaying **(a)** one ring, **(b)** two rings and **(c)** several rings. The arrows indicate spot defects in the grooves. From left to right, the cultured pearls are 10.5, 15.5 and 11.5 mm long. Photos by J.-P. Gauthier.

Preliminary observation of the circled samples with the unaided eye revealed characteristic defects in the grooves (Figure 2). To understand their origin, 34 cultured pearls were chosen for this study: 21 drop-shaped, five near-round and eight capsule-shaped. The 34 samples, ranging from 11 to 19 mm long, were sliced by author JF using a diamond saw. The cutting plane (Figure 3a) was always chosen near these defects so as to observe both (1) the defects and their extension within the cultured pearl, and (2) the profile of the surface shaped by the circling. The cultured pearls were cut in half or into thick slices, and the cut surfaces were then polished on an oiled aluminium disc charged with 3,000 mesh diamond powder.

The samples were examined and photographed with a Leica S8 APO binocular microscope equipped with a Canon PowerShot S70 digital camera. When possible, the thick slices were photographed in both transmitted illumination and between crossed polarisers to provide better contrast.

RESULTS

The 34 circled cultured pearls sliced for examination displayed evidence of a rotational axis, as indicated by the direction of circling. For the drop-shape samples (the most common shape we encountered), we refer here to the tapered side as the upper pole or 'apex', and the opposite, rounded side as the lower pole or 'base'. We classified the 34 samples into three categories, depending on the number of circles perpendicular to the rotational axis:

- One circular groove, in the equatorial plane (12 cultured pearls)
- Two circular grooves, symmetrical with respect to the equatorial plane (17 cultured pearls)
- Multiple circles (five cultured pearls)

Category 1: One Equatorial Circle

Figure 4 represents the typical case of a Ming cultured pearl with a single groove. The groove on such samples always appeared in the plane through the maximum diameter of the bead nucleus, perpendicular to the rotational axis, even if the groove appeared off-centre due to a sample's drop shape. For this condition, we use the term *equatorial groove*. We also observed that a single groove almost always contained two spot defects (Figures 4a and 4b), diametrically opposite and often large, although one of them was sometimes barely visible. These defects were often composed of cavities, but sometimes they were protrusions or bumps (red arrows in Figure 4).

In the slice shown in Figure 4c, it is apparent that the two diametrically opposed defects originated at the orifices of the hole drilled in the nucleus before the

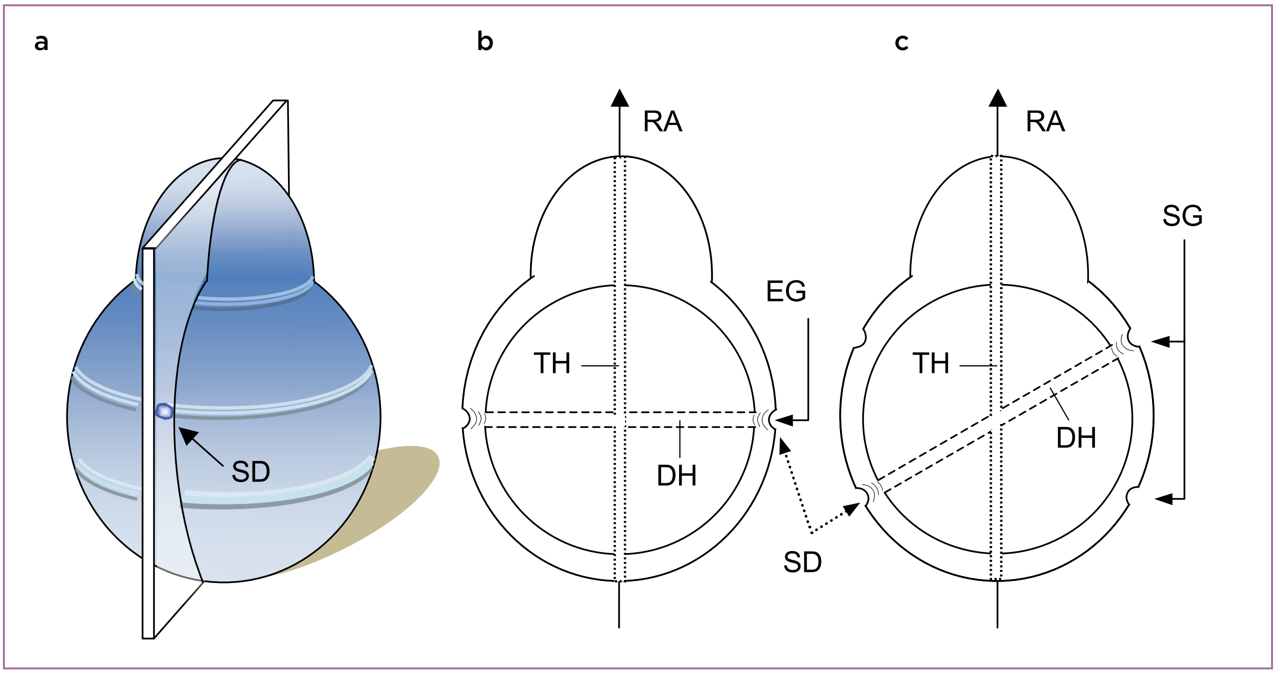

Figure 3: These sketches illustrate **(a)** a vertical slice through a circled Ming cultured pearl with spot defects (SD) visible on one circle; **(b)** a section showing a nucleus drill hole (DH) perpendicular to the rotational axis (RA), generating a single equatorial groove (EG); and **(c)** a section in which the drill hole through the nucleus is tilted with respect to the rotational axis of the cultured pearl, generating a pair of symmetrical grooves (SG). TH is the threading drill hole, which is usually, as shown here, oriented along the rotational axis. Drawing by J.-P. Gauthier.

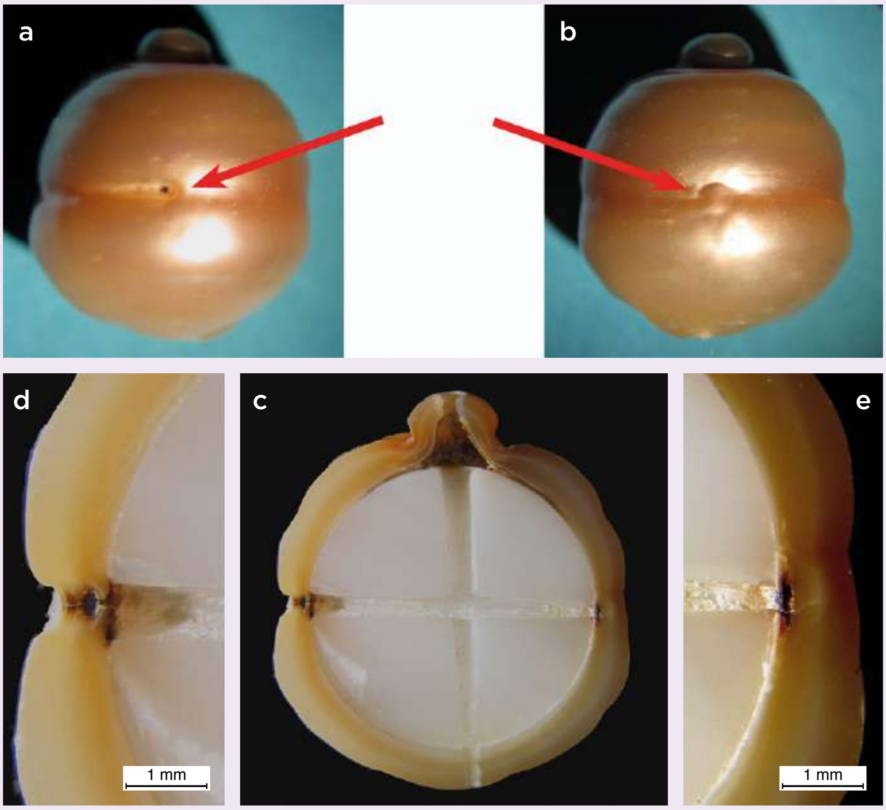

Figure 4: In this cultured pearl (12 mm long) with one 'equatorial' groove, each view of the two opposite sides **(a, b)** shows a defect in the equatorial plane perpendicular to the vertical rotational axis. In this case, the defects appear as a small depression on one side and a bump on the other side (red arrows). **(c)** A cross-section of this cultured pearl (2.5-mm-thick slice), observed between crossed polarisers and viewed parallel to the rotational axis, displays the defects originating from the openings of the horizontal hole drilled in the nucleus. **(d, e)** A closer view of the defects shows they are characterised by dark desiccated organic matter, mainly on the left side where the matter probably corresponds to the graft. Photos by J.-P. Gauthier.

pearl cultivation process. The dark mass seen only on one end of this hole (Figure 4d) might correspond to organic matter, possibly residue from the graft introduced into the drill hole. Outside both ends of the hole, in the perinuclear region, brown organic layers account for a lack of nacre deposition during the early stages of cultured pearl growth, followed by resumed nacre growth, leading to a depressed tubular region on one side (Figures 4a and 4d) and to a small bump on the other side (Figures 4b and 4e).

The vertical hole seen in Figure 4c was drilled along the rotational axis after cultivation for threading.

Category 2: Pair of Circles

Figures 5a and 5b show a sample of the second category, equally typical, of a Ming cultured pearl with a pair of grooves. In this, as in all similar samples, only one defect appears in each groove (indicated by red arrows in Figure 5).

The slice depicted in Figure 5d clearly shows the tilt angle of the nucleus drill hole relative to the equatorial plane. Considering the formation of the grooves as a result of cultured pearl rotation in the host mollusc, this tilt angle explains the systematically opposite position of the defects compared to the bead centre, the two grooves being located symmetrically in relation to the equatorial plane of the bead and the presence of only a single defect within each groove (see also Figure 3c).

The depth of the grooves is greatest at the location of the defect, and becomes progressively shallower with increasing rotational distance away from it. Thus the direction of the cultured pearl's rotation can be inferred (from the right to the left in Figures 5a and 5b, indicated by green arrows), as previously pointed out by Gauthier et al. (2014). The cut section (Figure 5d) illustrates how the furrows are less pronounced on the sides opposite the spot defects (blue arrows). Figures 5e and 5f are enlarged views of the nucleus drill hole openings. A dark mass of organic matter lies in the right-hand opening, which is probably the side in which the graft was introduced.

The apex of this cultured pearl has a protrusion surrounding a bulge (Figure 5c), which might be responsible for the anchorage of its rotational axis in the soft tissue of the gonad. Again, the threading hole was drilled along the rotational axis.

Category 3: Multiple Circles

The third category comprises multi-circled Ming cultured pearls. In addition to the presence of one or two grooves, along with all features present in categories 1 and 2, these had additional circles, each generated by a defect

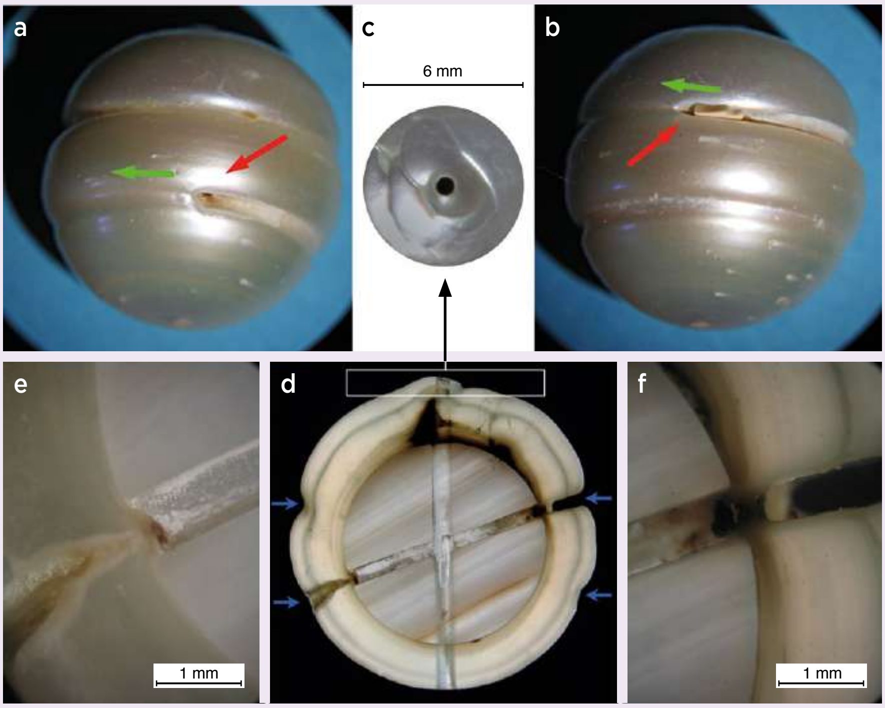

Figure 5: A cultured pearl (14 mm long) with two equatorial grooves is shown in two opposite views **(a, b)**. Red arrows point to the single defect in each groove, and green arrows indicate the rotation direction of the cultured pearl during its growth. **(c)** A top view of the cultured pearl shows a small dome at the apex responsible for fixing its rotational axis. **(d)** The profile of the grooves is highlighted (blue arrows) on this cross-section slice (2 mm thick), observed between crossed polarisers. Also shown are enlarged views **(e, f)** of each end of the bead drill hole. Photos by J.-P. Gauthier.

of various width. The positions of these defects were random. In the two former cases, the two diametrically opposed defects and the rotational axis defined the plane along which a specimen was sliced for examination. In this third case, which we will discuss briefly, it was not possible to incorporate all of the defects into a single thick slice.

Drilling of the nucleus bead can explain the existence of two grooves on most circled cultured pearls having a fixed rotational axis. For those with more than two grooves, another cause of circling needs to be found, but this is beyond the scope of the present study. Nevertheless, it should be noted that additional circles are usually generated at spot defects quite similar in appearance to those due to the nucleus drill hole, as shown in Figure 6. This beaded cultured pearl may have incorporated another, much smaller, non-beaded cultured pearl that grew independently in the gonad. Known by the Japanese name *tokki pearl* (Krzemnicki et al., 2011), this structure could be responsible for the drop shape of this sample. The overall shape dictated the orientation of the rotational axis. The apparent attachment point between the two cultured pearls is also another cause of circling (blue arrow in Figures 6a and 6c).

Three main defects are visible in Figure 6a. Two of them lie in a single plane that passes through the rotational axis, and their profile is visible on the slice from this cultured pearl (green arrows in Figure 6c). At the centre of the section is a cylindrical cavity almost perpendicular to the slice that corresponds to the nucleus drill hole. This slightly tilted drill hole generated the two near-equatorial grooves, quite close together. The combination gives rise to an equatorial ridge (red arrow). The two defects highlighted in Figure 6b lie precisely within these grooves. Before slicing the sample, one might assume that one of the defects was positioned directly above an orifice of the nucleus drill hole, but this was not the case.

ADDITIONAL RESULTS

We examined several additional Ming cultured pearls to better understand the nature of the circling and its presence or absence. These included a multi-circled sample with a pair of opposite spot defects near the poles, as well as several non-circled cultured pearls that were not yet drilled for threading (eight drop-shaped, 15 round and three baroque). In addition, to evaluate potential confusion with the beaded Ming products, we examined a non-beaded mantle-grown Chinese freshwater cultured pearl.

Ming Cultured Pearl with a Pair of Defects near the Poles

Figure 7 illustrates a multi-circled Ming cultured pearl belonging to category 3 above, which provides an interesting example regarding the tilt angle of the drill hole with respect to the rotational axis. It displays at least

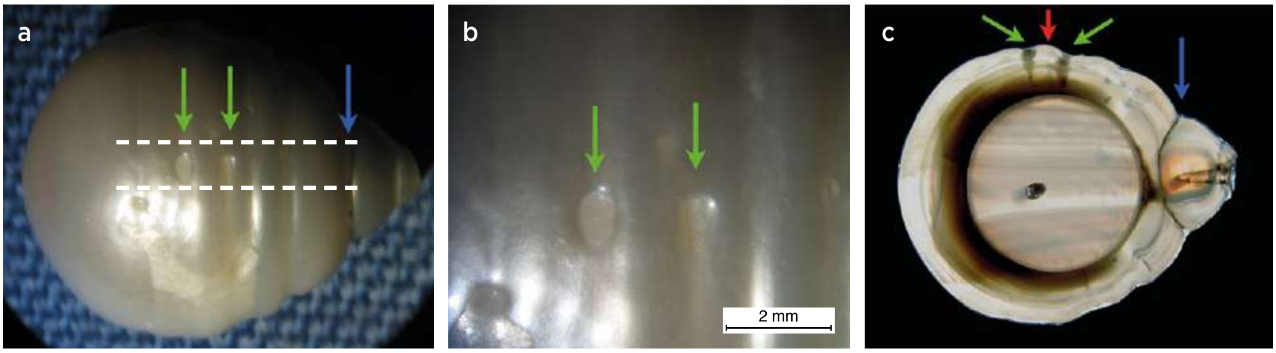

Figure 6: This multi-circled cultured pearl (14 mm long) displays **(a)** an external appearance with circles (e.g. green arrows) and another type of defect (blue arrow). The dashed lines represent the planes of the cuts that yielded the 1-mm-thick slice in (c). **(b)** Enlargement reveals details of the spot defects (e.g. green arrows). **(c)** A slice of this sample observed between crossed polarisers shows the profile of two spot defects (green arrows) lying in the grooves created by the drill hole being slightly tilted relative to the equatorial plane of growth rotation. The dark oval near the centre of the nucleus is an oblique cut through the nucleus drill hole. Also note the presence of a bump between the two defects (red arrow). A possible 'tokki pearl' is visible at the apex. Photos by J.-P. Gauthier.

seven grooves with three random defects appearing only on one side, with two of them in the same vertical plane (red arrows in Figure 7b). In addition, two diametrically opposite defects appear near the upper and lower poles (green arrows in Figures 7c and 7d). Based on our previous findings, these should correspond to the orifices of the nucleus drill hole. This was confirmed by the slice shown in Figure 7e. The nucleus drill hole (dashed red line in Figure 7e) is positioned at a slight angle from the threading hole (i.e. near the rotational axis).

The proximity of one orifice to the upper pole suggests that the end where the graft was introduced could be involved in the development of the apical dome. In this case, the large size of the cavity was enough to create a protrusion that induced a fixed axis of rotation. However, the protrusion was slightly deflected relative to the axis of the nucleus drill hole, leading to the formation of circumpolar grooves. The origin of the dome being due to the graft environment is not a general case, as already discussed for categories 1 and 2 above, in which the cavity near the orifice does not extend enough to create a bump on the surface.

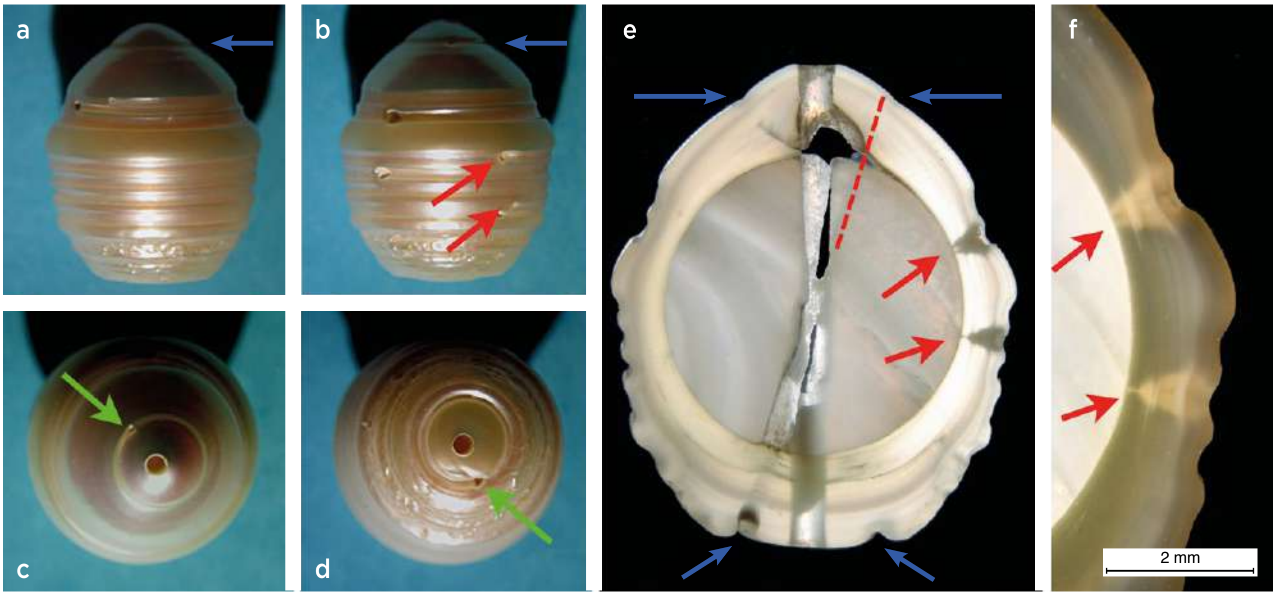

Figure 7: Another multi-circled cultured pearl (13 mm long) has a nucleus drill hole slightly tilted relative to the rotational axis. Two opposite lateral views **(a, b)** display several rings. Views of the apex **(c)** and base **(d)** show defects symmetrical with respect to the nucleus centre, marking the presence of the orifices of the nucleus drill hole (green arrows) and generating specific grooves (blue arrows in a, b and e). **(e)** A slice (2 mm thick) along a plane through the rotational axis and two defects (indicated by red arrows) is shown here between crossed polarisers. The threading drill hole is vertical, while the dashed red line indicates the nucleus drill hole direction. The organic mass of the graft, removed during the slicing process, was lying in the apical cavity. **(f)** An enlarged view of the defects is shown here in reflected light. Photos by J.-P. Gauthier.

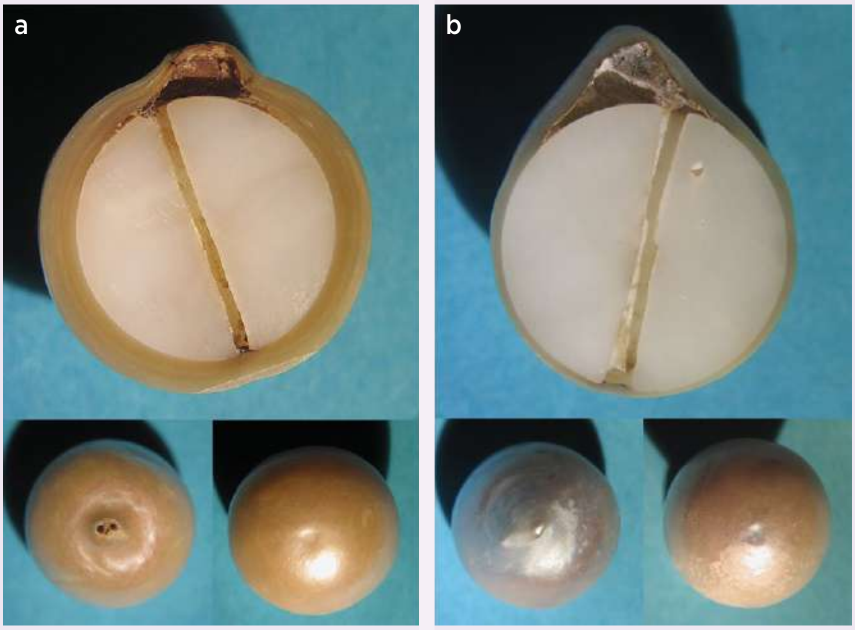

Figure 8: Two drop-shaped Ming cultured pearls (**a:** 11 mm long, **b:** 13.5 mm long) of low quality, without circles and not drilled for threading show nucleus drill holes slightly tilted with respect to the rotational axis. The apical bumps are related to the graft placed in one end of the drill hole of the bead nucleus. Photos of the apex and base of each cultured pearl before it was sliced are shown at the bottom (left and right, respectively). Photos by J.-P. Gauthier.

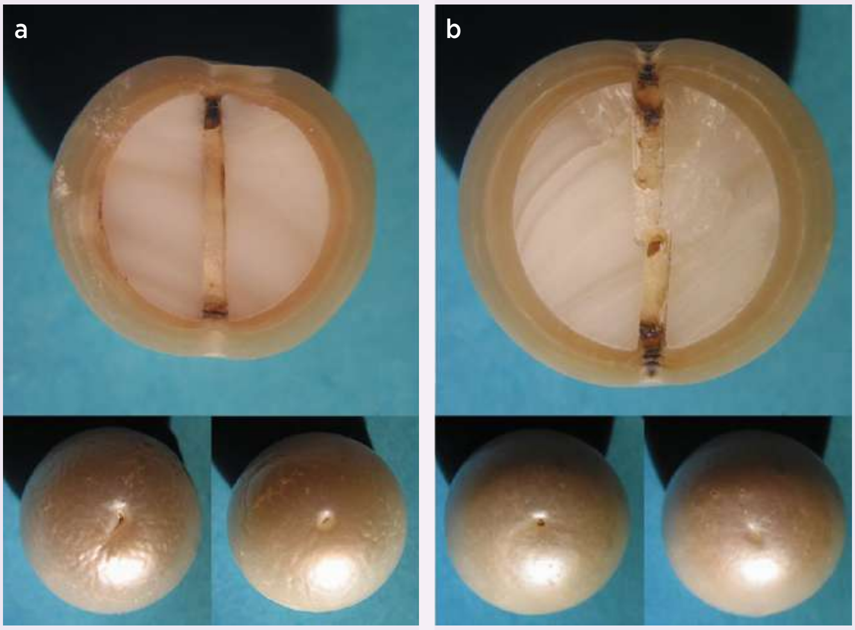

Figure 9: Two round Ming cultured pearls (**a:** 12 mm, **b:** 13.5 mm) of low quality, without circles and not drilled for threading show upper and lower spot defects that correspond to the extremities of the nucleus drill hole (see left and right photos, respectively, of the apex and base of each cultured pearl before it was sliced). Their round shape allowed them to rotate around axes of various directions, so no circling was generated. Photos by J.-P. Gauthier.

Non-Circled Drop-Shaped Ming Cultured Pearls

One might wonder whether all Ming cultured pearls with a symmetric shape along their rotational axis should display circling. The eight non-circled drop-shaped Ming cultured pearls that we examined were of unmarketable low quality and had not been drilled for threading. All of them were near-round, with a protrusion at the apex. In addition, all samples showed a hole or depression at the centre of the apex protrusion and a slight circular depression at or near the centre of the lower pole. These features are illustrated by two samples in Figures 8a and 8b.

The cultured pearls were sliced along their rotational axis, which revealed that all of them had a nucleus drill hole that was slightly tilted with respect to the rotational axis (as illustrated in the previous example), and yet none displayed any circling. The bump at the apex probably corresponds to the end of the nucleus drill hole where the graft was introduced. However, the cavities associated with the grafts were perhaps large enough to prevent the upper drill holes from imprinting on the nacreous envelope, thus explaining the lack of circles. The basal depressions were slight enough to also avoid basal circles.

Non-Circled Round Ming Cultured Pearls

Non-circled round Ming cultured pearls, often of high quality, also exist in the market. The 15 undrilled low-quality round samples that we examined all showed two opposite spot defects, similar to the examples described above. However, without the bumps that created the drop shapes documented above, these cultured pearls turn, but not around a fixed axis. Hence they move in multiple orientations, thus avoiding the formation of circles. Two examples are shown in Figure 9, and the interiors of the other 13 round cultured pearls were quite similar.

Round Ming cultured pearls of good quality sometimes also exhibit such marks due to the drilled bead nucleus (Figure 10). The two opposite spots consist of slight depressions, indicating the position of each end of the nucleus drill hole. In such a case, a threading hole drilled along this axis would entirely eliminate the surface defects.

Such defects are entirely absent from round Ming cultured pearls of high quality. These depressed areas most likely were present during the early stage of growth, but progressively disappeared as nacre deposition accumulated, and as the round cultured pearl rotated around a randomly shifting axis.

Non-Circled Baroque Ming Cultured Pearls

Three baroque Ming cultured pearls were examined, since in principle they did not rotate (as shown by their shape). As expected, we noticed the presence of two opposite spot defects on all three samples, marking the existence of a nucleus drill hole. As an example, one of the samples is shown in Figure 11.

Mantle-grown Non-beaded Cultured Pearl

It is worth mentioning that non-beaded mantle-grown cultured pearls sometimes have defects quite similar to those reported in this study of beaded Ming cultured pearls. An example that could cause confusion is shown

Figure 10: This round Ming cultured pearl (11 mm) of good quality shows two diametrically opposed slight defects due to the hole drilled through the nucleus bead. Photos by T. N. Bui.

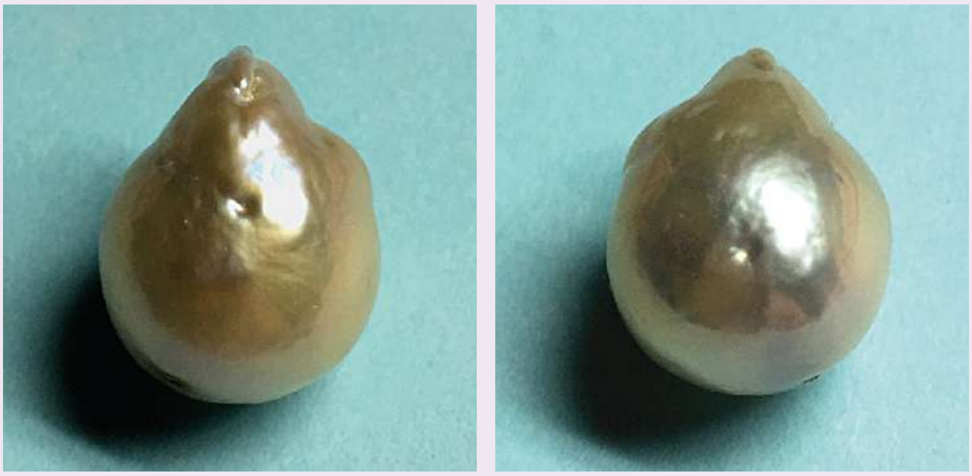

Figure 11: A baroque Ming cultured pearl (11 × 13.5 mm) shows two opposite spot defects marking the presence of a nucleus drill hole, but the lack of circling indicates that it did not rotate during its formation. Photos by T. N. Bui.

in Figure 12a. The appearance of this Chinese mantle-grown cultured pearl with two major grooves is very similar to a beaded Ming cultured pearl containing a nucleus drill hole that is tilted with respect to the rotational axis. However, a closer examination reveals that the two circles are not symmetrical with respect to the equatorial plane of a possible bead nucleus, even if the position of such a bead cannot be defined precisely. Moreover, the lower circle has a spot defect, but none is visible opposite on the upper circle, as would be expected for the presence of a bead with a drill hole. Microradiography might clarify this situation, if necessary.

A slice through this cultured pearl parallel to the rotational axis and passing through the spot defect (Figure 12b) confirmed the absence of a bead nucleus. The defect originated from the interior of the cultured pearl, but at the surface it closely resembles a spot that could have been generated by a drilled nucleus.

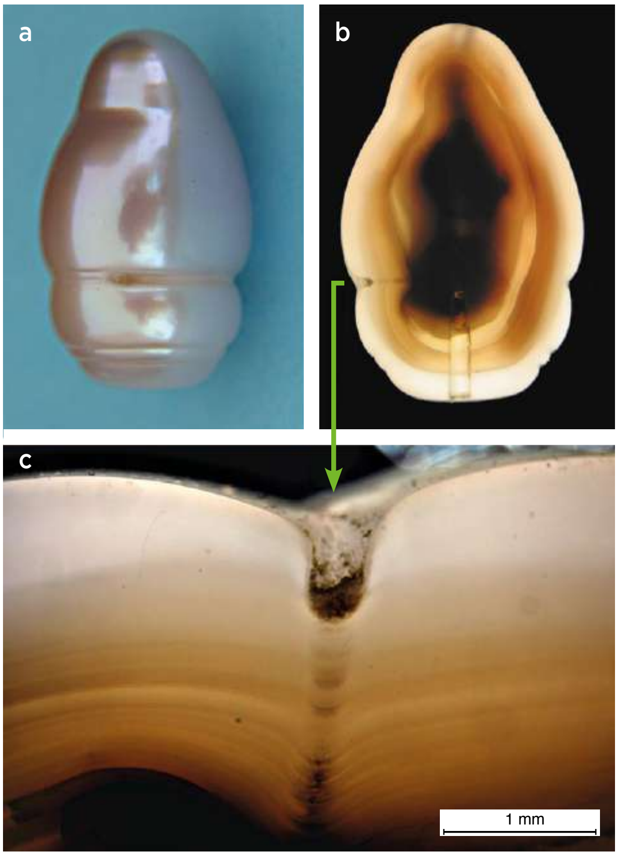

Figure 12: This non-beaded mantle-grown Chinese freshwater cultured pearl (**a:** 18.5 mm long) contains defects that induced circling due to rotation around a fixed axis. A cross-section slice (**b:** 2 mm thick) observed between crossed polarisers shows the profile of a defect (green arrow) lying in one of the grooves. **(c)** Enlargement of the defect illustrates features similar to those observed in beaded Ming cultured pearls. Photos by J.-P. Gauthier.

DISCUSSION

Circling is a feature frequently encountered on saltwater and freshwater cultured pearls, and is suggestive of a fixed rotational axis perpendicular to the circles. This rotational movement, for a long time only theoretical, was finally demonstrated in a recent experiment (Gueguen et al., 2015), and one possible mechanism for inducing such rotation was suggested by Cartwright et al. (2013). An internal defect, emerging at the cultured pearl's surface and generating circles, was suggested by Gauthier et al. (2014) and later confirmed by Cuif et al. (2018) on pearls cultured in black-lip oysters. In rare cases, the orientation of the initial fixed rotational axis can change suddenly and take another fixed position (Gauthier et al., 2015).

The Role of the Drill Hole in Creating Spot Defects and Circling

Our study has shown that a specific type of circling on Ming cultured pearls is generated by the presence of the hole drilled in the bead nucleus before pearl cultivation in order to introduce a graft into the gonad simultaneously (Hänni, 2011). However, the influence of this nucleus drill hole may be seen even on non-circled cultured pearls.

During the early stages of pearl cultivation, organic layers facing the drill-hole orifices settle poorly or do not biomineralise, leading to depressed areas more-or-less visible on the surface during the latter growth stages, when more uniform nacre deposition occurs. The cultured pearl's rotation and the possible presence of pits unrelated to the nucleus drill hole modify this simple mechanism, and thus may create the following situations for the circling and spot defects:

1. Drop-shaped cultured pearls (formed around a fixed rotational axis), with a bead nucleus drill hole that is:

- perpendicular to the rotational axis (category 1): *one groove, with two opposite spots on this groove.*
- tilted at a significant angle relative to the rotational axis (category 2): *two grooves with one spot each, opposite with respect to the bead centre*.
- tilted relative to the rotational axis, plus the presence of defects (pits) unrelated to the bead drill hole (category 3): *additional circles*.
- slightly tilted with respect to the rotational axis: *no grooves if the nucleus drill hole does not touch the nacreous envelope; two opposite spot defects near the poles*.

2. Round-shaped cultured pearls (random, multiple rotational axes):
    - *no grooves, two opposite spots*, eventually removed by thread drilling, or
    - *no grooves, no spots*, if the later stage of biomineralisation makes them disappear (top quality).
3. Baroque cultured pearls (no rotation): *no grooves, two spots*.

The Role of the Graft

Cochennec-Laureau et al. (2010) noted that, during surgical insertion of the graft into the pearl pouch of Polynesian black-lip oysters, tissue debris (gametes and haemocytes) can be introduced at the same time. In addition, depending on the surgical preparation of the graft (cutting of the donor oyster's mantle), it can become necrotic causing organic debris. Both tissue alterations may lead to deformation and/or a change in the functional integrity of pearl sac development. The absence of pearl sac epithelial cell homogeneity induces modifications of the nacre layer deposits.

A bump near one end of the bead drill hole corroborates the graft's influence. Moreover, if the graft slides out of the bead hole, a bump more distant from the hole also could be explained in the same way. Such excrescences induce the anchorage of the cultured pearl in the pearl sac, leading it to rotate around a fixed axis. In such an instance, the presence of the bead drill hole may induce the circling.

The Role of Epithelial Cells of the Pearl Sac

The pearl biomineralisation process is very similar to the repair of the shell of a living pearl oyster, as described by Caseiro and Gauthier (1997) after piercing a *Pinctada margaritifera* valve with a drill bit. The pallial epithelium (i.e. consisting of cells of the type that form a pearl sac) covered the hole very quickly (within a day) with an organic layer for emergency repair, followed later by the deposition of fibrous aragonite and tablets of mother-of-pearl. With regard to the current study, which involves pearls cultured with a hybrid freshwater *Hyriopsis* mussel, the epithelium of the pearl sac also appears to have initially deposited organic layers (as shown in Figures 4d and 4e) and then started the conventional process of biomineralisation.

This observation suggests that the deposition of matter by the epithelial cells depends strongly on the cellular quality of the pearl sac or its environment (e.g. its contact with the bead). Facing a nucleus drill hole, a mollusc produces organic layers more-or-less deficient in biomineral, and the return to normal nacre deposition seems delayed. As the cultured pearl rotates, cells that previously faced a hole come into contact with a solid part of the bead, but they do not immediately produce mineral layers, as evidenced by the persisting groove, and this occurs for all cells located along the circular path travelled by the hole. We can thus understand the formation of the spot defects, which develop thereafter into grooves during cultured pearl rotation about a fixed axis.

CONCLUSION

The observations described here on circled Ming cultured pearls and extended to non-circled ones provide, by means of classical microscopy, a dataset that helps explain the mechanism of occurrence of certain types of circling, including the development of one, two or more, or no such circles. Only those rotating around a fixed axis during growth present the specific grooves described here. Conversely, circles are absent from round cultured pearls for which the rotational axis changes direction continuously during growth, and from baroque cultured pearls that do not rotate. Such samples may present only two opposite defects—holes or crater-like depressions—that disappear during the growth of top-quality round cultured pearls. The graft introduced into the bead nucleus drill hole can have a major influence on a cultured pearl's shape, inducing a bump, which is responsible for fixing the rotational axis. The early formation of spot defects—which then develop into grooves during rotation relative to the orifices of the nucleus drill hole or other cavities existing near the bead—can be attributed to the behaviour of the adjacent epithelial cells.

REFERENCES

Cartwright J.H.E., Checa A.G. and Rousseau M., 2013. Pearls are self-organized natural ratchets. *Langmuir*, **29**(26), 8370–8376, http://doi.org/10.1021/la4014202.

Caseiro J. and Gauthier J.P., 1997. L'huître aux lèvres noires, *Pinctada margaritifera*. II. Altération créée par perçage central de la valve - Comparaison avec les altérations naturelles. *Revue de Gemmologie* A.F.G., No. 133, 12–16.

Cochennec-Laureau N., Montagnani C., Saulnier D., Fougerouse A., Levy P. and Lo C., 2010. A histological examination of grafting success in pearl oyster *Pinctada margaritifera* in French Polynesia. *Aquatic Living Resources*, **23**(1), 131–140, http://doi.org/10.1051/alr/2010006.

Cuif J.-P., Perez-Huerta A., Lo C., Belhadj O. and Dauphin Y., 2018. On the deep origin of the depressed rings on pearl surface illustrated from Polynesian *Pinctada margaritifera* (Linnaeus 1758). *Aquaculture Research*, **49**(5), 1834–1847, http://doi.org/10.1111/are.13638.

Gauthier J.-P., Gutierrez G. and Serrar M., 2014. La "piqûre", un défaut à l'origine du cerclage des perles chez *Pinctada margaritifera*. *Revue de Gemmologie A.F.G.*, No. 187, 6–8.

Gauthier J.-P., Gutierrez G., Serrar M. and Bui T.N., 2015. Rares perles cerclées à double axe de rotation. *Revue de Gemmologie A.F.G.*, No. 194, 4–7.

Gueguen Y., Czorlich Y., Mastail M., Le Tohic B., Defay D., Lyonnard P., Marigliano D., Gauthier J.-P., Bari H., Lo C., Chabrier S. and Le Moullac G., 2015. Yes, it turns: Experimental evidence of pearl rotation during its formation. *Royal Society Open Science*, **2**(7), article 150144, 8 pp., http://doi.org/10.1098/rsos.150144.

Hänni H.A., 2000. Gem News: Freshwater cultured "Kasumiga pearls," with Akoya cultured pearl nuclei. *Gems & Gemology*, **36**(2), 167–168.

Hänni H.A., 2011. Ming pearls: A new type of cultured pearl from China. *Journal of the Gemmological Association of Hong Kong*, **32**, 23–25.

Ito E., 1996. Study on the mechanism of formation of "circle pearls": An approach from the nacreous structure. *Journal of the Gemmological Association of Japan*, **21**(1–4), 33–44, http://doi.org/10.14915/gsjapan.21.1-4_33 (in Japanese with English abstract).

Ito M., 2009. Improving pearl quality by grafting and husbandry methods. *Aqua Tips*, **20**(1), 1–8.

Ito M., 2011. Circle and spot formation mechanisms and changes in luster, color, and roundness of cultured pearls by grafting methods in *Pinctada margaritifera*. *Gems & Gemology*, **47**(2), 148.

Karampelas S., 2012. Gem News International: Large natural-color freshwater cultured pearls with drilled beads. *Gems & Gemology*, **48**(2), 148–149.

Kishore P. and Southgate P.C., 2015. Does the quality of cultured pearls from the black-lip pearl oyster, *Pinctada margaritifera*, improve after the second graft? *Aquaculture*, **446**, 97–102, http://doi.org/10.1016/j.aquaculture.2015.04.024.

Kishore P. and Southgate P.C., 2016. The effect of different culture methods on the quality of round pearls produced by the black-lip pearl oyster *Pinctada margaritifera* (Linnaeus, 1758). *Aquaculture*, **451**, 65–71, http://doi.org/10.1016/j.aquaculture.2015.08.031.

Krzemnicki M.S., Müller A., Hänni H.A., Gut H.-P. and Duggelin M., 2011. Tokki pearls: Additional cultured pearls formed during pearl cultivation: External and internal structures. *32nd International Gemmological Conference*, Interlaken, Switzerland, 13–17 July, 56–58.

Ky C.-L., Blay C., Sham-Koua M., Lo C. and Cabral P., 2014. Indirect improvement of pearl grade and shape in farmed *Pinctada margaritifera* by donor "oyster" selection for green pearls. *Aquaculture*, **432**, 154–162, http://doi.org/10.1016/j.aquaculture.2014.05.002.

Ky C.-L., Blay C., Aiho V., Cabral P., Le Moullac G. and Lo C., 2015a. Macro-geographical differences influenced by family-based expression on cultured pearl grade, shape and colour in the black-lip 'pearl oyster' *Pinctada margaritifera*: A preliminary bi-local case study in French Polynesia. *Aquaculture Research*, **48**(1), 270–282, http://doi.org/10.1111/are.12880.

Ky C.-L., Demmer J., Sham-Koua M. and Cabral P., 2015b. Development of cultured pearl circles and shape after initial graft and second nucleus insertion in the black-lipped pearl oyster *Pinctada margaritifera*. *Journal of Shellfish Research*, **34**(2), 319–328, http://doi.org/10.2983/035.034.0214.

Ky C.-L., Nakasai S., Molinari N. and Devaux D., 2015c. Influence of grafter skill and season on cultured pearl shape, circles and rejects in *Pinctada margaritifera* aquaculture in Mangareva lagoon. *Aquaculture*, **435**, 361–370, http://doi.org/10.1016/j.aquaculture.2014.10.014.

Laurs B.M., 2012. Gem News International: Tucson 2012. *Gems & Gemology*, **48**(1), 54–55.

Ogimura T., Futami K., Katagiri T., Maita M., Gonçalves A.T. and Endo M., 2012. Deformation and blemishing of pearls caused by bacteria. *Fisheries Science*, **78**(6), 1255–1262, http://doi.org/10.1007/s12562-012-0545-x.

Strack E., 2011. An overview of production techniques for Chinese freshwater cultured pearls. *32nd International Gemmological Conference*, Interlaken, Switzerland, 13–17 July, 51–55.

The Authors

Prof. Jean-Pierre Gauthier and Jacques Fereire
Centre de Recherches Gemmologiques, Laboratoire de Planétologie et Géodynamique, 2 rue de la Houssinière, BP 92208, 44322 Nantes Cedex, France
Email: jpk.gauthier@gmail.com

Thanh Nhan Bui
Université catholique de Louvain, Louvain-la-Neuve, Belgium

Acknowledgements

This work was funded by Almini Beijing Trading Co. Ltd (亚米尼北京贸易有限公司), China. The authors warmly thank Mostafa Serrar and Gilles Gutierrez (Laboratory ICP-Texinfine, Lyon, France) and Nathalie Cochennec-Laureau (Ifremer, La Trinité-sur-Mer, France) for their valuable contributions.

Conferences

AGA LAS VEGAS

The Accredited Gemologists Association's 2018 Las Vegas conference took place on 1 June during the JCK Show in Nevada, USA. Attended by 67 people, the event was chaired by AGA president **Stuart Robertson** and featured five speakers.

Dr Wuyi Wang (Gemological Institute of America, New York, New York) covered advances in the growth and identification of synthetic diamonds. In the past 10–15 years, both HPHT and CVD technologies for gem diamond synthesis have made significant progress, in both quality and quantity of specimens produced. Millions of synthetic gem diamonds—in melee sizes (e.g. Figure 1) and as larger crystals—are now produced annually. It is highly likely that growth technology will continue to improve, and that more D-to-Z and fancy-colour synthetic diamonds will enter the jewellery market. Disclosure of whether a diamond is natural or synthetic, or has been treated to enhance its appearance, is crucial. This disclosure requires that instrumentation technology and identification processes keep pace with new developments to help ensure that every synthetic diamond is definitively identified.

Alberto Scarani (Magilabs, Rome, Italy) described fluorescence spectroscopy for near-colourless diamond screening and coloured stone analysis using his EXA instrument. In the screening mode, the instrument indicates 'pass' for natural diamonds and 'refer' for synthetic diamonds and simulants (although in rare cases, some very pure, low-nitrogen type IaA natural diamonds are referred for further testing). The instrument's 'advanced' mode is used to display the fluorescence emission spectrum of a sample, which is useful for further differentiating near-colourless natural from synthetic diamonds and imitations, as well as testing some coloured diamonds and identifying emerald filling substances, separating natural/synthetic/heated spinel and evaluating coloured stones for the presence of Cr^{3+}.

Dr Thomas Hainschwang (GGTL Laboratories, Balzers, Liechtenstein) began his presentation by reviewing different instrumentation he has developed specifically for gem testing, most of which uses luminescence imaging for separating natural from synthetic diamonds—including the new D-Tect machine marketed by HRD Antwerp for testing near-colourless diamonds rejected by most screening devices (see p. 181 of this issue of *The Journal* for more information). Then he reviewed his ambitious ongoing diamond treatment project, in which he and his team are collecting data on carefully pre-selected natural and synthetic diamonds before and after irradiation, heat treatment and HPHT processing.

Jon Phillips (Corona Jewellery Co., Toronto, Ontario, Canada) discussed the advantages and disadvantages of five different commercial diamond screening units, and emphasised that no machine 'does it all' for the average jeweller. Prospective buyers of a screening unit should understand how the machine works, its ease of use, details of its warranty and any service contracts, availability of in-house training, its up-front cost and delivery time.

Martin Rapaport (Rapaport Diamond Corp., New York, New York) shared his ideas on synthetic diamonds in the marketplace, both presently and in the future. He sees De Beers' recently announced initiative of selling 'Lightbox' synthetic diamonds as a way to push down other sellers of synthetics, and he feels that the company is prioritising making money over promoting natural diamonds. He emphasised that there is already a lot of jewellery containing melee-sized synthetic diamonds (mainly produced in China) on the market, and predicted that the price of natural diamond melee could eventually fall to that of synthetic melee.

Brendan M. Laurs FGA

Figure 1: These near-colourless melee-sized rough synthetic diamonds (2–3 mm each) were grown in China. Photo by Jianxin (Jae) Liao, © GIA.

22ND MEETING OF THE INTERNATIONAL MINERALOGICAL ASSOCIATION

On 13–17 August 2018, the quadrennial meeting of the International Mineralogical Association (IMA) was hosted by the Geological Society of Australia and took place at the Melbourne Convention and Exhibition Centre in Melbourne, Victoria, Australia. The conference was attended by approximately 550 people, and featured a series of plenary lectures and several parallel sessions of oral presentations on a variety of mineralogical topics. A 536-page abstracts volume can be downloaded from the conference website at www.ima2018.com/ima2018-abstracts. Notably, the conference featured two sessions on gems: 'Sciences Behind Gemstone Treatments' (Figure 2) and 'Recent Advances in Our Understanding of Gem Minerals'. In addition, various presentations of interest to gemmologists were given in other sessions that focused on mineral museums, granitic pegmatites and diamond geology. Oral presentations attended by this author are profiled below.

Several presentations featured topics related to coloured stones. **Grant Hamid** (Hamid Bros. Gem Merchants, Melbourne, Victoria, Australia) reviewed developments during the past 50 years with gem corundum localities, synthetics and treatments (see also the Gem-A Conference report in *The Journal*, Vol. 34, No. 8, 2015, p. 717). **Dr Frederick (Lin) Sutherland** (Australian Museum, Sydney) and co-authors presented new geochemical and radiometric age data for rubies from Myanmar. U-Pb isotopic age determinations of zircon inclusions in Mong Hsu rubies yielded 23.9 ± 1.0 million years (Ma) and of titanite inclusions in a ruby from Mogok (Thurein Taung) gave 32.4 ± 1.0 Ma. Trace-element plots showed a clear separation between the Mong Hsu and Mogok rubies, as well as differences from rubies derived from eastern Australian gemfields. **Dr Isabella Pignatelli** (University of Lorraine, Nancy, France) and colleagues used X-ray tomography and trace-element analysis to characterise some new trapiche rubies from the Khoan Thong placer in Luc Yen, northern Vietnam. They deduced that the corundum in the dendritic arms formed at the same time as the interstitial corundum of the trapiche crystals.

Philippe Belley and **Dr Lee Groat** (University of British Columbia, Vancouver, Canada) performed trace-element fingerprinting of cobalt-blue spinel from Baffin Island in Canada in comparison with other localities. They found two types of Co-bearing spinel: low V and/or Cr (showing the best blue colour) and high V and/or Cr combined with low Mn and possibly some Fe (corresponding to purple samples). All showed Ni enrichment. **Dr Gaston Giuliani** (IRD and CRPG, University of Lorraine, Nancy, France) and co-authors reviewed the geology of demantoid deposits. They defined Type I deposits as being hosted by serpentinised ultramafic rocks within ophiolitic sequences (e.g. Italy, Russia, Iran and Pakistan) and Type II deposits as Ca-Mg skarns (e.g. Madagascar and Namibia). Oxygen isotope values can be used to separate those from Madagascar and Namibia as well as from Italy and Iran. **Dr Allan Pring** and colleagues (Flinders University, Adelaide, Australia) analysed 200 opal samples from various localities using X-ray diffraction (for pre-screening), Raman and far-infrared spectroscopy and nuclear magnetic resonance. The samples were categorised according to opal-A (i.e. amorphous: from Australia, Slovakia and the USA), opal-CT (i.e. cristobalite and tridymite: some samples from Australia) or opal-C (i.e. cristobalite: very rarely encountered). **Bahareh Shirdam** and colleague (University of Tehran, Iran) examined the photoluminescence spectra of turquoise with 290 nm excitation. The main luminescence peaks were positioned at 361, 392 and 455 nm, and the 410–570 nm region showed variations related to rare-earth elements and other trace impurities.

There was one diamond presentation, given by **Dr Sally Magaña** (Gemological Institute of America [GIA], Carlsbad, California), who examined spatial variations and the effects of heating on radiation stains in green diamonds. Because the green colour of these stains turns brown within minutes when heated to 550–600°C, the natural irradiation must take place relatively near the earth's surface (i.e. at less than 30 km depth). Confocal Raman depth profiling and photoluminescence mapping at liquid-nitrogen temperature showed differences in the depth penetration and spatial patterns between natural- and laboratory-irradiated stains, and therefore may help distinguish the origin of a green diamond's colouration.

Gem treatments featured prominently at the conference, particularly on corundum. **Dr Visut Pisutha-Arnond** and co-authors (Gem and Jewelry Institute of Thailand [GIT], Bangkok) reported on blue-diffused sapphires produced from colourless natural and synthetic starting materials. Chemical analysis across slices of both natural and synthetic samples showed an enrichment in Ti along with various other elements (e.g. Be and Li, as well as Fe and Ga in the synthetics) in the diffused blue colour layer. The blue layer was thinner in the synthetics than in the natural corundum, but larger samples of the synthetic starting material could be successfully diffused because of its lack of inclusions and consistent chemical composition. Co-author **Thanapong Lhuaamporn** gave a presentation for **Thanong Leelawatanasuk** (GIT, Bangkok) on the characteristics of blue sapphire enhanced by a relatively new process using heat and pressure. Sri Lankan sapphires that did not react favourably to traditional heat treatment were placed in a specially designed crucible containing graphite and a small amount of water, and were heated multiple times of short duration under conditions of <1,800°C and <1 kbar. FTIR spectroscopy of the sapphires after treatment showed four main patterns created by strong OH-related absorptions that have not been seen in traditionally heated Sri Lankan sapphires. **Dr Pornsawat Wathanakul** (Kasetsart University, Bangkok, Thailand) and colleagues performed traditional heating experiments on Sri Lankan sapphires and observed changes in their infrared spectra. The intensity of the 3309 cm^{-1} band was orientation dependent, so the samples had to be carefully oriented to obtain meaningful data. Also, the use of the 3309 cm^{-1} band to detect heat treatment only worked for sapphires with a relatively low Ti content (i.e. < 0.05 wt.% TiO_2), and therefore generally could be applied to metamorphic but not magmatic sapphires. **Aumaparn Phlayrahan** (Kasetsart University, Bangkok, Thailand) and co-authors studied the influence of Ti content on the 3309 cm^{-1} infrared absorption band in heat-treated ruby. The band only appeared in samples containing moderate-to-high Ti (i.e. 100–200+ ppm), and only when the samples were heated to ≥1,200°C, due to the high affinity of Ti^{4+} for the OH^- liberated from diaspore and/or boehmite during the heating process.

Chengsi Wang and colleagues (Gemmological Institute, China University of Geosciences, Wuhan) reported preliminary results of a synchrotron-radiation X-ray absorption spectroscopy study of natural and treated Oregon sunstone. Yellow Oregon labradorite underwent Cu diffusion treatment to produce red and

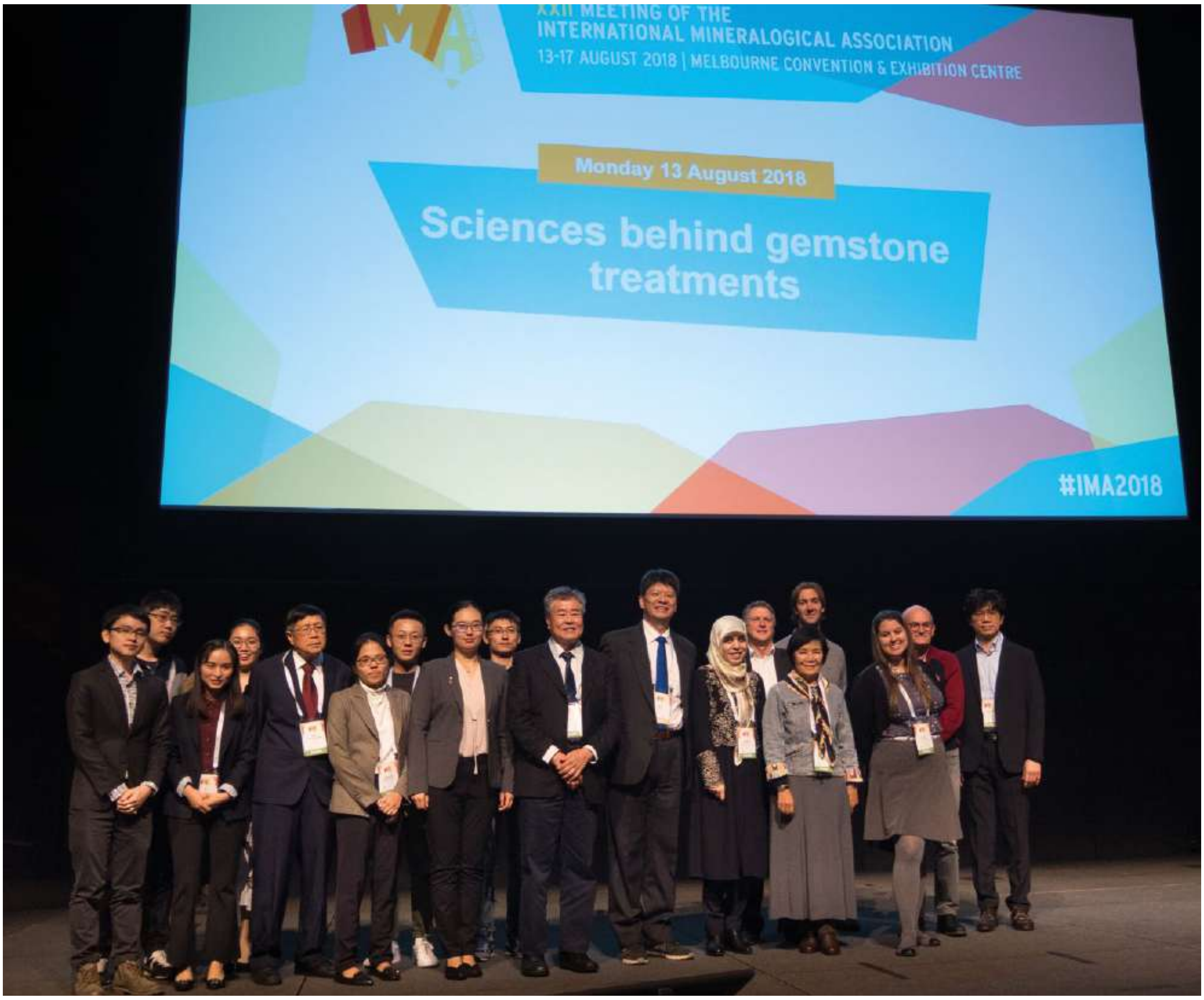

Figure 2: Oral and poster presenters of the IMA session titled 'Sciences Behind Gemstone Treatments' gather together. Photo by B. M. Laurs.

green zones that are typical of natural Oregon sunstone. In the red and green zones of the diffused samples (and in the red zone of an untreated Oregon sunstone), the copper was likely present as nanoparticles of Cu^{+} and/or Cu^{2+} (rather than Cu^{0}, as reported previously), with the different colours possibly related to the copper valance state and the local environment. **Tay Thye Sun** (Far East Gemological Laboratory, Singapore) reviewed the development and identification of various jadeite treatments since the 1980s, and differentiated between A-jade (untreated), B-jade (bleached and polymer impregnated), C-jade (dyed) and, most recently, D-jade (jadeite doublet with a white base and green cap).

Gem localities were covered in 10 presentations. **Wim Vertriest** (GIA, Carlsbad, California) reviewed the challenges of performing field studies of ruby and sapphire deposits. The discovery of new deposits is unpredictable, and these localities may show rapid and unexpected developments (including being abandoned) that are driven by various factors influenced by the gem trade (e.g. response to heat treatment or resemblance to stones from famous localities). **Dr Ian Graham** (University of New South Wales, Sydney, Australia) and co-authors examined alluvial sapphires from Orosmayo, Argentina, using microscopy (for morphological studies) and the analysis of trace elements and oxygen isotopes. They inferred that the sapphires formed due to metasomatic exchange between mantle-derived carbonatised lamprophyres and crustal felsic magmas, and they were later brought to the surface by ascending intermediate magmas. **Kandy Wang** (University of New South Wales) and colleagues reported new oxygen isotope ratios ($\delta^{18}O/\delta^{16}O$) for cabochon-quality rubies from Paranesti, north-eastern Greece. The oxygen isotope compositions ranged from –0.3‰ to +1.3‰; such a narrow range straddling 0‰ has not previously been documented for metamorphic corundum. **Peter Lyckberg** (Museum of Natural History, Luxembourg) reviewed gems and minerals from granitic pegmatites of Afghanistan and Pakistan. While those in Afghanistan are a major source of gem-quality tourmaline, spodumene and morganite, the pegmatites in Pakistan are known mainly for producing aquamarine, topaz and a variety of rare minerals. In another presentation, **Lyckberg** recounted his experiences in 2013–2018 with mining topaz, heliodor and smoky quartz from 'chamber'-type pegmatites in Volodarsk, Ukraine. One particularly notable pocket in 2017 formed a large vertically oriented cavity that yielded more than 6 tonnes of topaz, including large crystals weighing 96 and 230 kg each; a 9,000 ct topaz was subsequently faceted. **Dr Lee Groat** (University of British Columbia, Vancouver, Canada) reviewed recent advances in coloured stone exploration in Canada. Using geochemistry, hyperspectral imagery and drone footage, he and his team have identified several targets for emerald in the Canadian Cordillera, and also for sapphire and spinel on Baffin Island. In a pair of presentations, **Dr William Simmons** and **Dr Karen Webber** (Maine Mineral & Gem Museum, Bethel, Maine, USA) and colleagues obtained new U-Pb age dates for zircon and apatite from gem-bearing pegmatites in Oxford County, Maine. The ages range from ~250 to 270 Ma, which are about 30 Ma younger than the Sebago pluton, so the pegmatites cannot be related to fractional crystallisation of this pluton as previously proposed. Instead, the pegmatites may have formed from the crystallisation of anatectic melts generated during post-orogenic extension prior to the rifting of Pangea. The pegmatite magmas could have been generated by decompression melting of leucosomes in the metamorphic basement rocks, and they eventually ascended to ~8 km where they crystallised at 2.5 kbar conducive for pocket formation. **Jeffrey Morrison** (New England Mineral Association, Yarmouth, Maine, USA) and co-authors described mining for tourmaline and other minerals at the Havey pegmatite in Poland, Maine. The mine is known for producing fine gem tourmaline with a consistent bluish green colour (see *The Journal*, Vol. 34, No. 5, 2015, pp. 394–395). **Kemala Wijayanti** (Padjadjaran University, Bandung, Indonesia) and colleagues performed SEM, XRF and petrographic analyses on green jasper from the southern part of Java, Indonesia. Samples from three localities (Bungbulang, Klawing and Samigaluh) contained inclusions of chlorite ± limonite and had trace amounts of Fe, Mg, Al and Mn.

Australian gem deposits were the subject of several presentations. **Dr Ahmadjan Abduriyim** (Tokyo Gem Science, Saitama, Japan) and colleagues performed U-Pb age dating of zircon megacrysts from three localities in the New England sapphire fields (Kings Plains, Swan Brook and Mary Anne Gully) in New South Wales. The ages defined two main formational events during 216–174 Ma and 45–37.7 Ma. In addition, U-Pb age dating of syngenetic zircon inclusions in blue sapphires from Inverell (also in New South Wales) gave ages of 34.9 ± 1.4 Ma, similar to the Eocene range mentioned above for some of the zircons. **Nick Raffan** (University of New South Wales) examined an alluvial sapphire deposit at Tomahawk Creek in the Anakie gemfields of central Queensland. This area is known for producing large colour-zoned green/yellow sapphires, including the 82.4 ct Tomahawk Tiger. **Dr Simon Pecover** (Pan Gem Resources Pty Ltd, Palm Grove, Queensland) presented evidence for the

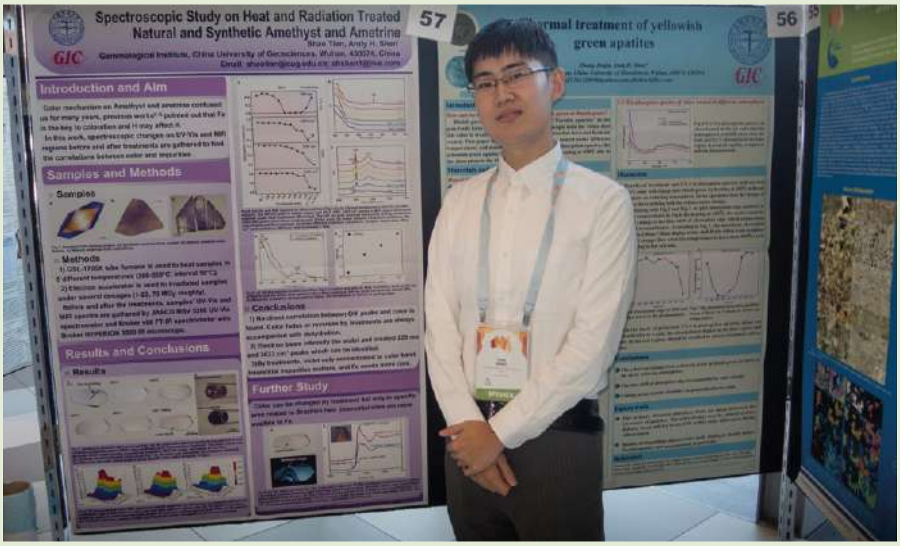

Figure 3: The IMA poster sessions featured nine presentations related to gems, including Tian Shao's spectroscopic study of heat-treated and irradiated natural and synthetic amethyst and ametrine. Photo by B. M. Laurs.

vigorous flow of opal-forming fluids in some Australian opal deposits. In such a scenario, he invoked shear-induced ordering of silica spheres to form play-of-colour opal, which alternated with layers of potch opal (i.e. lacking play-of-colour) due to disordered deposition of silica spheres. **Dr Peter Downes** (Western Australian Museum, Northbridge) and co-authors examined variscite and associated phosphate minerals from the Mt Deverell deposits in the Gascoyne region of Western Australia. The variscite has been mined since the 1970s, and forms veins <12 cm wide that cross-cut silicified mudstone and siltstone of Proterozoic age. It ranges from pale green to green to blue and contains traces of Cr and V.

In other presentations, **Dr Hao Wang** and co-authors (Swiss Gemmological Institute SSEF, Basel, Switzerland) reviewed advances in the origin determination of coloured stones using laser ablation inductively coupled plasma time-of-flight spectroscopy (i.e. with GemTOF instrumentation; see *The Journal*, Vol. 35, No. 3, 2016, pp. 212–223). Using two data analysis techniques—principal components analysis (PCA) and t-distributed stochastic neighbour embedding (t-SNE)—he and his team have made significant progress in using trace elements to separate blue sapphires from Kashmir and Madagascar, and also to distinguish emeralds from various localities. **Dr Ruslan Kostov** (University of Mining and Geology 'St. Ivan Rilski', Sofia, Bulgaria) described gem minerals and gold from archaeological finds in the Balkans (south-eastern Europe). The materials in the artefacts included nephrite, jadeite, serpentinite, talc, malachite, rock crystal, chalcedony, jasper, turquoise and jet. **Zhiqing Zhang** and **Dr Andy Shen** (Gemmological Institute, China University of Geosciences, Wuhan) used FTIR spectroscopy to analyse KBr pellets made from 52 amber samples from various localities, including the Baltic Sea, Myanmar, China (Fushun), Mexico (Chiapas) and the Dominican Republic. The spectral features could be used to separate all but those from Fushun and Myanmar.

The two gem sessions also included nine posters (e.g. Figure 3), which covered the low-pressure, high-temperature treatment of brown type Ia diamond; spinel from Tanzania; lead glass-filled ruby; heat treatment of blue sapphire, tanzanite and greenish yellow apatite; heated and irradiated gem materials (i.e. dark green tourmaline and natural/synthetic amethyst and ametrine); and chrysocolla chalcedony from Taiwan. The posters were displayed in an exhibition area where delegates could also interact with instrument manufacturers, publishers, professional organisations and mineral dealers.

Three additional oral presentations were given at an evening reception hosted by the Gemmological Association of Australia on 14 August. **Dr Gaston Giuliani** described the geological occurrence of Colombian emeralds, and also traced their early mining history. **Dr Lee Groat** recounted gem-exploration activities on Baffin Island, where the major challenges are the sparse infrastructure (with accompanying large expenses necessary to mobilise work parties in this area), extensive permitting and the presence of polar bears that are known to stalk humans for their next meal. **This author** closed the evening with an update on tourmaline, demantoid and diamond mining in Namibia (see *The Journal*, Vol. 36, no. 1, pp. 8–9 and 16–18).

Brendan M. Laurs FGA

Learning Opportunities

CONFERENCES AND SEMINARS

Fabergé Museum International Academic Conference: Jewellery Art of the 19th and Early 20th Centuries
20–22 September 2018
St Petersburg, Russia
https://fabergemuseum.ru/en/news/article/118

Goldsmiths' Fair 2018
25 September–7 October 2018
London
www.goldsmithsfair.co.uk/talks
Note: Includes a seminar programme

2018 GIA Symposium: New Challenges. Creating Opportunities
7–9 October 2018
Carlsbad, California, USA
https://symposium.gia.edu

ASMOSIA XII: Association for the Study of Marble & Other Stones in Antiquity International Conference
8–14 October 2018
Izmir, Turkey
www.asmosia2018.com

2nd World Emerald Symposium
12–14 October 2018
Bogotá, Colombia
www.emeraldsymposium.com

CIBJO Congress 2018
15–17 October 2018
Bogotá, Colombia
www.cibjo.org/congress2018

Canadian Gemmological Association Gem Conference 2018
19–21 October 2018
Vancouver, British Columbia, Canada
http://canadiangemmological.com/events-conferences/upcoming-conferences

Friends of Mineralogy, Pacific Northwest Chapter, 2018 Symposium—Minerals of California
19–21 October 2018
Kelso, Washington, USA
http://pnwfm.org/2017/12/19/2018-symposium-minerals-of-california

The Munich Show: Mineralientage München
26–28 October 2018
Munich, Germany
https://munichshow.com/en/the-munich-show/public-days/highlights
Note: Includes a seminar programme

Singapore Jewellery & Gem Fair 2018
26–29 October 2018
Singapore
www.singaporejewellerygemfair.com/JewelTalk
Note: Includes seminar programme

Gem-A Conference 2018
3–4 November 2018
London
https://gem-a.com/event/conference

7º Simpósio Brasileiro de Geologia do Diamante (7th Brazilian Symposium on Diamond Geology)
4–9 November 2018
Salvador, Bahia, Brazil
www.simposiododiamantebahia.com.br/en/
Note: Optional field trip to the Braúna diamond mine

Geological Society of America 130th Annual Meeting
4–7 November 2018
Indianapolis, Indiana, USA
https://community.geosociety.org/gsa2018/home
Session of interest: 'Gemological Research in the Twenty-First Century—Characterization, Exploration, and Geological Significance of Diamonds and Other Gem Minerals'

16th Swiss Geoscience Meeting
30 November–1 December 2018
Bern, Switzerland
https://geoscience-meeting.ch/sgm2018
Note: Includes a gemmology session

21st FEEG Symposium
19–20 January 2019
Vicenza, Italy
www.feeg-education.com/symposium
Note: Takes place during the Vicenzaoro international gold and jewellery show

AGTA Gemfair
5–10 February 2019
Tucson, Arizona, USA
www.agta.org/tradeshows/gft-seminars.html
Note: Includes a seminar programme

2019 Tucson Gem and Mineral Show
14–17 February 2019
Tucson, Arizona, USA
www.tgms.org/show
Note: Includes a seminar programme

Inhorgenta Munich
22–25 February 2019
Munich, Germany
www.inhorgenta.com/events-news/inhorgenta-forum
Note: Includes a seminar programme

Gem-A Midlands Branch Conference
23 February 2019
Birmingham
Email louiseludlam@hotmail.com

Hasselt Diamond Workshop 2019: SBDD XXIV
13–15 March 2019
Hasselt, Belgium
www.uhasselt.be/UH/SBDD/SBDD-XXIV

Initiatives in Art and Culture (IAC) 9th Annual International Gold Conference
4–5 April 2019
New York, New York, USA
http://artinitiatives.com

American Gem Society Conclave 2019
8–10 April 2019
Seattle, Washington, USA
www.americangemsociety.org/page/conclave2019

55th Gemboree 2019
19–22 April 2019
Rockhampton, Queensland, Australia
http://aflaca.org.au/gemboree
Note: Includes a seminar programme

European Gemmological Symposium 2019
24–26 May 2019
Idar-Oberstein, Germany
www.dgemg.com/en/organisation/16-newsletter/termine/385-european-gemmological-symposium-2019.html

Geological Society of Namibia 50th Anniversary Conference
1–4 September 2019
Windhoek, Namibia
www.gssa.org.za/?p=4214
Note: Possible field trip to diamond mining areas in Namibia

EXHIBITIONS

Europe

Empire of the Sikhs
Until 23 September 2018
The Brunei Gallery,
School of Oriental and African Studies,
University of London
http://www.soas.ac.uk/gallery/empire-of-the-sikhs

Pearls: Treasures of the Seas and Rivers
Until 1 October 2018
State Historical Museum, Moscow, Russia
www.shm.ru/shows/11652

The Art of Power: Habsburg Women in the Renaissance
Until 7 October 2018
Schloss Ambras, Innsbruck, Austria
www.schlossambras-innsbruck.at/en/visit/exhibitions/the-art-of-power

Splendours of the Subcontinent: A Prince's Tour of India 1875–6
Until 14 October 2018
The Queen's Gallery, Buckingham Palace, London
http://tinyurl.com/y84c2dr9

The Splendour of Power
Until 21 October 2018
Museet på Koldinghus, Kolding, Denmark
www.koldinghus.dk/uk/exhibitions-2017/the-splendour-of-power-2018.aspx

Le Trésor de Preslav
Until 5 November 2018
Louvre Museum, Paris, France
http://mini-site.louvre.fr/trimestriel/2018/Agenda_juin_aout_2018/10

Russia: Royalty & the Romanovs
9 November 2018–28 April 2019
The Queen's Gallery, Buckingham Palace, London
http://tinyurl.com/ybecrdbj

Designers & Jewellery 1850–1940: Jewellery & Metalwork from The Fitzwilliam Museum
Until 11 November 2018
The Fitzwilliam Museum, Cambridge
http://tinyurl.com/ybvy7oj6

Bijoux-Bijoux! Costume Jewellery from Chanel to Dior
13 November 2018–27 January 2019
Kunstgewerbemuseum, Berlin, Germany
www.smb.museum/en/exhibitions/detail/bijoux-bijoux-modeschmuck-von-chanel-bis-dior.html

Horta & Wolfers: Reopening of the Wolfers Frères Jewellery Store, 1912
Until 30 December 2018
Art & History Museum, Brussels, Belgium
www.kmkg-mrah.be/expositions/horta-wolfers

The Portland Miniatures: Joel Arthur Rosenthal
Until 31 December 2018
The Harley Gallery, Worksop, Nottinghamshire
www.harleygallery.co.uk/exhibition/the-portland-miniatures-joel-arthur-rosenthal

From Zeus to Earth and from Chile to Neapolis
Until 31 December 2018
Ilias Lalounis Jewelry Museum, Athens, Greece
http://lalaounis-jewelrymuseum.gr/en/exTdetails.asp?exid=39

East Meets West – Jewelled Splendours of the Art Deco Era
Until 6 January 2019
Pforzheim Jewellery Museum, Germany
www.schmuckmuseum.de/en/current.html

Hidden Gems: Scotland's Agates
Until 6 January 2019
National Museum of Scotland, Edinburgh
www.nms.ac.uk/national-museum-of-scotland/whats-on/hidden-gems-scotland-s-agates

BVLGARI. Tribute to Femininity. Magnificent Roman Jewels
Until 13 January 2019
The Moscow Kremlin Museums, Russia
http://tinyurl.com/yahq83nk

The Crown of Kerch: Treasures from the Dawn of European History
Until 29 September 2019
Neues Museum, Berlin, Germany
www.smb.museum/en/exhibitions/detail/die-krone-von-kertsch.html

North America

Centuries of Opulence: Jewels of India
Until 10 October 2018
GIA Museum, Carlsbad, California, USA
www.gia.edu/gia-museum-exhibit-centuries-opulence-jewels-india

American Jewelry from New Mexico
Until 14 October 2018
Albuquerque Museum, New Mexico, USA
www.cabq.gov/culturalservices/albuquerque-museum/exhibitions/american-jewelry

East Meets West: Jewels of the Maharajas from The Al Thani Collection
3 November 2018–24 February 2019
Legion of Honor Museum, San Francisco, California, USA
http://legionofhonor.famsf.org/exhibitions/east-meets-west

Jewelry: The Body Transformed
12 November 2018–24 February 2019
The Met, New York, New York, USA
www.metmuseum.org/exhibitions/listings/2018/jewelry

Crowns of the Vajra Masters: Ritual Art of Nepal
Until 16 December 2018
The Met Fifth Avenue, New York, New York, USA
https://metmuseum.org/exhibitions/listings/2017/crowns-of-vajra-masters

Fabergé Rediscovered
Until 13 January 2019
Hillwood Estate, Museum & Gardens, Washington DC, USA
http://hillwoodmuseum.org/faberge-rediscovered

Beadwork Adorns the World
Until 3 February 2019
Museum of International Folk Art, Santa Fe, New Mexico, USA
http://internationalfolkart.org/exhibition/3348/beadwork-adorns-the-world

Treasures of a Desert Kingdom: The Royal Arts of Jodhpur, India
9 March–2 September 2019
Royal Ontario Museum, Toronto, Ontario, Canada
www.rom.on.ca/en/exhibitions-galleries/exhibitions/rajasthan

OTHER EDUCATIONAL OPPORTUNITIES

Gem-A Workshops and Courses
Gem-A, London
https://gem-a.com/index.php/education/courses

- Understanding Gemstones
  5 October 2018, 10 and 28 January 2019
- Understanding Gemstone Testing
  12 October 2018, 11 and 29 January 2019
- Understanding Diamond Grading
  16 November 2018, 10 and 31 January 2019
- Understanding Diamond Simulants
  23 November 2018, 11 January 2019, 1 February 2019
- Investigating Gemstone Treatments (Intermediate)
  7 December 2018, 3 May 2019
- Ruby, Sapphire and Emerald (Intermediate)
  26 October 2018
- Investigating Jade and Its Imitations (Intermediate)
  19 October 2018, 8 March 2019
- Diamond Grading and Identification Course
  24–28 September 2018, 22–26 October 2018, 25 February–1 March 2019
- Investigating Gemstone Treatments
  7 December 2018
- Diploma Preparation (new for 2018, UK only)
  28 January–1 February 2019
  3 days practical, 2 days theory

Lectures with Gem-A's Midlands Branch
Fellows Auctioneers, Augusta Street, Birmingham
Email louiseludlam@hotmail.com

- Craig O'Donnell—Styles & Stones
  28 September 2018
- Paul Phillips—Photography & Micro Photography
  19 October 2018
- Vanessa Paterson—Amber
  30 November 2018

Lectures with the Society of Jewellery Historians
Society of Antiquaries of London, Burlington House, London
www.societyofjewelleryhistorians.ac.uk/current_lectures

- Christopher Thompson Royds—My Work as a Jeweller
  25 September 2018
- Anna Tabakhova—Clasps: 4000 Years of Fasteners in Jewellery
  23 October 2018
- Helen Ritchie—Designers and Jewellery: Jewellery and Metalwork from the Fitzwilliam Museum 1850–1940
  27 November 2018
- Martin Henig—Personal Cameos of Roman Date in the Content Family Collection
  22 January 2019
- Jack Ogden—TBA
  26 February 2019
- Peter Semrád—The Story Behind 'Hungarian' Opals
  26 March 2019
- Beth Wees—TBA
  25 June 2019
- Rachel Church—Brooches, Badges and Pins at the Victoria and Albert Museum
  26 November 2019

New Media

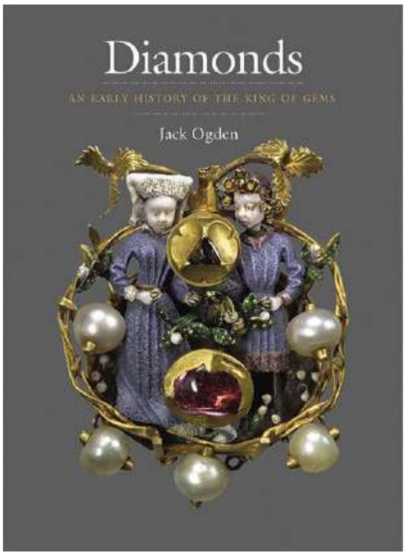

Diamonds—An Early History of the King of Gems

By Jack Ogden, 2018. Yale University Press, New Haven and London, http://tinyurl.com/Yale-Ogden-Diamonds, 408 pages, illus., ISBN 978-0300215663. £30.00 hardcover.

'The aim of this book is to consider the history of the trade in diamonds from India to Europe and the Near East, from its roots some two and a half thousand years ago until the early 1700s, when the diamond deposits in Brazil displaced India as the world's primary supplier' (Preface, p. x). This is what author Jack Ogden declares to be his intention, but in reality, this volume offers a lot more. Among other things, Ogden also delivers a history of the development of diamond cutting and its influence on jewellery styles, and he explains how the myths and legends from ancient times have gradually given way to real facts and figures. In 15 chapters, Ogden guides the reader through these topics.

In Chapter 1, 'The Diamond', Ogden presents what we know from the scarce old sources about what people in the ancient world believed to be the characteristics of diamonds—covering the well-known myths, from their indestructibility to their solubility in buck's blood, as well as the famous 'Valley of Gems'—and their social function in ancient cultures. Diamonds had always been rare and represented not only great wealth, but also high status and power. Interestingly, their oldest use seems to have been for grinding and as polishing powder for the cutting of other gems. In jewellery, only well-formed, uncut octahedra were used. Of the few surviving jewels, the oldest is a Hellenistic ring from Afghanistan of ca. 300 BC, after the Alexandrian Conquest.

Chapter 2 describes the role of diamonds in 'The Ancient World', where—not surprisingly—the most important source of information is Pliny's *Natural History*. Chapter 3 gives an outline of what old Eastern sources reveal about diamonds in 'Early Persia and the East'. All diamonds at the time came from India, but only smaller stones reached the Mediterranean World and these were initially used for cutting, drilling and grinding. Only after the increased contact with India following the expansion of the Macedonian kingdom by Alexander the Great were diamonds also used more and more in jewellery. In Chapter 4, Ogden describes the situation in 'Medieval Europe'. After the arrival of the Sasanian Persians and the westward expansion of Islam in the Near East, the old trade routes were almost cut off, and only small amounts of diamonds trickled into Europe. Diamonds were nearly forgotten during the so-called Dark Ages. This also explains why it is only after ca. 1200 AD that one finds the first clear documentary evidence for diamonds in medieval European jewellery. The first surviving jewels date from the later 1300s.

The following six chapters are dedicated to diamond polishing and cutting, 'the most fundamental development in the history of diamond' (p. 79). Chapter 5 considers 'The Dawn of Diamond Cutting in Europe'. According to the sparse evidence, the cutting process had probably been understood by 1300 AD. It all started with the discovery that the faces of diamond crystals could be polished with diamonds. Inevitably, this discovery led to diamond polishing in India, but it was in Europe where 'The Fifteenth-Century Technical Revolution' (Chapter 6) took place: the invention of a horizontal rotating iron wheel (scaife) and other tools, which are still in use to this day. The following chapters describe the different stages of diamond cuts from 'Renaissance Table and Point Cuts' (Chapter 7) to 'Renaissance Multifaceted Cuts' (Chapter 8) to 'The Early Brilliant Cut' (Chapter 9). Generally speaking, the simple cuts of tables and roses were eventually replaced by sparkling brilliants, made possible by the advancements of 'cutting-edge' cutting technology, and the innovative spirit of the cutters. Chapter 10 discusses 'Diamond Cutting in London', following England's rise as a colonial power. With the establishment of the East India Company in 1600, large quantities of diamonds began to reach England. Within a relatively short time, London became a major cutting and trading hub, and it was the main diamond cutting centre until Amsterdam and Antwerp took over about a century later.

Chapter 11 covers 'The Value and Assessment of Diamonds', where the author states that 'in the past, as today, diamonds were a sign of wealth, if not wealth itself, and their value was of concern to dealers and owners alike' (p. 203). Ogden follows diamond prices through the ages and the criteria for the assessment of the diamond qualities, as well as the motivations behind both. He stresses the great importance of honesty and experience, quoting Thakkura Pheru (India, 14th century): 'Those who fix a high price for an inferior gem or a low price for a superior gem, due to arrogance or avarice, will become lepers' (p. 231).

The last four chapters are dedicated mainly to India. They describe 'The Indian Diamond Mines' (Chapter 12), 'The Diamond Trade in India' (Chapter 13), 'Diamond Cutting in India and the East' (Chapter 14) and, finally, 'The Eclipse of Indian Diamonds' (Chapter 15). In all four chapters it becomes evident that the 'knowledge' described in ancient sources was mostly a compilation of myths and legends (e.g. the Valley of Gems). With growing contacts, first by people such as Marco Polo, and later by traders such as Jean-Baptiste Tavernier and the activities of the major trade organisations such as the East India Company, more and more first-hand information reached the Western World and created a detailed and realistic picture of the situation in the Orient.

After a short epilogue, the volume is rounded off with an appendix reproducing Nathanial Cholmley's *A Description of the Diamond-Mines* of 1677, followed by an impressive bibliography of 462 titles and an index, which contains primarily names and places, with less than a tenth of the entries devoted to general keywords.

With this book, Ogden does not claim to reinvent the wheel:

> This is not the first study of the history of diamonds and their cutting—there is Godehard Lenzen's 1970 study—but new research means that we can supplement or suggest some reconsideration of the findings of his and older works (Preface, p. x).

Nor does he claim to have exhaustively covered the topic:

> There will always be further archives, inventories and collections that could shed light on this subject, there is much of relevance out there in myriad languages (…) that will have to await consideration by those with the relevant skills (Preface, p. xi).

On the other hand, he states that 'this book has been interesting and enjoyable to research and write' (Preface, p. xi). I would like to add that reading it was equally enjoyable and interesting. It is written in an easily readable, yet eloquent, style and Ogden manages to present the history of diamonds as an exciting adventure, while at the same time he has written a well-researched scholarly work. Ogden's meticulous and painstaking approach leads to an almost flawless result (in fact, I stumbled over just one error: the author talks about 'the Florentine Diamond, now in Vienna' [p. 215], which is surprising, as this stone was stolen in 1918 and has never turned up again). To complement the text, this book is richly illustrated with pictures of old diamond jewels and images from old sources, some of which are rare and difficult to find.

All in all, Ogden's early history of diamonds is not only an impressive scholarly masterpiece, but is also a great pleasure to read which I would recommend to everyone.

Dr Rolf Tatje
Duisburg, Germany

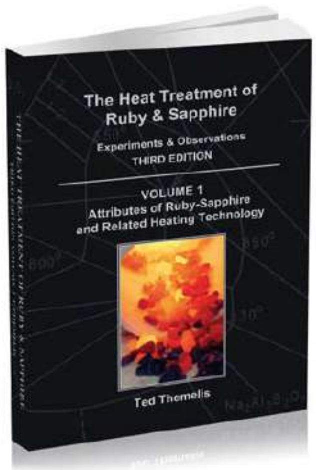

The Heat Treatment of Ruby & Sapphire: Experiments & Observations, 3rd edn., Vol. 1: Attributes of Ruby-Sapphire and Related Heating Technology

By Ted Themelis, 2018. Self-published, http://themelis.com/Books-Heat-TRS3.html, 294 pages, illus., ISBN 094-0965577. US$150.00 hardcover.

When I was invited to review this book I was very excited, since I have long been curious about the processes that happen when a gemstone is heated, but never had the chance to get actively involved. When I then held the book in my hand, I almost rejected the task because it was full of so much information that it seemed impossible to get through. However, the more

I read, the more I was captivated by it.

In his preface, Themelis points out that this book is not intended to be scientific, and the results presented are often based on trial and error without any explanations behind them. He also gives a short rundown on the instruments, furnaces and samples that he has used for his experiments.

The book then starts with a very informative chapter about the history of heating corundum, giving some early accounts, and then delving into more precise descriptions when heat treatment became more common in the 1970s. Themelis then goes into the history of heating corundum from certain origins.

Following the historical part, there is a wild mix of introductory subjects, including corundum definitions, disclosure issues, stability of heat treatments, values of the treated gems compared to their untreated counterparts, as well as information about the gem trade and various markets, economic impact, the value of gemstone reports, gemmologists in the trade, technologies for heat treatment, and the physical and chemical properties of corundum. For a laboratory gemmologist like myself, some of these subjects (e.g. various markets and worldwide heat-treatment facilities) were extremely interesting because I am not often exposed to them. However, I missed seeing a paragraph about trade shows, and also sample reports from the various laboratories (at least the better-known ones).

The next two chapters are dedicated to the properties of corundum and the effect of heat treatment on them. A detailed account of all possible colour impurities and irregularities is given, often with further explanations on their reaction to heat treatment, accompanied by numerous images of corundum from various localities, as well as charts for a better understanding. Themelis also describes different types of colour zoning and other defects such as twinning, parting, fissures, etc., and their effects on the outcome of heat treatment. A large part of the book is concerned with the description of internal features in corundum, again noting how they are affected by heat treatment. This includes not only mineral inclusions, but also fluid inclusions, 'silk' and staining in fissures. Material on the surface of a stone is also covered. A special section mentions inclusions separately in alphebetical order with their origins and melting points. The descriptions in these chapters are complemented by numerous images.

Starting with Chapter 5, the volume covers the practical side of heat treatment. It lists various heating parameters for different cases with detailed explanations of why it is important to choose certain steps, and explains the types of heating environments and the gases that are used. This is followed by a chapter that alphabetically lists additives in the heating process, with their chemical formulas, melting points and where and how they are used. Themelis then goes on to review other additives such as fertilisers, natural substances, etc., followed by helpful notes.

In Chapter 8, Themelis describes the entire methodology involved in heating corundum, starting with identifying rough material in the field and sorting it from other gem materials. He also gives an overview of classical gemmology, as well as advanced gemmological instruments for identification found in major gemmological laboratories, before continuing with a sub-chapter on the chemical cleaning of corundum. He lists all the acids that are used in various cleaning processes, generally with a description of the substance it is supposed to remove, the necessary equipment and a detailed description of how to clean the corundum. He then describes pre-burning processes and why they are performed, why shaping the rough stones may be necessary, how to assess certain features and attributes of the corundum, and how to classify it into different groups. Afterwards, he explains step by step how to determine the appropriate heating process, with many tips on what to watch out for when loading the crucible, choosing the right atmosphere, running the heating process, retrieving the stones and assessing the results.

In Chapter 9, Themelis gives a rundown of heating equipment from blow pipes to primitive furnaces to the most complicated electric furnaces. This chapter again gives many examples of which corundum is heated with which oven, together with some historical data from the 1980s. It is followed in Chapter 10 by an account of problems and damage that can occur during the heating process, be it failure of the instrument, overheating or contamination, as well as the effects fluxes may have on equipment.

The final chapter (Chapter 11) gives a classification of the heating processes for ruby and sapphire, accompanied by flow charts and before-and-after images of treated corundum. Here, I was a bit puzzled about the group classifications in the flow charts because I did not see an explanation why Themelis provided these group names without using them elsewhere to describe the processes (perhaps this will be done in Vol. 2).

In conclusion, this is a very thorough book, mainly addressed toward someone wanting to learn about heat treatment, but I also highly recommend it to the interested gemmologist as there is information that is not found elsewhere (e.g. types of fluxes and cleaning substances, the effect of heating on certain inclusions and the temperatures used for certain treatments). However, the book contains such a wealth of information based on experience that it is sometimes hard to combine the information found in the various chapters. The individual pages appear slightly overloaded with images and text, but this helps to keep the book at a reasonable size that is easy to use as a reference guide. Overall, I think it is a valuable book wherever heat treatment is concerned, and I am curious how Themelis will follow it in the second volume.

Dr Lore Kiefert FGA
Gübelin Gem Lab, Lucerne, Switzerland

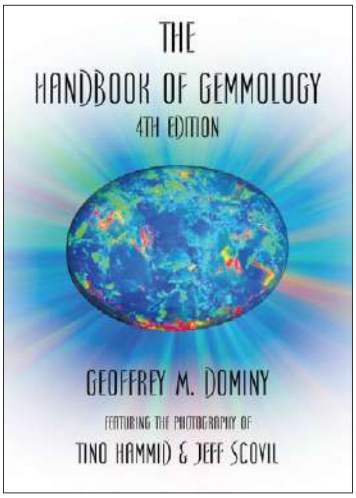

The Handbook of Gemmology, 4th edn.

By Geoffrey M. Dominy, 2017. Amazonas Gem Publications, Mallorca, Spain, http://handbookofgemmology.com, 1,342 pages, illus., ISBN 978-0991888238. US$49.95 eBook.

Now in its 4th edition, Geoffrey Dominy's digital *Handbook of Gemmology* continues its expansion into the gemmological field, creating an indispensable electronic reference that should be in every gemmologist's library. Running an impressive 1,342 pages, this edition aims to be a one-stop reference source, more easily carried and accessed than any traditional paper book of this size.

If downloaded as the 'flip-book' option, the *Handbook* comes complete with a handy overlay function that details the interactive features of the book and helps the user get the maximum potential from this format. Thumbnail previews allow the equivalent of quickly flicking through a traditional paper book, enabling sections to be easily located. The book also can be downloaded as a PDF file which, for technophobes, still allows a high level of interactivity and searchability. Colour-coded bookmarks, highlights and positionable 'post-it' notes are available, thus making each person's copy a truly unique and individual book. These features provide an interesting crossover from paper to digital format, and are bound to prove useful to those not wishing to mark up a traditional paper book. Another way to access the eBook is to log in and view it online, so there is no need to take up space on one's hard drive.

Using a columnar format, and high-quality images throughout, Dominy illustrates each chapter, often with full-page views of gemstones or features, bringing his customary style to all areas of the book.

Certain areas enjoy greater detail and more in-depth discussion than previous editions. For example, when considering atoms and bonding, Dominy includes s, p, d and f orbitals in a way that the lay person can follow. This is beyond the information provided by most other gemmological courses, but with advances in treatments and synthesis, it is increasingly important to have a greater understanding of such properties in gem materials.

Each crystal system also gets its own explanation, often covering several pages, and is related back to familiar household items, such as the tetragonal system that is explained by way of a milk carton. Crystallographic concepts are often difficult for students to grasp, which makes this a useful teaching tool. Within the same chapter the author also lists an extensive range of magnetic/paramagnetic reactions from various gem materials, an area that I have always found interesting but lacking in most mainstream texts. Dominy provides a reasonably extensive list of these magnetic reactions, covering the main gem materials that are found in today's jewellery market.

Spectroscopy and light absorption are covered in another chapter, and a variety of spectra are provided, with colour illustrations accompanied by lists of important absorption lines. With an ever-expanding use of laboratory equipment, these spectral lines play an increasing role in gemmological testing. This is demonstrated at the end of the chapter, where the visible spectrum is overlaid onto spectral traces obtained from a spectrophotometer, which allows direct comparisons to be made and eases the transition from traditional to modern laboratory gemmology.

The section on refraction covers detailed use of the refractometer and underlying theory, and gives an excellent visual representation of the distant-vision or spot method for obtaining a reading from a non-planar surface.

This is an area that many students struggle with, and this may prove useful in teaching centres globally. Beyond this, Dominy considers alternative ways of determining the RI value(s) of a stone, including Alan Hodgkinson's 'Visual Optics' and the use of immersion cells for estimating RI (and assisting with observing internal features).

In the chapter that discusses polarised light, Dominy covers the enantiomorphism of quartz, and shows how left- and right-handedness can be determined in a way often overlooked in all but the highest levels of gemmological education. Filters are also dealt with in great detail, not only in terms of results, but also regarding their construction and usage, whether something as simple as crossed polarisers or a full filter set.

The chapter on specific gravity has been updated to show a more visual representation of the various methods and principles, making it easier for the non-specialist to understand and increasing its potential use for students.

An interesting addition to this edition is a section on building a smartphone microscope camera, which is useful given the high quality of images now obtainable from most phones. In place of simply holding a smartphone over a microscope eyepiece, Dominy details how a simple apparatus can be constructed that supports the phone at a suitable distance and position for images to be captured. The pages immediately after this provide an extensive range of inclusion images, showcasing what can be done with the right equipment.

Subsequent chapters cover composite gems and synthetics. Each is covered in detail, with images and diagrams to highlight key features and what to look for when faced with specimens that are potentially laboratory grown. Synthetic diamond, as might be expected, is covered in its own in-depth section, which goes beyond prior editions of this book. Modern production techniques (both HPHT and CVD) are covered in detail, and accompanied by numerous images showing rough and cut examples. Where this edition significantly exceeds all previous ones is a description of the advanced technology currently in use to detect synthetic diamonds, even down to melee sizes. Although most readers will not have a chance to see or use these tools, Dominy gives a good explanation of their capabilities, as well as when—and in which sequence—they should be used.

The important area of treatments is given greater consideration, spanning more than 60 pages of high-quality information and illustrations, bringing the reader up to date with the latest developments. This provides an essential reference source for all levels of reader.

Both diamond and coloured stone grading are dealt with in detail. The former is to be expected in any gemmological text nowadays, but the extensive detail provided on the latter—including systems, nomenclature and processes—exceeds most other texts.

Next are a series of chapters dedicated to gem identification and ordered by colour, which are very useful for any student. Following these is an extensive 'Gemfacts' section that provides in-depth coverage of 17 gem materials. Last are a series of appendices that make useful references.

In conclusion, this updated version of *The Handbook of Gemmology* builds upon previous successes, expanding and enhancing the prior editions with new and in-depth information. Given the digital portability of this work, and the range of formats in which it is available, this continues to be a ground-breaking publication, and an essential tool for any level of gemmologist.

Editor's note: A two-volume 5th anniversary printed edition of *The Handbook of Gemmology* was released in May 2018 for €309.00 in Europe and €329.00 elsewhere.

Andrew S. Fellows FGA DGA
Birmingham City University, Birmingham

Other Book Titles

COLOURED STONES

Turquoise: The World Story of a Fascinating Gemstone, updated edn.
By Joe Dan Lowry, 2018. Gibbs Smith, Layton, Utah, USA, 256 pages, ISBN 978-1423650898.
US$75.00 hardcover.

DIAMOND

Evolution of Magmatic and Diamond-forming Systems of the Earth's Lower Mantle
By Anna V. Spivak and Yuriy A. Litvin, 2018. Springer, Cham, Switzerland, 108 pages, ISBN 978-3319785172.
€109.99 hardcover or €91.62 eBook.

GENERAL REFERENCE

The Jeweller's Directory of Gemstones
By Judith Crowe, 2018. Herbert Press, Bloomsbury, London, 176 pages, ISBN 978-1912217182. £20.00 softcover.

INSTRUMENTATION

Confocal Raman Microscopy
Ed. by Jan Toporski, Thomas Dieing and Olaf Hollricher, 2018. Springer, Cham, Switzerland, 596 pages, ISBN 978-3319753782. €140.17 softcover or €118.99 eBook.

Scanning Electron Microscopy and X-Ray Microanalysis, 4th edn.
By Joseph I. Goldstein, Dale E. Newbury, Joseph R. Michael, Nicholas W. M. Ritchie, John Henry J. Scott and David C. Joy, 2018. Springer-Verlag, New York, New York, USA, 550 pages, ISBN 978-1493966745. US$129.00 hardcover or $99.00 eBook.

JEWELLERY AND *OBJETS D'ART*

Boucheron: Free-Spirited Jeweler
By Anita Coppet, 2018. Abrams, New York, New York, USA, 216 pages, ISBN 978-1419734908. US$80.00 hardcover.

Fabergé: His Masters and Artisans
By Ulla Tillander-Godenhielm, 2018. Unicorn Publishing Group, London, 272 pages, ISBN 978-1911604204. £30.00 hardcover.

Seals and Status: Power of Objects
Ed. by John Cherry, Jessica Berenbeim and Lloyd de Beer, 2018. British Museum Press, London, 225 pages, ISBN 978-0861592135. £40.00 softcover.

Sustainable Jewellery: Principles and Processes for Creating an Ethical Brand
By Jose Luis Fettolini, 2018. Promopress, Barcelona, Spain, 176 pages, ISBN 978-8416851201. €27.00 softcover.

Gem-A Notices

Gifts to the Association

Gem-A is most grateful to the following for their generous donations, which will support continued research and teaching:

Jonathan Bartky, Ariel Treasures, Livingston, New Jersey, USA, for two samples of red aventurescent quartzite from Tanzania, marketed as Cherry Tanzurine.

Dr Marco Campos Venuti, Seville, Spain, for three cabochons of green-to-yellow opal from Brazil and four cabochons of trapiche-like ametrine from Brazil.

Denis Ho, Hong Kong, for a selection of African sapphires and a folding lightbox.

Adam Pearl, Cleveland, Ohio, USA, for four rough pieces of colourless cordierite from Tanzania.

Dr Lola Rafieva, London, for various beads and jewellery including coral, glass, bone and plastic.

Estelle Weiner, Cheadle, for diamond-cutting tools that once belonged to her mother, Rebecca Staal.

New Head of Education

Gem-A is delighted to announce the appointment of Nysa Pradhan as our new Head of Education. Nysa started on 28 August 2018, and is leading and developing Gem-A's worldwide educational activities. While being based at Gem-A's headquarters in London, Nysa will be visiting our teaching centres and shows around the world, so you may be seeing her sometime soon.

Gem-A Annual General Meeting

Gem-A members are invited to attend our AGM on Tuesday 2 October 2018 from 18:30 to 21:00 at the Goldsmiths Centre, Britton Street, London. Gem-A members can log onto our website to access AGM documents, and may also join us for drinks at 18:00 before the meeting.

Gem-A Conference 2018: Bringing together the greatest minds in gemmology

Gemmologists from around the world will gather in London for the annual Gem-A Conference 3–4 November. The Conference boasts an incredible line-up of speakers, including expert gemmologists from every area of the field, exclusive workshops and trips including private viewings of museum collections. Registration closes on Sunday 21 October 2018. Make sure you don't miss out on the gemmological event of the year. Register now at https://gem-a-conference-2018.eventbrite.co.uk.

Literature of Interest

COLOURED STONES

Anorthite with uvarovite garnet inclusions. E-A. Jeong, *Wooshin Gem Lab Magazine*, **5**, 2018, 16–20, www.wooshinlab.com/LabStory/Research/Read.wgk?ArticleID=212.*

Beauty created by light: Color change gemstones. M.-R. Heo, *Wooshin Gem Lab Magazine*, **5**, 2018, 28–31, www.wooshinlab.com/LabStory/Research/Read.wgk?ArticleID=212.*

Cause of tri-colour change effect of a rare garnet. Y. Shen and P. Ye, *Journal of Gems & Gemmology*, **20**(2), 2018, 17–23 (in Chinese with English abstract).

Colour grading system of emerald. Y. Zuo, C. Carmona, L. Liu, F. Wu, D. Fortaleche and Q. Lin, *Journal of Gems & Gemmology*, **20**(2), 2018, 9–16 (in Chinese with English abstract).

A common origin for Thai/Cambodian rubies and blue and violet sapphires from Yogo Gulch, Montana, U.S.A.? A.C. Palke, J. Wong, C. Verdel and J.N. Ávila, *American Mineralogist*, **103**(3), 2018, 469–479, http://doi.org/10.2138/am-2018-6164.

Gemmological and mineralogical characteristic of "Lanshui" jadeite [green jadeite from Guatemala]. L. He, J. Liu, C. Long and B. Liao, *Journal of Gems & Gemmology*, **20**(2), 2018, 31–37 (in Chinese with English abstract).

The gemological characteristics of American "mica jade" [clinostrengite]. H. Zhu, B. Sun, F. Yan, P. Wang and X. Zhao, *Superhard Material Engineering*, **29**(4), 2017, 64–66 (in Chinese with English abstract).

Gemological characterization of sapphires from Yogo Gulch, Montana. N.D. Renfro, A.C. Palke and R.B. Berg, *Gems & Gemology*, **54**(2), 184–201, http://doi.org/10.5741/GEMS.54.2.184.*

Infrared and Raman spectra of high-quality turquoise from Hubei and Anhui, China: Characteristics and significance. C. Wen-jun, G. Shi, Y. Wang, J. Ren, Y. Yuan and H. Dai, *Spectroscopy and Spectral Analysis*, **38**(4), 2018, 1059–1065 (in Chinese with English abstract).

Inhabituel quartz de Madagascar imitant naturellement une grandidierite [Unusual Madagascar quartz naturally imitating grandidierite]. J.-M. Arlabosse, *Revue de Gemmologie A.F.G.*, No. 202, 2018, 6–9 (in French).

Isotopes [*sic*] signatures of gem minerals. G. Giuliani and A.E. Fallick, *Wooshin Gem Lab Magazine*, **5**, 2018, 2–9, www.wooshinlab.com/LabStory/Research/Read.wgk?ArticleID=212.*

Out of the blue...dealing with kyanite. A. Vaia, *Rivista Italiana di Gemmologia/Italian Gemological Review*, No. 4, 2018, 41–43.

Paraíba tourmaline revisited. C. Milisenda, *InColor*, No. 39, 2018, 34–41, www.gemstone.org/incolor/39.*

The provenance of nephrite in China based on multi-spectral imaging technology and gray-level co-occurrence matrix. D. Chen, M. Pan, W. Huang, W. Luo and C. Wang, *Analytical Methods*, **10**, 2018, 4053–4062, http://doi.org/10.1039/c8ay01274a.

The Raman spectroscopy study of gem-quality serpentine from Soghan, Kerman Province, Iran. B. Shirdam and S. Aslani, *Wooshin Gem Lab Magazine*, **5**, 2018, 24–27, www.wooshinlab.com/LabStory/Research/Read.wgk?ArticleID=212.*

Reverse dichromatism in gem andalusite related to total pleochroism of the Fe^{2+}-Ti^{4+} IVCT. B. Rondeau, S. Chamard-Bois, E. Fritsch, F. Notari and B. Chauviré, *Spectrochimica Acta Part A: Molecular and Biomolecular Spectroscopy*, **204**, 2018, 611–619, http://doi.org/10.1016/j.saa.2018.06.053.

Role of Ti content on the occurrence of the 3309-cm^{-1} peak in FTIR absorption spectra of ruby samples. A. Phlayrahan, N. Monarumit, S. Satitkune and P. Wathanakul, *Journal of Applied Spectroscopy*, **85**(3), 2018, 385–390, http://doi.org/10.1007/s10812-018-0662-0.

The story of the Smithsonian's Brazilian topaz crystals. E.S. Meieran, *Mineralogical Record*, **49**(3), 2018, 449–451.

Study on EDXRF method of turquoise composition. L. Liu, M. Yang, L. Ren, A. Shen and C. He, *Spectroscopy and Spectral Analysis*, **38**(6), 2018, 1910–1916 (in Chinese with English abstract).

Tanzurine, cherry-red and emerald-green quartz from Tanzania. J.S. White and L.D. Dickson, *Rocks & Minerals*, **93**(3), 2018, 250–257, http://doi.org/10.1080/00357529.2018.1428863.

Tsavorite…50 years later. C. Simonet, *InColor*, No. 39, 2018, 28–30, www.gemstone.org/incolor/39.*

CULTURAL HERITAGE

Carnelian, agate, and other types of chalcedony: The prehistory of Jebel al-Ma'taradh and its semi-precious stones, Emirate of Ra's al-Khaimah. V. Charpentier, O. Brunet, S. Méry and C. Velde, *Arabian Archaeology and Epigraphy*, **28**(2), 2017, 175–189, https://doi.org/10.1111/aae.12090.

An Early Byzantine engraved almandine from the Garibpet deposit, Telangana State, India: Evidence for garnet trade along the ancient Maritime Silk Road. H.A. Gilg, K. Schmetzer and U. Schüssler, *Gems & Gemology*, **54**(2), 2018, 149–165, http://doi.org/10.5741/GEMS.54.2.149.*

Early historic gemstone bead manufacturing centre at Bhutiapali, the middle Mahanadi Valley, Odisha. P.K. Behera and S. Hussain, *Journal of Multidisciplinary Studies in Archaeology*, **5**, 2017, 269–282.

The mineral collection of Russian Empress Catherine II. N.V. Borovkova, *Mineralogical Almanac*, **23**(2), 2018, 4–18.

Mining, macro-regional interaction and ritual practices in the south-central Andes: The first evidence for turquoise exploitation from the late Prehispanic and Inca periods in north-western Argentina (Cueva Inca Viejo, Puna de Salta). G.E.J. López, F.I. Coloca, M. Rosenbusch and P. Solá, *Journal of Archaeological Science: Reports*, **17**, 2018, 81–92, http://doi.org/10.1016/j.jasrep.2017.09.036.*

The weight of ritual: Classic Maya jade head pendants in the round. C.T. Halperin, Z.X. Hruby and R. Mongelluzzo, *Antiquity*, **92**(363), 2018, 758–771, http://doi.org/10.15184/aqy.2018.65.

DIAMONDS

The Alto Paranaíba region, Brazil: A continuing source for pink diamonds? D.B. Hoover, J. Karfunkel, D. Walde, R.A.V. Moraes, G. Michelfelder, F.E. Renger, L.C.B. Ribeiro and K. Krambrock, *Australian Gemmologist*, **26**(9–10), 2018, 196–204.

Application of laser Raman spectroscopy method in research of diamond. F. Han, S. Li, L. Zhu, Y. Nie, K. Yu, J. Wang, T. Su, M. Hu and H. Xiao, *Journal of Synthetic Crystals*, **47**(5), 2018, 1060–1065 (in Chinese with English abstract).

Black diamonds from Marange (Zimbabwe): A result of natural irradiation and graphite inclusions. K.V. Smit, E. Myagkaya, S. Persaud and W. Wang, *Gems & Gemology*, **54**(2), 2018, 132–148, http://doi.org/10.5741/GEMS.54.2.132.*

Blue boron-bearing diamonds from Earth's lower mantle. E.M. Smith, S.B. Shirey, S.H. Richardson, F. Nestola, E.S. Bullock, J. Wang and W. Wang, *Nature*, **560**(7716), 2018, 84–87, http://doi.org/10.1038/s41586-018-0334-5.

Les diamants de Golconde [Golconda diamonds]. C. Juncker, A. Herreweghe and A. Delaunay, *Revue de Gemmologie A.F.G.*, No. 202, 2018, 22–26 (in French).

Diamond exploration potential of the northern East European Platform. E. Shchukina and V. Shchukin, *Minerals*, **8**(5), 2018, http://doi.org/10.3390/min8050189.*

Diamonds help solve the enigma of Earth's deep water. K.V. Smit and S.B. Shirey, *Gems & Gemology*, **54**(2), 2018, 220–223, www.gia.edu/gg-issue-search?ggissueid=1495265158591&articlesubtype=diamondsfromthedeep.*

Essential books on diamond. A.J.A. Janse, *Australian Gemmologist*, **26**(9–10), 2018, 217–223.

The first Australian diamond. R.F. Hansen and L.J. Rennie, *Australian Gemmologist*, **26**(9–10), 2018, 205–216.

Multidisciplinary constraints on the abundance of diamond and eclogite in the cratonic lithosphere. J.M. Garber, S. Maurya, J.-A. Hernandez, M.S. Duncan, L. Zeng, H.L. Zhang, U. Faul, C. McCammon, J.-P. Montagner, L. Moresi, B.A. Romanowicz, R.L. Rudnick and L. Stixrude, *Geochemistry, Geophysics, Geosystems*, **19**(7), 2018, 2062–2086, http://doi.org/10.1029/2018gc007534.

Natural-color blue, gray, and violet diamonds: Allure of the deep. S. Eaton-Magaña, C.M. Breeding and J.E. Shigley, *Gems & Gemology*, **54**(2), 2018, 112–131, http://doi.org/10.5741/GEMS.54.2.112.*

Only a matter of time…[Argyle pink diamonds]. *Gems&Jewellery*, **27**(2), 2018, 20–21.

The pursuit of colour. Part 1. The rise to prominence of fancy coloured diamonds post 1970. C. Green, *Australian Gemmologist*, **26**(9–10), 2018, 226–239.

Specific internal structure of diamonds from Zarnitsa kimberlite pipe. A. Ragozin, D. Zedgenizov, K. Kuper and Y. Palyanov, *Crystals*, **7**(5), 2017, article 133, 10 pages, http://doi.org/10.3390/cryst7050133.*

Surface dissolution features and contact twinning in natural diamonds. T. Lu, J. Ke and Z. Qiu, *Neues Jahrbuch für Mineralogie, Abhandlungen*, **195**(2), 2018, 145–153, http://doi.org/10.1127/njma/2018/0108.

FAIR TRADE

From a trust-based to a transparency-based industry: How technology drives changes in the gemstone industry. D. Nyfeler, *GemGuide*, **37**(4), 2018, 8–11.

Mapping small-scale mineral production networks: The case of alluvial diamonds in Ghana. J. McQuilken and G. Hilson, *Development and Change*, **49**(4), 2018, 978–1009, http://doi.org/10.1111/dech.12403.

Will they be named blood rubies? The complex settlement of Gemfields opens new implications of social responsibility [Mozambique rubies]. P. Minieri, *Rivista Italiana di Gemmologia/Italian Gemological Review*, No. 4, 2018, 32–39.

GEM LOCALITIES

Between rice paddies and karst pinnacles: The Luc Yen gemstone mining area. A. Trivier, *InColor*, No. 39, 2018, 16–26, www.gemstone.org/incolor/39.*

Emerald from the Fazenda Bonfim deposit, northeastern Brazil: Chemical, fluid inclusions and oxygen isotope data. J.S. Santiago, V. da S. Souza, B. de C. Filgueiras and F.A.C. Jiménez, *Brazilian Journal of Geology*, 2018, 16 pages, http://doi.org/10.1590/2317-4889201820170130.*

The four gemstones from Yunnan Province, China. A. Nakajima, *Journal of the Gemmological Society of Japan*, **33**(1–4), 2018, 3–12, http://doi.org/10.14915/gsjapan.33.1-4_3 (in Japanese with English abstract).

Gems of Italy [chalcedony to epidote]. *Rivista Italiana di Gemmologia/Italian Gemological Review,* No. 4, 2018, 20–29.

Madagascar sapphire: Crystal blue persuasion. E.B. Hughes and R.W. Hughes, *Rivista Italiana di Gemmologia/Italian Gemological Review*, No. 4, 2018, 44–54.

Mantle and deep crustal xenoliths in basalts from the Bo Rai ruby deposit, eastern Thailand: Original source of basaltic ruby. C. Sutthirat, C. Hauzenberger, T. Chualaowanich and T. Assawincharoenkij, *Journal of Asian Earth Sciences*, **164**, 2018, 366–379, http://doi.org/10.1016/j.jseaes.2018.07.006.

Mozambique Paraiba tourmaline deposits – An update. F. Pezzotta, *InColor*, No. 39, 2018, 52–56, www.gemstone.org/incolor/39.*

Nouveau et premier gisement de saphirs en Iran [New and first deposit of sapphires in Iran]. G. Panczer, N.M. Pak and G. Riondet, *Revue de Gemmologie A.F.G.*, No. 202, 2018, 4–5 (in French).

Paraiba – A miner's perspective [Quintos mine, Brazil]. *InColor*, No. 39, 2018, 58–62, www.gemstone.org/incolor/39.*

Paraiba tourmaline from Brazil: The neon-blue burn. T. Hsu, *InColor*, No. 39, 2018, 42–50, www.gemstone.org/incolor/39.*

Petro – chemical and spectral signatures on corundum bearing Precambrian amphibolites in Sullia area, Dakshina Kannada District, Karnataka, India. H.T. Basavarajappa and N.E. Maruthi, *Journal of Emerging Technologies and Innovative Research*, **5**(7), 2018, 75–83.

Petrochemistry, mineral chemistry, and pressure–temperature model of corundum-bearing amphibolite from Montepuez, Mozambique. A. Fanka and C. Sutthirat, *Arabian Journal for Science and Engineering*, **43**(7), 2018, 3751–3767, http://doi.org/10.1007/s13369-018-3172-8.

La pierre verte de Nouvelle-Zélande : Aux couleurs des espoirs maoris [The green stone of New Zealand: In the colours of the Maori hopes]. I. Reyjal, *Revue de Gemmologie A.F.G.*, No. 202, 2018, 18–21 (in French).

The Telirio mine, Minas Gerais, Brazil [brazilianite]. A. Bartorelli and C. Cornejo, *Mineralogical Record*, **49**(3), 2018, 401–429.

INSTRUMENTATION

Looking for the light [luminescence]. L. Faber, *Gems&Jewellery*, **27**(2), 2018, 12–14.

Nanoparticle-enhanced laser induced breakdown spectroscopy for the noninvasive analysis of transparent samples and gemstones. C. Koral, M. Dell'Aglio, R. Gaudiuso, R. Alrifai, M. Torelli and A. De Giacomo, *Talanta*, **182**, 2018, 253–258, http://doi.org/10.1016/j.talanta.2018.02.001.

An overview of synthetic diamond detection – Methods and instruments. J. Chapman and B. Deljanin, *Australian Gemmologist*, **26**(9–10), 2018, 209–216.

MISCELLANEOUS

Creative, entrepreneurial, and branding strategy for a novel jewellery line. A.D. Mavromoustakaki, M.S. thesis, School of Economics, Business Administration & Legal Studies, International Hellenic University, 2018, 90 pages, https://repository.ihu.edu.gr/xmlui/handle/11544/29100.*

De Beers's diamond mine in the 1880s: Robert Harris and the Kimberley searching system. M. Pointon, *History of Photography*, **42**(1), 2018, 4–24, http://doi.org/10.1080/03087298.2018.1429095.*

The past and present of platinum. S. Turner, *Gems&Jewellery*, **27**(2), 2018, 22–24.

Price estimation model of jade bracelet based on RBF neural network. K. Deng, P. He, X. Zhou and W. Zhang, *IOP Conference Series: Materials Science and Engineering*, **381**, 2018, article 012100, 7 pages, http://doi.org/10.1088/1757-899x/381/1/012100.*

Your friend the inclusions. The detective at the party of inclusions. Third episode. L. Costantini and C. Russo, *Rivista Italiana di Gemmologia/Italian Gemological Review*, No. 4, 2018, 7–13.

NEWS PRESS

About a quadrillion tons of diamonds may be hiding in Earth. A. Interrante, *Newsweek*, 16 July 2018, www.newsweek.com/diamond-found-earth-1026382.*

Blockchain used to track gems to counter blood diamonds and fakes. T. Shapshak, *Forbes*, 10 May 2018, http://tinyurl.com/y7t8tvx3.*

De Beers has scorned lab-made diamonds for years. Now it will sell them – for as little as $200. A. Bhattarai, *Washington Post*, 29 May 2018, http://tinyurl.com/ycbgp4ep.*

Ethical concerns grow over Kimberley Process diamond charter. H. Sanderson, *Financial Times*, 21 March 2018, www.ft.com/content/76019f26-01f5-11e8-9e12-af73e8db3c71.

Hill of gems, gems of labour – Mining in the borderlands [Chanthaburi, Thailand]. A.R. Chowdhury and A. Abid, *Kyoto Review of Southeast Asia*, 2018, https://kyotoreview.org/yav/gems-of-labour-mining-in-the-borderlands.*

This porcelain is tougher than it looks [developed by jewellery designer Wallace Chan]. R. Felder, *New York Times*, 20 July 2018, www.nytimes.com/2018/07/20/fashion/jewelry-porcelain-wallace-chan.html.*

Researchers offer new details how they found a 300-year-old ship that sank with $17 billion in treasure. L. Landrum, CNN, 23 May 2018, www.cnn.com/2018/05/22/world/colombia-shipwreck-discovery-trnd/index.html.*

Tokenised diamonds to test limits of cryptocurrency investing. D. Weinland and K. Varagur, *Financial Times*, 6 May 2018, www.ft.com/content/24110758-4dcf-11e8-97e4-13afc22d86d4.

What the FTC diamond ruling means for consumers and diamond marketers. P.N. Danziger, *Forbes*, 2 August 2018, http://tinyurl.com/y9eamj4t.*

ORGANIC GEMS

Characteristics of Burma blood amber and other colors of ambers. R. Xiao and J. Kang, *Superhard Material Engineering*, **30**(2), 2018, 54–58 (in Chinese with English abstract).

Could a nut replace an elephant? [vegetable ivory or tagua nut] *Gems&Jewellery*, **27**(2), 2018, 16–17.

Identification of an unknown variegated bracelet [shell materials]. X. Song and Q. Zhang, *Journal of Gems & Gemmology*, **19**(5), 2017, 37–47 (in Chinese with English abstract).

Mid-infrared spectroscopy for characterization of Baltic amber (succinite). E. Wagner-Wysiecka, *Spectrochimica Acta Part A: Molecular and Biomolecular Spectroscopy*, **196**, 2018, 418–431, http://doi.org/10.1016/j.saa.2018.02.053.

Raman spectroscopy coupled to chemometrics to discriminate provenance and geological age of amber. M.D. Peris-Díaz, B. Łydżba-Kopczyńska and E. Sentandreu, *Journal of Raman Spectroscopy*, **49**(5), 2018, 842–851, http://doi.org/10.1002/jrs.5357.

Up close and really personal: Putting human elements into jewels. M. Chabrol, *InColor*, No. 39, 2018, 68–70, www.gemstone.org/incolor/39.*

PEARLS

Cultured pearls from Lake Kasumigaura: Production and gemological characteristics. A. Abduriyim, *Gems & Gemology*, **54**(2), 2018, 166–183, http://doi.org/10.5741/GEMS.54.2.166.*

Gulf pearls: Then and now. J. Hann, *Gems&Jewellery*, **27**(2), 2018, 32–35.

Récente découverte en Indonésie d'une perle de Melo de dimension inhabituelle [Recent discovery in Indonesia of a Melo pearl of unusual size]? T.N. Bui and J.-P. Gauthier, *Revue de Gemmologie A.F.G.*, No. 202, 2018, 16–17 (in French).

SIMULANTS

Gemmological characteristic of two new malachite imitations. L. Yu, R. Liao and J. Guo, *Journal of Gems & Gemmology*, **20**(2), 2018, 47–56 (in Chinese with English abstract).

Investigating fake rough. G. Choudhary, *Gems&Jewellery*, **27**(2), 2018, 26–29.

Melee size diamond simulants in a ring. E.-O. Jo, H.-E. Moon and K.-W. Kwak, *Wooshin Gem Lab Magazine*, **5**, 2018, 21–23, www.wooshinlab.com/LabStory/Research/Read.wgk?ArticleID=212.*

Nouvelle imitation de diamant brut en moissanite synthétique [New imitation of rough diamond made of synthetic moissanite]. A. Delaunay and E. Fritsch, *Revue de Gemmologie A.F.G.*, No. 202, 2018, 15–16 (in French).

Structures désordonnées d'imitations d'oeil-de-chat en fibres de verre [Disordered structures in fiber-glass cat-eye imitations]. J.-P. Gauthier, J. Fereire and A. Laurent, *Revue de Gemmologie A.F.G.*, No. 202, 2018, 10–14 (in French with English abstract).

SYNTHETICS

Features of synthetic diamonds. S. Eaton-Magaña and C.M. Breeding, *Gems & Gemology*, **54**(2), 2018, 202–204, http://doi.org/10.5741/GEMS.54.2.202.*

Gemmological characteristic of HPHT synthetic diamonds. H. Zhu, H. Liu, Y. Cheng, J. Li and D. Wang, *Superhard Material Engineering*, **30**(1), 2018, 61–66 (in Chinese with English abstract).

Morphology of flux-grown crystals. M. Tachibana, *Journal of the Gemmological Society of Japan*, **33**(1–4), 2018, 13–19, http://doi.org/10.14915/gsjapan.33.1-4_13 (in Japanese with English abstract).

Synthesis and characterization of purple $NaAlSi_2O_6$ jadeite under high pressure and high temperature. L. Zhao, H. Ma, C. Fang, L. Ding and X. Jia, *Journal of Crystal Growth*, **499**, 2018, 30–34, http://doi.org/10.1016/j.jcrysgro.2018.07.034.

The untold story of Douros synthetic rubies. A. Malossi, *Rivista Italiana di Gemmologia/Italian Gemological Review*, No. 4, 2018, 57–68.

TREATMENTS

Effect of heat treatment on the luminescence properties of natural apatite. P. Chindudsadeegul and M. Jamkratoke, *Spectrochimica Acta Part A: Molecular and Biomolecular Spectroscopy*, **204**, 2018, 276–280, http://doi.org/10.1016/j.saa.2018.06.056.

Influence of annealing on the properties of silicon carbide at high temperature and high pressure condition. Z. You-jin, L. Wang, F. Wang, G. Zuo and H. Huang, *Journal of Synthetic Crystals*, **46**(10), 2017, 2073–2076 (in Chinese with English abstract).

COMPILATIONS

***G&G* Micro-World.** Mushroom in copal • Gilalite altered to cuprite in quartz • Colour zoning in chameleon diamond • Merelaniite inclusions in tanzanite • Microlite in topaz • Perettiite and tusionite inclusions in phenakite • Horse-shaped mica inclusion in sapphire • Star spinel with four or six rays • Glass imitation of demantoid with horsetail inclusions • Wurtzite phantom in quartz. *Gems & Gemology*, **54**(2), 2018, 224–232, www.gia.edu/gg-issue-search?ggissueid=1495265158591&articlesubtype=microworld.*

Gem News International. Colour-change grossular from Ethiopia • Green-blue Maxixe beryl • Trapiche-like amethyst from Brazil • 12-rayed star sapphire from Thailand • Chemical composition of Gold Sheen sapphire • Type IIa diamond with $CaSiO_3$-walstromite inclusion • Gemstones and Sustainable Development Knowledge Hub • *Selecting Gem Rough: A Guide for Artisanal Miners* • Etching on HPHT synthetic diamonds • Nephrite bracelet with filled cavity • DiamondView imaging of glass-filled ruby • Wax-impregnated jade with strong fluorescence • IAC conference on responsible gold. *Gems & Gemology*, **54**(2), 2018, 233–254, www.gia.edu/gg-issue-search?ggissueid=1495265158591&articlesubtype=gni.*

Gemmological Intelligence. Diamond breakage during cutting • Software for assessing a faceted diamond's apparent size • Hexagonal etch pits on a diamond crystal • Engagement ring trends. *Australian Gemmologist*, **26**(9–10), 2018, 240–253.

Lab Notes. 1.91 ct faceted afghanite • Beryl/glass assemblage imitating emerald • 17.09 ct HPHT-treated type IIb blue diamond • Natural melee found in synthetic diamond parcel • Repaired diamond • Cat's-eye amphibole and jadeite • 'Horse conch' pearls • Star sapphire with transparent core • Cabochons from *Crassostrea virginica* shell • Green-blue irradiated CVD synthetic diamonds • 5.01 ct pinkish orange CVD synthetic diamond • 15.32 ct near-colourless HPHT synthetic diamond. *Gems & Gemology*, **54**(2), 2018, 206–218, www.gia.edu/gg-issue-search?ggissueid=1495265158591&articlesubtype=labnotes.*

CONFERENCE PROCEEDINGS

XXII Meeting of the International Mineralogical Association. Melbourne, Victoria, Australia, 13–17 August 2018, 536 pages, www.ima2018.com/ima2018-abstracts.*

Amberif 2017: Amber Work of Nature in Human Hands. Gdańsk, Poland, 24 March 2017, 44 pages, http://tinyurl.com/y7u8k6u6.*

Amberif 2018: International Symposium—Amber. Science and Art. Gdańsk, Poland, 22–23 March 2018, 168 pages, http://tinyurl.com/y9ucpvxw.*

**Article freely available for download, as of press time*